DEVELOPMENT OF A CULTURED TISSUE SUBSTITUTE TO REPAIR THE AGEING RETINA

Audra Miral Alice Shadforth
Bachelor of Science (Biomedical Science)

A thesis submitted in fulfilment of the requirements for the degree of Doctor of Philosophy

School of Biomedical Sciences
Faculty of Health
Queensland University of Technology

2015

Abstract

Degenerative diseases of the retina, especially age-related macular degeneration (AMD) have profound effects on vision and thus significantly impair quality of life. Currently, the only treatment available for AMD patients involves the intravitreal injection of anti-vascular endothelial growth factor (anti-VEGF) agents that can help to modulate aberrant vascular growth. However, this symptom affects only 15 % of AMD patients. Furthermore, the anti-VEGF agents do not repair structural changes that occur as a result of the natural history of AMD progression. The structural changes originating in three tissue layers known as Ruysch's complex, have been linked to a number of local and systemic complications, that can result in monocular and bilateral blindness. Theoretically, the replacement of these three tissue layers, namely the retinal pigment epithelium (RPE), the acellular Bruch's membrane, and the choriocapillaris would be the best therapeutic option for all AMD patients as it would reconstruct the subretinal architecture. The development of cell-based therapies for the treatment of degenerative retinal diseases has therefore attracted much interest within the fields of ophthalmology and regenerative medicine.

Ideally, a cultured tissue substitute would include a functioning monolayer of RPE, a suitable biomaterial substitute for Bruch's membrane (thin, mechanically strong and permeable) and choroidal vascular endothelial cells that could anastomose with the patient's vasculature, helping to anchor the complex upon implantation. A major hurdle in the development of a cell-based therapy is the identification of an appropriate biomaterial substitute for Bruch's membrane. Recently *Bombyx mori* silk fibroin (hereafter referred to as fibroin) membranes, made to a similar thickness as a healthy Bruch's membrane (3 μm), have been found to support the attachment and growth of RPE cells (Shadforth et al., 2012). Thus this thesis aims to explore the feasibility of using fibroin membranes as a biomaterial substitute in the reconstruction of Ruysch's complex. The project set out to evaluate the functionality of RPE cells grown on fibroin membranes, evaluate the feasibility of modifying fibroin membranes to include extracellular matrix (ECM) components vital to the

native structure of Bruch's membrane, and establish a co-culture model of Ruysch's complex *in vitro*.

In the first research study (Chapter 3), the human cell line ARPE-19 was used to establish confluent cultures of RPE cells on fibroin membranes and were maintained under conditions designed to promote maturation. As a control, parallel cultures were established and maintained to maturity on commercial porous polyester cell culture well inserts (Transwell®), the current gold standard epithelial culture substrate. Cultures established on both materials were examined for evidence of trans-epithelial resistance (TER), features of RPE cell morphology and metabolism, specific phagocytic function (via uptake of vitronectin-coated microspheres) and apical/basal growth factor secretion. Cultures established on either material developed a cobblestoned morphology with partial pigmentation within 12 weeks, however, cultures grown on fibroin displayed a rounder apical surface with a more dense distribution of microvilli-like projections. Negligible change in TER was observed for cultures grown on either material, however this result is in keeping with prior studies of ARPE-19 cell function. Examination by immunocytochemistry, at 16 weeks, revealed a generally similar distribution pattern for RPE-specific cytoplasmic and membrane-bound proteins. Cultures grown on either material displayed specific phagocytic function and polarised secretion of growth factors was routinely detected in the conditioned medium collected from above and below both membrane types. These findings demonstrated that RPE cell functions on fibroin membranes are equivalent to those observed for standard test materials (polyester membranes).

After confirming RPE functionality on fibroin membranes, focus was shifted to the native structure of Bruch's membrane, namely its central core of elastin (Chapter 4). The specific structural and functional roles the Bruch's membrane fulfils within the outer retina, creates a complex list of requirements for a biomaterial substitute. This thesis evaluated the feasibility of incorporating an elastin component to the fibroin membranes. It was hypothesized the modified fibroin membranes may provide a potential delivery vehicle for both RPE cells and ECM components into diseased or injured tissues. Two basic strategies were explored: (1) membranes were prepared from blended solutions of fibroin and tropoelastin, or (2) layered constructs were prepared from sequentially cast solutions of fibroin, tropoelastin and fibroin. The retention of tropoelastin within blend and layered constructs was confirmed by

immunolabelling and Fourier-transform infrared spectroscopy (FTIR). The RPE cell response to fibroin membranes was not affected by the presence of tropoelastin. Interestingly, blend membranes displayed superior strength and elasticity when compared to the layered constructs, however, the standard fibroin membranes and the layered constructs demonstrated a Young's modulus in the range of a healthy Bruch's membrane. Further work will be required to optimise the interaction between the two proteins, however, the findings of this study support the potential use of fibroin membranes for the co-delivery of RPE cells and tropoelastin.

In the final research study (Chapter 5), a co-culture model of Ruysch's complex was developed *in vitro*, using the fibroin membranes as a substitute for Bruch's membrane. This study demonstrated that the fibroin membrane was able to act as a physical barrier between the two cell types, while facilitating communication between the mature monolayer of RPE cells and the choroidal-derived vascular endothelial cells that were seeded within a collagen type I gel. The fibroin membrane, suspended in our custom-designed culture chamber, was able to support the three-dimensional collagen gel for the entirety of the culture period and the co-culture complex could be described as being an *in vitro* representation of the subretinal architecture. Further refinement and development of this co-culture complex could provide insights into the mechanisms of interaction between the two cell types, and its use as a model of AMD disease will likely be the ultimate test of function, prior to pre-clinical trials.

The implantation of fibroin membranes into an animal model to study safety, efficacy and surgical handling will be ultimately paramount to understand the immunogenicity and degradation rate of fibroin membranes in the subretinal space. The tissue engineered complex developed in this project is in many ways comparable to Ruysch's complex, however, considerable future efforts will be required to create an implant suitable for human patients. The outcomes described in this thesis provide a foundation for the use of fibroin membranes as a Bruch's membrane substitute and offer a stepping stone for future studies in RPE transplantation.

List of Publications

The following is a list of published manuscripts that have been incorporated into this thesis.

Chapter 3

Shadforth AMA, Suzuki S, Theodoropoulos C, Richardson NA, Chirila TV, and Harkin DG (2015) A Bruch's membrane substitute fabricated from silk fibroin supports the function of retinal pigment epithelial cells in vitro.

Journal of Tissue Engineering and Regenerative Medicine,doi:10.1002/term.2089.

Chapter 4

Shadforth AMA, Suzuki S, Alzonne R, Edwards GA, Richardson NA, Chirila TV, and Harkin DG (2015) Incorporation of human recombinant tropoelastin into silk fibroin membranes with the view to repairing Bruch's membrane.

Journal of Functional Biomaterials 6: 946-62.

The following is a list of publications that are not directly related to the work performed in this thesis but were published throughout candidature.

1. Shadforth AMA, Chirila TV, Kwan ASL, Harkin DG, and Chen FK (2016) Biomaterial templates for the culture and transplantation of retinal pigment epithelial cells: a critical review. In: TV Chirila (Ed.), *Biomaterials and Regenerative Medicine in Ophthalmology* (2nd Edition). Woodhead Publishing Limited. *In press*
2. Suzuki S, Dawson RA, Chirila TV, Shadforth AMA, Hogerheyde TA, Edwards GA, and Harkin DG (2015) Treatment of Silk Fibroin with poly(ethylene glycol) for the enhancement of corneal epithelial cell growth. *Journal of Functional Biomaterials* 6: 345-66.
3. Paterson SM, Shadforth AMA, Shaw JA, Brown DH, Chirila TV, and Baker MV (2013) Improving the cellular invasion into PHEMA sponges by incorporation of the RGD peptide ligand: The use of copolymerization as a means to functionalize PHEMA sponges. *Materials Science and Engineering: C* 33: 4917-22.
4. George KA, Shadforth AMA, Chirila TV, Laurent MJ, Stephenson S-A, Edwards GA, Madden PW, Hutmacher DW, and Harkin DG (2013) Effect of the sterilization method on the properties of *Bombyx mori* silk fibroin films. *Materials Science and Engineering: C* 33: 668-74.

The following is a list of presentations and papers in refereed conference proceedings throughout candidature.

1. Shadforth AMA, Suzuki S, Theodoropoulos C, Richardson NA, Chirila TV, and Harkin DG (2015) Ultrathin silk fibroin membranes as prosthetic Bruch's membrane. The Association for Research in Vision and Ophthalmology, Asia meeting (Asia-ARVO). Yokohama, Japan. Poster presentation.
2. Shadforth AMA, Harkin DG, Chirila TV, Weiss A, Hutmacher DW, Feigl BK (2013) An in vitro 3-D cell culture model for studying pathomechanisms in AMD. The Association for Research in Vision and Ophthalmology, Annual meeting. Seattle, Washington, USA. Poster presentation.

List of Awards and Funding

- Dora Lush Biomedical Research Postgraduate Scholarship, National Health and Medical Research Council, Australian Government (2014-2015)
- Project Grant, Co-Investigator 1, Macular Disease Foundation Australia $200,000 (2014-2015)
- Madeline Lenz Eye Research Fellowship, Prevent Blindness Foundation, Queensland (2012-2013)

Keywords

Ageing, age-related macular degeneration, *Bombyx mori* silk fibroin, Bruch's membrane, cell biology, cell culture, choriocapillaris, choroid, epithelium, eye, fibroin, ophthalmology, retina, retinal pigment epithelium, silk, tissue engineering, transplantation, vasculature.

Statement of Originality

The work contained in this thesis has not been previously submitted to meet requirements for an award at this or any other higher education institution. To the best of my knowledge and belief, the thesis contains no material previously published or written by another person except where due reference is made. All research contained within this thesis was conducted by the author with the following exceptions. Dr Shuko Suzuki prepared all silk fibroin biomaterials used in this thesis and performed subsequent mechanical testing protocols.

Signature: QUT Verified Signature

Date: 5/11/15

Acknowledgements

Coming to the end of my PhD, I can't help but sit in awe of this entire process. In many ways this has been a journey of transformation and metamorphosis, with times of heartache and times of triumph. I have experienced and achieved so many personal milestones, many of which felt like I would need to scale Everest to even get close. These milestones were not just accomplished, they were conquered! None of this would have been possible without the support of many people and I hope I have been able to convey to them in person, just how much I appreciate everything they have done for me.

To my supervisors, Associate Professor Damien Harkin, Professor Traian Chirila, and Dr Neil Richardson, I thank you for your guidance and for your support. Thank you for being my teachers, for sharing your knowledge, and providing me with limitless time and energy. Damien, I don't think it is an overstatement to say, everything I am as a scientist is because of you.

To the Queensland University of Technology, I thank you for accepting my project proposal and supporting my candidature. I also thank you for an employment contract as a Postdoctoral Scientist.

To the National Health and Medical Research Council of Australia, I thank you for awarding me a Postgraduate Research Scholarship. To the Macular Disease Foundation of Australia, I thank you for the incredible work you do in raising awareness and for giving us your precious support in funding this research project.

To the Queensland Eye Institute, the QEI Board of Directors, and Professor Mark Radford, I thank you for giving me the space to perform my research, and for taking a risk and investing in me and my ideas. The QEI Research Team is made up of an incredible bunch of human beings, and I am honoured beyond words to have a place amongst that group. A special heartfelt thank you to Natalie, Shuko, Christina, Fiona, and Jenny.

To Dr Peter Woolf, thank you for looking after my eyes, for taking an interest in my studies, and for pestering your son to find me a job. That fateful morning changed my life.

To Amy, Keelan, Jonnica and Ray, Aunty Sandra and Uncle Neville, thank you for your never-ending love and support. I would not be the person I am without you.

To Mum, thank you for always believing in me. This thesis is dedicated to you.

And finally, to my husband Ashley. Thank you my darling for loving me and for sharing this wonderful life with me. Thank you for understanding my dreams, and for sometimes pushing me even higher. Every day your support is unwavering, and I thank you for every lunch you have packed, and for every minute you have sat in the car waiting for an experiment to finish, or the last sentence to be written. For every text message pep talk, for every hug, kiss, and fist pump, I thank you. I love you, and I am so very excited for the beautiful new adventure we have ahead of us.

Table of Contents

List of Abbreviations

AF	Attachment Factor
ALC	anterior lens capsule
AMD	age-related macular degeneration
ANOVA	analysis of variance
anti-VEGF	anti-vascular endothelial growth factors
ARPE-19	immortalised human RPE cell line
BSA	bovine serum albumin
CNVM	choroidal neovascular membranes
CO_2	carbon dioxide
CRALBP	cellular retinaldehyde-binding protein
ECM	extracellular matrix
EGF	epidermal growth factor
ELISA	enzyme-linked immunosorbent assay
FBS	fetal bovine serum
FGF	fibroblast growth factor
FITC	fluorescein isothiocyanate
FTIR	Fourier-transform infrared spectroscopy
HBB	HEPES binding buffer
HBSS	Hank's buffered salt solution
hESCs	human embryonic stem cells
hiPSCs	human induced pluripotent stem cells
HMDS	hexamethyldisilazane
HUVECs	human umbilical vein endothelial cells
IPE	iris pigment epithelium
LVF	laminin–vitronectin–fibronectin combination
MerTK	MER proto-oncogene tyrosine kinase
MMPs	matrix mellatoproteinases
Na^+/K^+-ATPase	sodium potassium ATPase
PBS	phosphate buffered solution
PEDF	pigment epithelium derived factor

PEO	poly(ethylene oxide)
POS	photoreceptor outer segments
QEI	Queensland Eye Institute
RCS rats	Royal College of Surgeons rats
RF6A	microvascular endothelial cell line
RPE	retinal pigment epithelium
RPE65	RPE-specific cytoplasmic isomerohydrolase
SEM	scanning electron microscopy
TCP	tissue culture plastic
TEM	transmission electron microscopy
TER	transepithelial resistance
TIMP-3	tissue inhibitor of metalloproteinase-3
VEGF	vascular endothelial growth factor
ZO-1	zona occludens-1

List of Figures

Chapter 1: Introduction

1.1 DESCRIPTION OF RESEARCH PROBLEM INVESTIGATED

Retinal degeneration, especially AMD, is a leading cause of blindness in the Western world. Patients suffer from extensive visual impairment due to degenerative change in the retina and its adjacent layers, loss of functioning cells, abnormal vascular ingrowth, and subsequent scar formation at the macula. Cell transplantation has been explored, with limited success, as a potential treatment and one of the reasons for this lack of success is the lack of a suitable substratum as support for the cells to be transplanted.

Globally, AMD is estimated to affect almost 8 million people (Gordois et al., 2012). In Australia, it is the most common (56.9%) cause of blindness (presenting visual acuity of less than 6/60) and is primarily seen in older people. It is predicted that in the coming decade the number of Australians who will have low vision or lose their sight will double to almost 1 million people (Hong et al., 2013). The direct health cost of AMD worldwide was approximately US$300 billion in 2010 (Gordois et al., 2012). Having no curative treatment for AMD means the need for resources will continue to increase with ongoing care requirements. Patients, caregivers, doctors, and society in general carry a substantial economic burden when considering the consequences of AMD (Köberlein et al., 2013). Vision loss caused by AMD can affect one or both eyes and this causes a significant impact on the emotional wellbeing of patients (Williams et al., 1998). The loss in independence, participation in society and overall quality of life, can exacerbate a functional decline in patients, resulting in depression, increased incidence of falls and injuries, and the consequential physical and financial burdens (Köberlein et al., 2013). It is estimated 3.4 million ‘healthy life years’ were lost globally due to AMD in 2010 (Gordois et al., 2012).

The use of anti-VEGF agents for treatment of the neovascular (wet) form of AMD has revolutionized the prognosis of this devastating condition. Stabilisation (even improvement) of vision is a common outcome of this therapy option. Unfortunately, anti-VEGF therapy is accompanied by a significant treatment burden; examinations, evaluations, and intravitreal injections need to be performed on a

monthly schedule for best visual outcomes (Lanzetta et al., 2013). Additionally, complications have been associated with continuous use of anti-VEGF drugs delivered by intravitreal injection. These adverse events, unrelated to the underlying ocular disease, include potentially serious intraocular bacterial infection (endophthalmitis), acute intraocular inflammation, retinal detachments and sustained elevated intraocular pressure that may require anti-glaucoma treatments (Falavarjani & Nguyen, 2013). Non-ocular haemorrhage and systemic wound-healing issues have also been reported with continuous anti-VEGF treatments (Bodnar, 2014). Moreover, anti-VEGF therapies do not address the broader pathology of AMD involving the degenerative structural changes in the outer retina.

The primary problem is that a biomaterial which mimics the native thickness and mechanical properties of Bruch's membrane, supports RPE cell function, and could be implanted and left in the subretinal space as a Bruch's membrane prosthesis is yet to be identified. The evaluation of novel biomaterials that could be used in this context for RPE transplantation is an ongoing area of research that is required for the development of a viable treatment option for a devastating disease that affects our ageing population.

1.2 DEFINITIONS AND KEY CONCEPTS

Outer retina – classification is defined by metabolic blood supply from the choroidal vasculature. Typically the outer retina is described as the photoreceptors, the retinal pigment epithelium, Bruch's membrane and the choriocapillaris.

Ruysch's complex – a historical term for the three tissue layers between the photoreceptors and the choroidal vasculature. These three layers are the retinal pigment epithelium, Bruch's membrane, and the microvascular choriocapillaris.

Retinal pigment epithelium (RPE) – a monolayer of pigmented epithelium that makes up the outermost layer of the sensory retina and supports the metabolic function of the photoreceptor cells.

Bruch's membrane – an extracellular matrix structure, rested on by the basal surface of the RPE monolayer, which acts as a molecular sieve and supports the functions of the RPE and the choriocapillaris.

Choriocapillaris – the microvascular component of the multilayered choroidal vasculature. The choriocapillaris is a fenestrated network of capillaries, not unlike

the glomerulus of the kidney, which is structurally and functionally vital to RPE and photoreceptor cell survival.

RPE transplantation – due to the important functions performed by healthy RPE in support of the photoreceptor cells of the sensory retina, and the age-related changes that occur in this pigmented monolayer, it is theorised that removing the aged RPE and replacing them with new, fresh RPE cells will halt any further photoreceptor degeneration, preventing blindness. Unfortunately, the transplantation of RPE into human patients with appropriate clinical improvements in vision has proven more complex. The current theory is that RPE cells will need to be transplanted as a functioning monolayer on a biomaterial substrate.

Bruch's membrane prosthesis – a theory proposed by Professor Susan Binder and colleagues in 2007 (Binder et al., 2007), which requires an appropriate biomaterial substrate to act as a support for the culture of RPE cells *in vitro*, as well as act as a Bruch's membrane substitute upon transplantation for as long as needed, possibly indefinitely.

1.3 OVERALL OBJECTIVES OF THE STUDY

The overall objective of the study is to evaluate fibroin as a biomaterial of choice in the development of a cultured tissue substitute, which mimics Ruysch's complex, in the context of RPE transplantation. This is a fundamental step in the development of a viable therapeutic treatment, for diseases such as AMD. The novel biomaterial evaluated in this study was derived from fibroin, the structural protein isolated from the cocoon of the *Bombyx mori* silkworm.

The scope of this research study was confined to the development and evaluation of an *in vitro* cell culture study, which used immortalised cell lines and the observation of morphological features that would be consistent with biological functioning. The evaluation of fibroin as a biomaterial in this context however, informs future studies that could use more appropriate RPE cell sources suitable for RPE transplantation (autologous human RPE, and induced pluripotent stem cell-derived RPE), as well as provides a novel contribution to the literature on the suitability of fibroin as a Bruch's membrane prosthesis.

1.4 SPECIFIC AIMS OF THE STUDY

1. To examine RPE cell functionality when grown on fibroin membranes
2. To use different methods to incorporate an elastin component in fibroin membranes
3. To co-culture RPE and choroidal-derived vascular endothelial cells either side of fibroin membrane

1.5 HYPOTHESES

1. We hypothesise that fibroin membranes will support RPE cell functionality.
2. We hypothesise that the incorporation of an elastin layer/component will improve the functionality of fibroin membranes and allow it to better mimic native Bruch's membrane.
3. We hypothesise a co-culture system will be supported by a fibroin membrane, and there will be a functional/morphological advantage to the tri-layer construct in the context of RPE transplantation.

Chapter 2: Literature Review

2.1 RUYSCH'S COMPLEX AND ITS IMPORTANCE TO VISION

Ruysch's complex is a historical term used to describe three layers of the outer retina between the photoreceptor outer segments and the choroidal vasculature (Fig. 2.1). The three layers of Ruysch's complex are the retinal pigment epithelium (RPE), Bruch's membrane, and the microvascular choriocapillaris (de Jong, 2006)

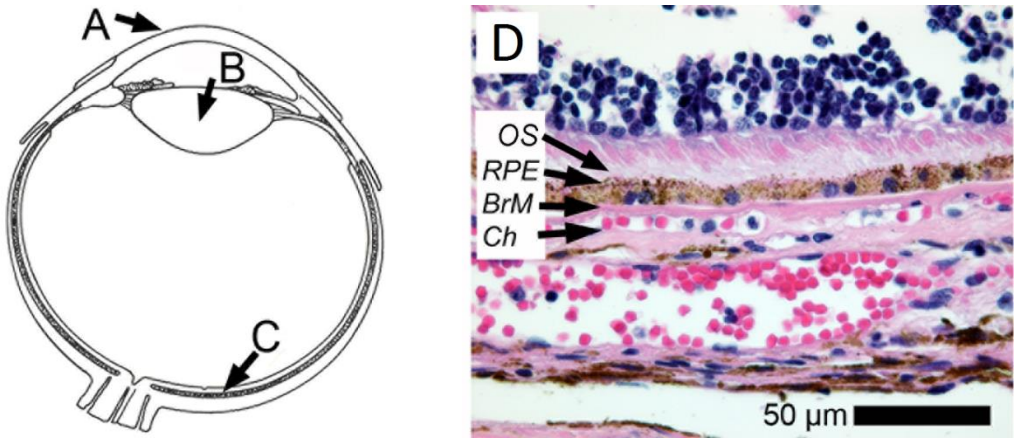

Figure 2.1. A schema of the eye demonstrates the principal refractive elements of the visual pathway, the cornea (A) and the lens (B). The retina (C) lines the internal posterior surface of the eye and contains the sensory components of the visual pathway. A histological preparation (D) reveals the proximity of the photoreceptor outer segments (OS) to the retinal pigment epithelium (RPE), and the underlying Bruch's membrane (BrM) and choriocapillaris (Ch). These three layers (RPE, BrM and Ch) are collectively named Ruysch's complex. Source: D.G. Harkin.

2.1.1 Retinal Pigment Epithelium

The RPE is a monolayer of pigmented cells derived from the neuroectodermal layer of the optic cup and constitutes the outermost layer of the sensory retina. The metabolic activities of the RPE are vital for the local homeostasis and maintenance of the overlying photoreceptors and the underlying blood supply, the choroidal vasculature. The unique and specialised functions performed by the RPE (Fig. 2.2), include the directional transport of nutrients and waste, daily phagocytosis of shed photoreceptor outer segments, regeneration of the Vitamin A-based chromophore required in the visual cycle, and polarised secretion of growth factors (Strauss, 2005).

The RPE cell exhibits an apical–basal polarity characteristic of a transporting epithelium, with apical tight junctions binding neighbouring RPE cells together to form the outer blood-retinal barrier (Rizzolo, 1997). This barrier induces transcellular transport and in conjunction with asymmetrical membrane protein distribution, allows directional transport of glucose, retinol (Vitamin A) and fatty acids to the photoreceptors. Equally important, this active transport process removes ions, metabolic waste products and water from the subretinal space (Strauss, 2005). The removal of water from the subretinal space is vital for photoreceptor health (Marmor, 1998). Furthermore, the highly folded basal membrane of the RPE helps to increase the surface area required for absorption and secretion.

The RPE cells extend apical microvilli into the subretinal space and ensheathe the photoreceptor outer segments. The apically localised transmembrane integrin, αVβ5, mediates retinal adhesion and promotes circadian-controlled phagocytosis of shed outer segments (Nandrot et al., 2006). Once engulfed, the segments are broken down by lysosomal activity within the RPE cell. This process is integral to the visual cycle, allowing the regeneration of the Vitamin A-based chromophore, trans-retinol, using the RPE-specific cytoplasmic isomerohydrolase, RPE-65 (Strauss, 2005). The chromophore, oxidised to 11-cis-retinal, is bound to the cellular retinaldehyde-binding protein (CRALBP), before being released by the RPE cell to be taken up by the photoreceptors. Mutations in the phagocytic signalling protein MER proto-oncogene tyrosine kinase, commonly referred to as MerTK, the cytoplasmic isomerase RPE-65, or the binding protein CRALBP induce significant pathology of the photoreceptors, as seen in retinitis pigmentosa (Travis et al., 2007).

Interestingly, geographical differences can be seen in RPE cells. In the macula, for example, RPE cells are small and tightly packed (14 μm × 12 μm/cell). By contrast, peripheral RPE cells, are relatively larger (60 μm/cell) and variable in height (Strauss, 2005; Harman et al., 1997; Panda-Jones et al., 1996). As the RPE cells in the macula are densely packed, the area appears darker (Feeney-Burns et al., 1984). The melanin granules within the RPE cytoplasm help to absorb radiant energy focused by the lens onto the retina, which is beneficial to visual acuity by preventing light reflection and dispersed light from interfering with the signal received by the photoreceptors (Boulton, 1998). The intense heat generated in this area is dissipated by the choroidal perfusion. It has also been shown that RPE cells of the macula

demonstrate higher degradation enzyme activities allowing for the maintenance of greater numbers of macular photoreceptors compared with RPE cells in the peripheral retina (Strauss, 2005).

Photoreceptor and vasculature health is maintained by polarized secretion of various trophic factors by the RPE. In particular, the secretion of vascular endothelial growth factor (VEGF) and pigment epithelium derived factor (PEDF) by the RPE has been implicated in the maintenance of photoreceptor health, immune privilege and the integrity of the surrounding vasculature (Kay et al., 2013; Strauss, 2005).

2.1.2 Bruch's membrane

The highly folded basal membrane of the RPE rests on Bruch's membrane, a collagen- and elastin-rich extracellular matrix structure (Booij et al., 2010). Stacked linear elastin fibers form a perforated sheet that is interposed between grid-like layers of collagen. The basement membranes of the RPE cells and the choriocapillaris endothelium basement membrane complete the pentalaminar structure (Marshall et al., 1998).

Bruch's membrane acts in support of the outer blood-retinal barrier, as a semi-permeable sieve. The organisation of each fibrous layer forms an arrangement of pores (Marshall et al., 1998). Movement through Bruch's membrane is primarily passive and molecules less than 70 kDa in size are able to diffuse freely (Booij et al., 2010). As stated earlier, photoreceptor health relies on the apical to basal removal of water from the subretinal space by the RPE, returning it to the general circulation. The unobstructed movement of nutrients, water and waste products through Bruch's membrane is vital for retinal health (Marshall et al., 1998).

Located between the RPE and its blood supply, Bruch's membrane is under pressure-induced stress oscillating with cardiac rhythm (Bonilha, 2008). It has been suggested that the central layer of elastin in Bruch's membrane, may act as a dampener to the pulsations of the choroidal vasculature that could potentially disrupt the RPE and photoreceptor outer segments (Leure-duPree, 1968). There is debate as to the origin of Bruch's membrane during development. The RPE and choroid are capable of synthesizing most of the extracellular components (Booij et al., 2010; Campochiaro et al., 1986); however the source of the elastin layer is still a matter for investigation (Strauss, 2005).

2.1.3 Choriocapillaris

The vascular structure that directly underlies Bruch's membrane is called the choriocapillaris. It is the innermost layer of the choroidal vasculature and is the metabolic blood supply of the RPE and photoreceptors (Strauss, 2005). The choriocapillaris is a network of continuous capillaries arranged in fan-shaped or triangular lobules that create a mosaic pattern enface to Bruch's membrane (H. R. Zhang, 1994). The structural integrity of the choriocapillaris, including the formation of fenestrations on the RPE side of the vascular endothelial cells, is maintained directly by growth factors secreted by the RPE (Kay et al., 2013). The vascular anatomy of this dense capillary network, especially at the posterior pole, forms a segmental blood supply that can support large quantities of blood at a high flow rate (H. R. Zhang, 1994). The choriocapillaris is often compared to the glomerular capillaries of the kidney, however the choriocapillaris has a blood flow 4 times higher than the kidney, and 28 times higher than the brain (Boron & Boulpaep, 2009; Strauss, 2005). Consequently, the subretinal area is an extremely oxygen-rich environment.

2.2 AGE-RELATED CHANGES AND THE INFLUENCE ON VISION HEALTH

Structural changes occur in Ruysch's complex with age. These changes include the accumulation of debris within the cytoplasm of the RPE cell, as well as deposition of sub-RPE deposits. There is also a breakdown in the barrier and transport capacity of Bruch's membrane and a reduction in the density and integrity of the choriocapillaris (de Jong, 2006). Human RPE cells display limited mitotic activity from two years of age, and degenerative changes tend to accumulate with age. Age-related changes can typically be seen in RPE cells with the atrophy of apical microvilli, disorganization of basal infoldings, the disappearance of melanin granules, and partially digested residues begin to clog the cytoplasm (Bonilha, 2008).

One particularly obvious age-related change within the RPE is the accumulation of lipofuscin. Lipofuscin is a heterogeneous material with a prominent yellow-brown pigment and is commonly known as the 'age pigment' as it typically accumulates throughout the body with age (Feeney, 1978). In the RPE, lipofuscin originates from the incomplete lysosomal digestion of phagocytosed photoreceptor outer segments. The resulting oxidised lipid residues start to accumulate in the basal

side of the RPE cells and can fill the entire cytoplasm by the 5th decade (Binder et al., 2007). As the cytoplasm becomes engorged, oxidative stress within the cell begins to appear (Bonilha, 2008). The visible light spectrum and the local oxygen-rich environment are able to generate reactive oxygen intermediates from these oxidized residues which can further inactivate the lysosomal and antioxidant enzymes within the cytoplasm (Wassell et al., 1999). This magnifies intracellular oxidative stress, forming a chronic feedback loop. The main lipofuscin flurophore A2E, can have phototoxic and detergent properties on membrane bound organelles and has been shown to induce apoptosis within cultured cells (Wassell et al., 1999)

With increasing age, Bruch's membrane thickens, calcifies and demonstrates an accumulation of oxidised waste products derived from RPE metabolism. Overall, these age-related changes have a negative effect on its' structural integrity and ability to facilitate fluid movement (Booij et al., 2010). In young eyes, the three fibrous layers (inner collagenous, elastin and outer collagenous) allow for maximum diffusion of nutrients and oxygen. As we reach our late thirties, there is an accumulation of debris and collagen crosslinking within Bruch's membrane which causes a reduction in effective pore size and a decrease in flow through the layers (Marshall et al., 1998). Elastolysis is a normal physiological process seen in ageing (Vrhovski & Weiss, 1998), and a 1 % decrease in elasticity of Bruch's membrane every year from the age of 21 has been demonstrated (Ugarte et al., 2006). The decrease in flexibility of the membrane can lead to brittleness and cracks (Bonilha, 2008). In later life, an increasing presence of hydrophobic lipids, arranged in the inner collagenous layer, known as 'the lipid wall', can severely reduce the water transport capacity through Bruch's membrane. This triggers further deterioration in transport capacity, inducing the deposition of basal laminar deposits below the RPE and along Bruch's membrane (Guymer et al., 1998).

Consistent with a thickening of Bruch's membrane with age (2 µm to 4.7 µm), there is a reduction in capillary lumen diameter from 9.8 µm to 6.5 µm (Ramrattan et al., 1994). There is also a 45 % decrease in the density of the choriocapillaris from the first decade of life to the tenth. The changes in this vasculature structure are thought to be caused by the impeded movement of trophic factors secreted by the RPE (Bonilha, 2008), and atrophy of the choriocapillaris (and the reduced blood supply) further disrupts the balance of growth factors secreted by the RPE (Bhutto &

Lutty, 2012). The age-related changes in Bruch's membrane also involve a disruption to extracellular matrix turnover. This can include an up-regulation in the expression and activation of extracellular matrix mellatoproteinases (MMPs), which have been shown to stimulate pathological angiogenesis (Hollburn et al., 2007). The degradation products of elastolysis alone have been shown to cause vasodilation, cellular migration and inflammation, especially in tissue that has already been damaged (Vrhovski & Weiss, 1998).

Conversely, changes to the corresponding enzyme inhibitors, especially the tissue inhibitor of metalloproteinase-3 (TIMP-3), may also have important clinical implications. TIMP-3 is unique among TIMPs as it is a normal component of the Bruch's membrane matrix structure (Fariss et al., 1997) and an accumulation of TIMP-3 within Bruch's membrane is considered a normal aging process (Kamei & Hollyfield, 1999). TIMP-3 can also bind to, and be stimulated by the extracellular glycoprotein, fibulin-3, which is another important component of Bruch's membrane. The regulatory roles of these molecules are not yet clear (Klenotic et al., 2004; Zhang & Marmorstein, 2010). However, the influence of these structural changes is highlighted when considering hereditary conditions when premature ageing of Bruch's membrane causes a similar presentation to AMD, but at a younger age, as seen in Sorsby fundus dystrophy (TIMP-3 mutation) and Malattia Leventinese, also known as Doyne honeycomb retinal dystrophy (EFEMP1/fibulin-3 mutation) (Nita et al., 2014; Sivaprasad et al., 2008). Age-related deterioration of the RPE, Bruch's membrane and the choriocapillaris can be a potential trigger for the onset of disease processes, such as AMD.

2.3 AGE-RELATED MACULAR DEGENERATION

The progression to advanced AMD pathology is a complex series of events that involve significant changes in Ruysch's complex. Two types of advanced AMD have been identified: dry and wet (de Jong, 2006). Dry AMD (the advanced form is also called geographic atrophy) is characterized by a confluent area of photoreceptor, RPE cell and choriocapillaris atrophies, which can lead to degeneration of the overlying neurosensory retina. Neovascular or wet AMD is characterised by choroidal neovascularisation that spreads apically through breaks in Bruch's membrane, the RPE monolayer, and into the sub- and intra-retinal spaces. This pathologic vascularisation starts as capillary-like vessels that are often

underdeveloped, leaky and can cause haemorrhagic detachments of the RPE and neurosensory retina that leads to disciform scarring (de Jong, 2006).

The aetiology of AMD is multi-factorial – including physiological ageing, genetic, inflammatory, and environmental factors. A key feature of early AMD pathology is the appearance of drusen. It has been suggested that drusen is the accumulation of lipofuscin and extracellular deposits beneath the RPE and within Bruch's membrane, the presence of which can further exacerbate the formation of drusen (Marshall et al., 1998). Although drusen can be present without a progression to disease, there is higher risk for progression to an advanced AMD pathology once its presence can be detected by the naked eye, especially once areas of soft indistinct drusen appear (de Jong, 2006). More recently, reticular pseudodrusen has also been recognised as an important predictor of AMD progression. These are focal deposits within the subretinal space and contain similar molecules to those observed in sub-RPE drusen. They are associated with atrophy of the outer retina, thinning of the choroid in the macular region, and geographic atrophy progression (Curcio et al., 2013; Curcio et al., 2005).

Different potential therapies for AMD treatment have been trialled including: dietary supplementation with vitamins and antioxidants; laser treatment with or without photosensitizing dye; submacular membranectomy with or without RPE transplantation or translocation; macular translocation surgery; radiotherapy; gene therapy; and pharmacological treatment (e.g. angiostatic steroid and anti-VEGF therapy) (Binder et al., 2007). Currently, anti-VEGF therapies are the most promising treatment and can improve and/or stabilize neovascular AMD when used on a monthly schedule (Lanzetta et al., 2013). However, a much larger proportion of AMD sufferers develop dry AMD for which no established treatment is available. Theoretically, restoration of visual function with anti-VEGF treatment relies on neovascularisation being the only pathology, specifically, the RPE cells and Bruch's membrane are still functioning and photoreceptors have not begun to degenerate (Thumann & Walter, 2008). As it is highly unlikely neovascularisation is the only pathology in patients who require anti-vascular therapies, a surgical intervention that replaces the damaged RPE cells, Bruch's membrane and choriocapillaris, thereby restoring the outer blood-retinal barrier, may still be the best curative approach for both types of advanced AMD.

2.4 RPE TRANSPLANTATION

Seminal experiments using Royal College of Surgeons (RCS) rats (Li & Turner, 1988) demonstrated that the inherited retinal degeneration that manifests in this animal model (a mutation prevents the RPE from phagocytosing shed photoreceptor outer segments) could be prevented by RPE cell transplantation. This form of retinal degeneration is seen in humans as a subtype of retinitis pigmentosa (Gal et al., 2000). After the first human submacular surgery to remove diseased tissue was performed by de Juan and Machemer (1988), surgical intervention for human AMD patients began to focus on the same transplantation principle (i. e., replace diseased RPE cells with healthy cells before photoreceptor degeneration could progress or even occur).

Extending upon the investigations of de Juan and Machemer (1998), Peyman et al., (1991) performed the first RPE transplantations in humans, whereby submacular scar excisions in two patients were followed by translocation of an autologous RPE pedicle flap or transplantation of an allogeneic adult RPE–Bruch's membrane-choroidal tissue explant. Both techniques involved significant surgical skill and surgical trauma. Unfortunately in this study, surgical trauma caused the ultimate failure for the pedicle flap technique, and allogeneic rejection caused failure of the explant technique. This attempt was followed by trials of transplantation of foetal human RPE patches (Algvere et al., 1994, 1999) after the removal of a subretinal membrane commonly identified as choroidal neovascular membranes (CNVM). These patients were able to fixate over the area of the RPE graft initially, but cystoid macular oedema ensued and eventually the grafts were encapsulated by fibrotic scars, which might be a result of immune rejection as none of the patients were immunologically suppressed.

The iris pigment epithelium (IPE) has been proposed as an autologous source of pigmented cells. IPE share the same embryonic origin as the RPE and possess similar morphological features such as pigmentation and tight junctions (Thumann et al., 1999, 2000). A simple biopsy can harvest sufficient cells for transplantation and they have been shown to acquire RPE-like morphology when injected into the subretinal space of rabbits and RCS rats (Thumann et al., 1999). However, transplantation of suspensions of autologous IPE cells has not resulted in a prolonged improvement of vision in AMD patients (Thumann et al., 2000). It was suggested

that this failure may have occurred because the transplanted IPE cells did not fully differentiate into cells that had the morphological and physiological properties of RPE cells *in situ*. Transplanted suspensions of autologous RPE cells have been reported to confer some improvement in eyes with wet type AMD after removal of CNVM (Binder et al., 2002). These eyes had significantly better reading acuity than the controls where only CNVM was removed. However, obtaining sufficient numbers of RPE cells was sometimes difficult, and in some patients the aspirated RPE cells were not transplanted because of insufficient numbers or haemorrhage.

In most of these studies, suspensions of isolated cells were injected into the subretinal space. Pivotal experiments by Tezel and Del Priore (1997) showed that RPE cells are anchorage-dependent and must re-attach to a substrate to prevent the initiation of apoptosis. The development of an RPE monolayer with proper cell polarity and function can only occur once re-attachment is successful. The significant structural and functional changes that occur within Bruch's membrane with age can have a profound and detrimental effect on RPE attachment, monolayer establishment and transplant survival (Sugino et al., 2011; Tezel et al., 1999; Tezel & Del Priore, 1999). Crafoord et al., (2002) confirmed this in their studies, finding that the photoreceptor cells survived well when transplanted IPE cells established into a monolayer, but the photoreceptors did not survive when the transplanted cells clustered into a mound-like shape. Moreover, RPE cells in suspension may not settle in the subretinal space but instead migrate into the vitreous cavity, whereby they become fibroblastic in nature and produce a contractile extracellular matrix, which can eventually contract in the form of epiretinal membrane or proliferative vitreoretinopathy (Hiscott & Sheridan, 1998; Pastor et al., 2002). These may result in macular pucker and retinal detachment, which will have a detrimental effect on the visual outcome.

Two surgical techniques to reconstitute submacular RPE (macular translocation and autologous RPE–Bruch's membrane–choroid transplantation) have been refined and used to restore foveal photoreceptor contact to an area of relatively healthy, albeit ageing RPE. The techniques have met with some success (patients have experienced a gain in visual acuity after surgery) and serve as a proof of the principle that some photoreceptor function can be restored in AMD (Van Zeeburg et al., 2012; Chen et al., 2009). Despite these encouraging results, the age of the patient (and their

cells) remains as an inhibiting factor for a reliable and reproducible treatment. The pre-operative viability of the photoreceptors and the state of disease advancement in the RPE cells has been previously suggested as the best predication for the progression of natural history of AMD irrespective of which therapy may be used (da Cruz et al., 2007). Therefore the precise timing of intervention is imperative. Essentially a therapy for AMD needs to be performed at earlier stages of degeneration so there is a better chance of preservation and restoration of function without untoward effects on the patient (Gouras, 1998). It is considered that a pre-made patch, which has a functioning monolayer of RPE cells and a Bruch's membrane substitute, will simplify the surgical technique and thus potentially, reduce complication rate. The identification of new sources of human RPE cells and exploring the option of custom-creating a healthy Bruch's membrane are two areas receiving increased attention.

2.5 PLURIPOTENT STEM CELLS AND THE RPE

A new field of cell biology emerged in 2007 when Shinya Yamanaka announced that human induced pluripotent stem cells (hiPSCs) had been derived from adult human fibroblasts (Takahashi et al., 2007). This seminal publication followed the isolation of the original pluripotent cells, human embryonic stem cells (hESCs), by James Thomson in 1998 (Thomson et al., 1998). As hiPSCs do not carry the ethical and moral oppositions that surround the use of human embryos, Yamanaka's discovery, confirmed concurrently by Thomson's group (Yu et al., 2007), was even more exciting. The existence of human pluripotent stem cells, either of an embryonic or induced (adult) origin, swiftly and permanently changed the future direction of biomedical research. A substantial amount of research has been conducted exploring the potential of pluripotent stem cells for modeling and treatment of human disease (Tabar & Studer, 2014).

Despite the initial widespread enthusiasm for this stem cell technology its appeal is somewhat reduced when the sophisticated biology of pluripotent stem cells and the complex technical issues related to the use of the cells is considered (Hayden, 2011). For example, a problem associated with the use of embryonic stem cells is the allogeneic source. As a consequence, it is highly likely that immunosuppression will be required for patients receiving differentiated hESCs as cell therapy. Traditionally, immunosuppressant treatment requires lifelong administration and significant

systemic health burdens. This required treatment is compounded by the continuing issue of teratoma formation by incomplete differentiation of embryonic stem cells (Wang et al., 2010). It may be possible to interrupt specific pathways of T-cell activation for an interim period of time after the implantation of an allogeneic hESC-derived graft, however these methods are yet to be optimised and evaluated in humans (Pearl et al., 2011; Rong et al., 2014). Reprogramming, the generation of hiPSCs from somatic cells, is a highly inconsistent process, and the best (high yield) protocol is yet to be completely defined (Borooah et al., 2013). Specific impediments to the translation of therapeutic stem cell technology include variation in differentiation potential between donor cell types (i.e. from a blood sample, skin biopsy), harnessing the signalling pathways that influence directed differentiation (converting the hESC or hiPSC to the desired cell fate) to adult-like physiology, optimising conditions for three-dimensional cytoarchitecture, a high incidence of mutational changes in differentiated cells, and the non-erasure of epigenetic memory of the donor cell source (Melville et al., 2013; Tabar & Studer, 2014). The utility of human pluripotent stem cells lies with their potential to differentiate into virtually any cell type. Protocols for generating differentiated cells from pluripotent stem cells follow two distinct paths, each with specific benefits and considerations. The first protocol type involves adherent cultures with growth factors being included and excluded from the culture medium at different time points; the second protocol utilizes suspension cultures able to generate embryoid bodies, and subsequent adherent culture time. Both protocol types involve selective isolation and manual dissection of the cells of choice, and extended culture time frames (Rowland et al., 2012). The distinctive pigmentation of RPE cells allows, with relative ease, the identification, dissection, culture and expansion of this cell type (Gamm et al., 2013). Consequently, RPE cells generated from pluripotent stem cells are being pursued with fervent interest.

The potential impact of pluripotent stem cell-derived RPE cells can be seen in the fields of regenerative medicine, pathology research and drug development studies. Currently, both hESC-RPE and hiPSC-RPE are being evaluated for use in the treatment of AMD. Trials are currently underway, (Phase I/II Clinical Trial; #NCT01344993) evaluating the safety and tolerability of a subretinal injection of hESC-RPE in patients with advanced dry AMD. After 4 months, ophthalmic examination indicated that the injection was well tolerated with cells attaching and

persisting throughout the trial period (Schwartz et al., 2012). Furthermore, the medium term (22 months) safety outcome was encouraging, with no development of uncontrolled proliferation, rejection or serious systemic adverse reaction (Schwartz et al., 2014). It is yet to be seen if an injection of hESC-RPE cells into the subretinal space will provide any functional improvement in humans.

The therapeutic value of monolayers of hESC-RPE cells grown on thin submicron membranes made from Parylene C, a synthetic polymer that has been used as a barrier coating on circuit boards and implantable medical devices, is currently being investigated in a collaborative program between the University of Southern California and the Doheny Eye Institute (Diniz et al., 2013; Ribeiro et al., 2013; Hu et al., 2012; Lu et al., 2012;). In particular, the feasibility of implanting this biomaterial substratum into the subretinal space of the RCS rat has been investigated (Hu et al., 2012) and the long-term survival of the implanted cells (up to 8 months) has been observed (Ribeiro et al., 2013). The group is yet to report a functional improvement in RCS rat visual function as a result of this implant, and how these results might translate into a human AMD patient.

Masayo Takahashi from RIKEN Center for Developmental Biology in Kobe, Japan is currently undertaking the first clinical study using hiPSCs in human patients (RIKEN Press Release, July 30, 2013). It is intended to establish hiPSC-RPE from six patients who have wet AMD, utilizing a collagen type I gel to create cell sheet monolayers (Kamao et al., 2014). The hiPSC-RPE cell sheets will be used as a graft and transplanted into the affected site of a single eye for each patient (after the CNVM is stabilised with a course of anti-VEGF drug, Ranibizumab, injections). The group have reported successful surgery for the first patient (Cyranoski, 2014). Functional integration and adverse reactions will be monitored over a three-year period. The significance of this clinical study, to researchers and AMD patients alike, cannot be overstated. The outcomes of this study will provide insight into the effectiveness of transplanting a sheet of RPE without reconstructing Bruch's membrane in treating advanced AMD. More broadly speaking, this study and the corresponding regulatory changes that have been made at government level will influence every aspect of hiPSC technology moving forward and is being closely watched by the scientific community (Reardon & Cyranoski, 2014).

2.6 BIOMATERIALS FOR RPE TRANSPLANTATION

Any biomaterial considered as a potential replacement for Bruch's membrane must fulfil a range of specific structural and functional criteria. For example, it will need to be supportive of cell attachment and differentiation, structurally thin yet surgically robust enough to be introduced into the subretinal space. The substitute will need to be biocompatible and immunologically inert with a controllable rate of biodegradation (Wang et al., 2006). Permeability of the biomaterial and a water transport capacity comparable to a young Bruch's membrane will be vital to prevent pooling at the RPE-substrate interface (da Cruz et al., 2007). Biomaterials that could be used as a potential substitute for Bruch's membrane and their capacity to support cell attachment and correct cell phenotype development have been explored and extensively reviewed a number of times (Binder, 2011; Hynes & Lavik, 2010). Some substrates (i.e. films and membranes) could support the delivery of the cell monolayer during surgery, whereas other substrates would need to be removed prior to monolayer transplantation (thermoresponsive polymers and gelatin). So far, there has not been a substrate that has all the necessary requirements.

An important consideration when selecting a biomaterial for this area is whether the transplanted RPE would eventually need to re-attach and/or interact with the aged Bruch's membrane. For example, will the biomaterial degrade quickly, exposing the transplanted cells to an aged Bruch's membrane? If the biomaterial will not expose the transplanted RPE cells to the aged Bruch's membrane, is it an appropriate addition to the subretinal environment? The thickness and permeability of biomaterials that have been tested for RPE cell attachment (and differentiation in some studies) to this point are often incompatible for implantation into the subretinal space.

Out of the multitude of studies that have evaluated potential substitutes for Bruch's membrane, only four have used differentiated RPE cultures and implanted them into animal models. The materials that have been used include collagen type I in cross-linked and uncross-linked forms (Bhatt et al., 1994), anterior lens capsule (Nicolini et al., 2000), the synthetic polymer called parylene C (Diniz et al., 2013) and commercial polyester membranes (Stanzel et al., 2014). Only one group used an animal cell source (Nicolini et al., 2000) that matched the animal host, the other groups used human cell sources (embryonic-derived RPE, fetal RPE and adult RPE

stem cells). The animal models used to test the safety, tolerability and survival of the implants included rabbits (Bhatt et al., 1994; Stanzel et al., 2014), pigs (Nicolini et al., 2000) and immuno-compromised nude rats (Diniz et al., 2013).

Bhatt et al (1994), showed great theory when designing their study. They hypothesised it would be better to implant a monolayer of RPE cells, they also removed the host RPE cells before implanting the RPE-biomaterial complex, and they used a material with a biological origin which would most likely degrade without potentially harmful by-products. They found the un-crosslinked collagen type I substratum was flexible and conformed to the surface of the host's intact Bruch's membrane. Little evidence of the uncross-linked collagen substrate was seen 6 weeks after surgery, however the retinal layers above the implant (identified by the pigmented cells that had been implanted into the unpigmented rabbit model) appeared normal. In contrast, the cross-linked collagen substratum did not degrade over the post-surgery monitoring time period, and there was obvious damage to the retinal layers above the implant. The authors suggested that by crosslinking the collagen, it may have condensed the structure and reduced the diffusion capability between the choroid and the photoreceptors. Similar to the uncross-linked collagen substrata, anterior lens capsule (ALC) was also well tolerated within the subretinal space (Nicolini et al., 2000). Unfortunately due to the elastic membrane-like nature of the ALC, it curled upon implantation in the subretinal space. The donor RPE cells were still attached to the ALC and were present at 2 weeks post-surgery however as they were curled up inside the ALC they were not presented to the photoreceptors. The authors recommended that the ALC would need to be structurally modified before it could be used as a viable Bruch's membrane substitute.

The most recent investigations have used synthetic materials, parylene C (Diniz et al., 2013) and polyester membranes (Stanzel et al., 2014). Both studies resulted in damage to the overlying retinal layers (presumably caused by a disruption to photoreceptor-choroid nutrient and waste transfer), however they were able to show survival of the implanted RPE cells on the synthetic substrata in the subretinal space. Diniz et al (2013) showed a monolayer of RPE cells survived better than a suspension of RPE cells injected into the subretinal space. They also confirmed differentiation of their embryonically-derived RPE cells by evaluating them in an immune-compromised nude rat model and no teratoma formation was observed.

Stanzel et al (2014) were the first to implant human adult RPE stem cells into an animal model, and the cells survived and kept their differentiated morphology and survived in the subretinal space over the monitoring period. Further work by this group is focussed on using a more porous substratum that will support native (more appropriate) nutrient and waste exchange.

2.7 SILK FIBROIN

There is much interest in using silk as a biomaterial (Gil et al., 2013; Harkin et al., 2011; Wenk et al., 2011; Murphy & Kaplan, 2009; Hakimi et al., 2007; Vepari & Kaplan, 2007; Wang et al., 2006; Altman et al., 2003;). Silk proteins belong to the family of fibrous proteins, which also includes collagens, elastins, and myosins, and already have a long history of use as a surgical suture material. There is an enormous range of silks, which are produced predominantly by the larvae of insects from the order Lepidoptera (i. e., moths and butterflies) and by spiders (Araneae) (Chirila et al., 2008).

Silkworm silk is a high molecular-weight polypeptide composite made up of two fibroin proteins; a light chain (25 kDa) and a heavy chain (325 kDa), joined together in a 1:1 ratio with a single disulphide bond. A sericin coat, made up of glue-like proteins, encases these core fibers (10-25 μm diameter) holding them together and forming the cocoon case (Chirila et al., 2008; Vepari & Kaplan, 2007; Altman et al., 2003). Historically there have been incidences of adverse tissue reaction linked to the sericin coat when silkworm silk is used in raw form, however, new protocols for the purification of fibroin, have eliminated this contamination and confirmed biocompatibility *in vitro* and *in vivo* (Meinel et al., 2005; Altman et al., 2003).

Due to its versatility and remarkable mechanical properties, regenerated aqueous solutions of *Bombyx mori* silk fibroin have been used to form a variety of biomaterials including films, sponges and electrospun mats (Chirila et al., 2008; Vepari & Kaplan, 2007). The primary structure of fibroin has significant homogeneity (highly repetitive amino acid sequence) and its secondary structure is composed of highly organised β-sheets. This arrangement is the basis of the material's high tensile strength (Wang et al., 2006; Altman et al., 2003). The structural stabilisation of biomaterials made using regenerated fibroin solution can be controlled by inducing β-sheet crystallinity using a temperature-controlled water

vapour annealing process (Hu et al., 2011). Fibroin is degradable, biocompatible and chemically modifiable (Vepari & Kaplan, 2007; Meinel et al., 2005).

2.8 SILK FIBROIN AND RPE

Membranes fabricated from silk fibroin, have been assessed and evaluated as a template for growing monolayers of RPE cells *in vitro*, and shows potential as a Bruch's membrane substitute. In a pilot study by our group (Kwan et al., 2010) fibroin was investigated as a substratum for RPE cultures both alone or coated with a selection of ECM proteins, in the presence or absence of serum. Using a human RPE cell line, ARPE-19 cells were seeded onto tissue culture plastic (TCP), fibroin membrane alone, or fibroin membranes coated with laminin, vitronectin, fibronectin, a laminin–vitronectin–fibronectin combination (LVF), or collagen type IV. Samples were cultured in media containing fetal bovine serum (FBS) for 72 hours, then fixed and stained with nuclear stain Hoechst, after which cells attached were counted. Experiments were repeated with serum-starved ARPE-19 cells, which were seeded on to the different substrata, and cultured under serum-free conditions for 24 hours. The results showed that ARPE-19 cell growth on the fibroin membrane was not significantly different ($p < 0.05$) to that observed using TCP and FBS-containing culture conditions. The ARPE-19 cell count on the fibroin membrane alone in serum-free culture conditions was 50% of that on standard TCP in FBS ($p = 0.01$). However, the cell counts on fibroin membranes coated with ECM proteins surpassed unmodified fibroin membrane alone (vitronectin > collagen IV > fibronectin > LVF > laminin). Furthermore, cell attachment on fibroin membranes coated with vitronectin or collagen IV in serum-free conditions was found to be comparable with that seen in medium containing FBS on TCP.

Following this preliminary study the attachment, growth and morphology of human RPE cells grown on membranes prepared from fibroin were assessed (Shadforth et al., 2012). Fibroin membranes measuring only a few microns in thickness that had been rendered porous by casting fibroin in the presence of low concentrations of poly(ethylene oxide) (PEO) were utilised. In considering the importance of nutrient/waste exchange *in vivo*, it was considered at the time to be the best representation of a prosthetic Bruch's membrane based on fibroin. Permeability of the membranes was evaluated using a horizontal diffusion cell and three model molecules (with molecular weights between 0.4 and 70 kDa) and were found to be 4-

fold more permeable than native Bruch's membrane. We conducted a morphological assessment of long-term ARPE-19 cultures (2 months) which resulted in the partial formation of tight junctional complexes (expected of ARPE-19 cells, assessed using ZO-1 immunocytochemistry) and extension of microvilli from the apical surface (visualised by electron microscopy). The feasibility of establishing primary cultures of adult human RPE cells on fibroin compared with conventional TCP was also evaluated. Primary adult RPE cultures established at a slower rate on fibroin, when compared to TCP, nevertheless they formed morphologically correct cultures and tight junctional complexes. Considering these encouraging results, fibroin membranes warrant further investigation as a Bruch's membrane substitute.

Strikingly, when biomaterial substrates are being tested and evaluated as a Bruch's membrane substitute, the adoption of correct cell morphology is most often the only "test" done on RPE cell cultures. Cells may have the correct morphology; however this does not confirm their functionality. A complete functional assessment of the RPE monolayer grown on fibroin membranes is needed to confirm it is capable of performing the vital functions required of a fully functional *in vivo* monolayer. Several groups have developed and performed functional tests on human adult RPE, human fetal RPE and RPE cells derived pluripotent stem cells (embryonic or induced adult origin) to confirm they have acquired RPE functions (Stanzel et al., 2014; Blenkinsop et al., 2013; Salero et al., 2012; Kokkinaki et al., 2011; Sonoda et al., 2009; Maminishkis et al., 2006). Considering the functional requirements of an *in vivo* RPE monolayer, *in vitro* testing of RPE cultures grown on fibroin membranes could include testing barrier function formation, visualising the polarisation of metabolic proteins, quantifying polarised growth factor secretion, and testing the selective phagocytic ability of the transmembrane integrin, αVβ5.

A major consideration in developing any biomaterial substitute for Bruch's membrane is to determine the necessity of including elastin in the formulation. As described previously, the native Bruch's membrane contains a central core of elastin. It has been reported that the elasticity of this membrane decreases with age leading to the appearance of breaks (Ugarte et al., 2006). As a consequence, there is a strong rationale to determine if the properties of a potential Bruch's membrane substitute can be improved with the incorporation of elastin. Elasticity is typically imparted to tissue by a process of elastic fiber assembly (Kozel et al., 2004). The elastic fiber

assembly, arranges elastin (secreted from cells as tropoelastin and converted by lysyl oxidase) with microfibrils to form elastin fibers. RPE cells have been shown to produce both microfibrils and lysyl oxidase (Wachi et al., 2005), so by incorporating the elastin precursor tropoelastin in the delivery substrate with new RPE cells, it may encourage a permanent Bruch's membrane template to be formed *in vivo*. Combined solutions of fibroin and recombinant human tropoelastin have been studied previously (Hu et al., 2011; Hu et al., 2010) and the resultant blended biomaterial membrane exhibited improved strength and elasticity, and was shown to support the attachment and proliferation of human mesenchymal stem cells.

2.9 INCORPORATING A VASCULAR COMPONENT

Creating a fully functional *in vitro* RPE-Bruch's membrane complex will be an important advance in developing an appropriate replacement for the diseased RPE and Bruch's membrane seen with age *in vivo*. However it is still missing an important subretinal structure, the choriocapillaris. It has been suggested that a layer of vascular endothelial cells should be added to the basal side of an RPE-Bruch's membrane transplant, creating an "ultimate bioprosthesis" (Binder et al., 2007). The vascular endothelial cells of this tri-layered complex may improve anchorage within the host vasculature upon transplantation and assist in re-establishing blood supply.

A simple trilayer model of this complex was established and described by Hamilton et al (2007). This *in vitro* model used ARPE-19 cells, denuded human amniotic membrane and human umbilical vein endothelial cells (HUVECs) to replicate the three *in vivo* layers. Results from this group show their trilayer culture is a promising model; however, the use of amnion and HUVECs pose several problems. Amnion, like any allogenically derived material, could be a source of infection and rejection to the eventual patient. More importantly, the thickness of amniotic membrane at 60-100 μm is not an appropriate substitute for the native Bruch's membrane (3 μm). Human amniotic membrane has also been found to be a source of growth factors (Shao et al., 2004) which could potentially alter the critical balance of growth factors required for normal retinal structure and function. HUVECs, derived from the vein of the umbilical cord, are a macrovascular cell type and may well lack the specific features required to replicate the distinct and small capillary vessels of the choriocapillaris. A microvascular endothelial cell line or

specifically choroidal-derived endothelial cells would be a better representation of the *in vivo* environment.

Choroidal vascular endothelial cells and RPE cells have been grown together in culture and the interaction was described by Sakamoto et al (1995). This group highlighted the heterogeneity and organ-specificity of vascular endothelial cells, and showed vessel formation by choroidal-derived vascular endothelial cells *in vitro* is modulated by RPE cells. Both cell types were isolated from bovine tissue. The choroidal-derived vascular endothelial cells were seeded within a collagen type I gel and the RPE cells were seeded on the surface of the polymerised gel. The presence of the RPE cells promoted angiogenesis of the vascular endothelial cells within the gel. Unfortunately the culture setup did not use a Bruch's membrane substitute, and there was no physical barrier (other than the collagen gel) between the two cell types. Therefore it was not truly representative of the subretinal architecture.

Another RPE-choroidal endothelial cell co-culture model has been established and was described by Fan et al (2002). They put special emphasis on using choroidal vascular endothelial cells derived from human tissue, and co-culturing the cell types with a definite interface between them. Fan and colleagues were also able to show functional interactions in their co-culture model. Unfortunately their co-culture setup allows these interactions to be studied primarily as an *in vitro* model only, with no ability to use it in an *in vivo* application. The co-cultures were assembled by placing cultures of mature ARPE-19 cells grown on Transwell® filters over human primary choroidal-derived vascular endothelial cells sandwiched within a collagen gel coating the TCP surface below. There was a functional interface between the two cell types however the complex was essentially two parts grown closely together. They did not attempt to recreate the Bruch's membrane-choriocapillaris architecture and it could not be considered as a single unit complex that could stand alone.

2.10 SUMMARY

There is a need to identify the ideal template for the growth of RPE cells with the aim of creating potential RPE transplantable constructs, as current clinical therapies are inadequate for treating the different presentations of AMD. Although there have been some advances in the development of potential templates for RPE cell growth and maintenance, it remains unclear as to what represents the best substratum (e.g.

material), the most suitable vascular components (e.g. underlying vascular scaffold), the best microenvironment (e.g. combination of growth factors), the ideal cell type, and the most appropriate timing of the surgery. Solving such problems and overcoming the current limitations of available biomaterials for RPE substrates will certainly make a positive contribution to those whose lives are impacted upon by AMD.

Chapter 3: Research Study One

Statement of Contribution of Co-Authors for Thesis by Published Paper

The authors listed below have certified* that:

1. they meet the criteria for authorship in that they have participated in the conception, execution, or interpretation, of at least that part of the publication in their field of expertise;
2. they take public responsibility for their part of the publication, except for the responsible author who accepts overall responsibility for the publication;
3. there are no other authors of the publication according to these criteria;
4. potential conflicts of interest have been disclosed to (a) granting bodies, (b) the editor or publisher of journals or other publications, and (c) the head of the responsible academic unit, and
5. they agree to the use of the publication in the student's thesis and its publication on the QUT ePrints database consistent with any limitations set by publisher requirements.

In the case of this chapter:

Shadforth AMA, Suzuki S, Theodoropoulos C, Richardson NA, Chirila TV, and Harkin DG. 2015. A Bruch's membrane substitute fabricated from silk fibroin supports the function of retinal pigment epithelial cells in vitro.
***Journal of Tissue Engineering and Regenerative Medicine*, doi: 10.1002/term.2089**

A Bruch's membrane substitute fabricated from silk fibroin supports the function of retinal pigment epithelial cells in vitro

3.1 ABSTRACT

Silk fibroin provides a promising biomaterial for ocular tissue reconstruction, including the damaged outer blood-retinal barrier of patients with AMD. The aim of the present study was to evaluate the function of RPE cells grown on fibroin membranes manufactured to a thickness similar to that of Bruch's membrane (3 μm). Confluent cultures of RPE cells (ARPE-19) were established on fibroin membranes and maintained under conditions designed to promote maturation over 4 months. Control cultures were grown on porous polyester cell culture well inserts (Transwell®). Cultures established on either material developed a cobblestoned morphology with partial pigmentation within 12 weeks. Negligible change in TER was observed for cultures grown on either material, however this result is in keeping with prior studies of ARPE-19 cell function. Immunocytochemistry at 16 weeks revealed a similar distribution pattern between cultures for F-actin, ZO-1, ezrin, cytokeratin pair 8/18, RPE-65 and Na^+/K^+-ATPase. Electron microscopy revealed that cultures grown on fibroin displayed a rounder apical surface with a more dense distribution of microvilli-like projections. Cultures grown on either material avidly ingested fluorescent microspheres coated with both vitronectin and bovine serum albumin (BSA), but not controls coated with BSA alone. VEGF and PEDF were routinely detected in the conditioned medium collected from above and below the two membrane types. Levels of PEDF were significantly higher than for VEGF on both membranes and a trend was observed towards larger amounts of PEDF in apical compartments. These findings demonstrated that RPE cell functions on fibroin membranes are equivalent to those observed for standard test materials (polyester membranes). As such, these studies support advancement to studies of RPE cell implantation on fibroin membranes in a pre-clinical model.

3.2 INTRODUCTION

Bruch's membrane is an important extracellular matrix structure within the outer retina. The structure and composition of this membrane allows it to act as a semi-permeable sieve between the RPE and the fenestrated capillaries of the choriocapillaris, collectively termed Ruysch's complex (de Jong, 2006). The barrier and permeability characteristics of Bruch's membrane are vital to sensory retina function and the maintenance of homeostasis within the subretinal space more generally (Booij et al., 2010). In patients with AMD, however, Bruch's membrane becomes thickened, brittle, cracked and filled with oxidised waste products. These changes promote alterations in the structural integrity of the choriocapillaris, a breakdown in the outer blood-retinal barrier, and loss of RPE cells, which ultimately leads to vision impairment through an accompanying loss of photoreceptors (Marmor & Wolfsenberger, 1998).

The transplantation of RPE cells as a therapeutic treatment for retinal degeneration has been extensively investigated in humans, however, the transplantation of RPE cells without addressing the structural defects in Bruch's membrane has not resulted in favourable therapeutic outcomes (Binder, 2011). The concept of implanting a prosthetic Bruch's membrane in conjunction with healthy RPE cells has therefore been proposed (Binder et al., 2007). Thus, instead of simply supporting RPE cell attachment and monolayer delivery during surgery, the biomaterial scaffold itself would act as an ongoing replacement for Bruch's membrane. This concept takes into consideration the important *in vitro* studies performed by Tezel and Del Priore (1997, 1999) and Tezel et al. (1999) which revealed that rejuvenation or replacement of Bruch's membrane was integral to RPE cell attachment, monolayer establishment, and consequently transplant survival.

A prosthetic Bruch's membrane should ideally be thin (3-5 μm), permeable, strong, flexible, biologically inert, and able to support the functions of RPE cells. While, numerous biomaterials have been examined for their potential to act as a scaffold to replicate native Bruch's membrane, few have been tested *in vivo*, and none have managed to incorporate all qualities required of an ideal Bruch's membrane replacement (Binder et al., 2011, 2007; Hynes and Lavik, 2010; Kwan et al., 2010).

Our group have previously proposed the use of fibroin (isolated from *Bombyx mori* cocoons) membranes as a potential Bruch's membrane substitute (Harkin et al., 2011; Shadforth et al., 2012). Fibroin, a fibrous protein produced by spiders, silk moths' larvae and numerous other insects, is responsible for the mechanical properties of silk. In our laboratories, fibroin-based membranes have been exploited for their potential to support the attachment, growth and differentiation of a range of ocular cells (Hogerheyde et al., 2014; Bray et al., 2013; George et al., 2013; Bray et al., 2012; Bray et al., 2011; Harkin et al., 2011; Madden et al., 2011; Chirila et al., 2008).

The properties that make fibroin attractive as a prosthetic Bruch's membrane include its tensile strength when manufactured as a very thin membrane, biocompatibility, permeability, and slow enzymatic degradation. We have previously demonstrated that fibroin membranes support the attachment and growth of RPE cells, but the functional properties of such cultures have remained unclear. We therefore present a detailed analysis of RPE function when grown to maturity on fibroin membranes. Our studies have been conducted using the spontaneously immortalised human RPE cell line, ARPE-19 (Dunn et al., 1996), that has been grown to maturity over 4 months in Miller's medium (Maminishkis et al., 2006). This analysis has been performed in parallel with control cultures grown on commercially available porous polyester cell culture membranes (Transwell®).

3.3 MATERIALS AND METHODS

3.3.1 Production of aqueous solutions of fibroin

The procedure has been previously described in detail by our group (Chirila et al., 2008). Briefly, dried *Bombyx mori* silkworm cocoons (Tajima Shoji Co. Ltd., Yokohama, Japan) were boiled in a solution of sodium carbonate containing 0.85 g of salt for each gram of cocoon material. This procedure removed the sericin outer coat from the core fibroin protein. The resulting fibrous material was washed and dried, and then dissolved (at 60 °C for 4 hours) in a concentrated solution of lithium bromide (9.3 M) to obtain a silk concentration of approximately 10 % wt./vol. The fibroin solution was subsequently filtered using syringe filters in succession with pore size 0.7 μm and 0.2 μm. This step is performed slowly to avoid shearing forces that could promote spontaneous gelation. The filtrate was dialyzed against water

using a dialysis cassette with a molecular mass cut-off of 3.5 kDa (Slide-A-Lyzer, Pierce Biotechnology) using 6 changes of water over 3 days. The resulting fibroin solution was filtered again as above and used to produce fibroin membranes.

3.3.2 Preparation of ultrathin membranes of fibroin

Fibroin membranes were cast using a custom-made casting table as described previously by our group (Bray et al., 2011). The thickness of fibroin membranes was measured using an upright micrometer and only areas of membrane 3 μm ± 1 μm thick were used. For structural stabilisation of fibroin membranes, β-sheet formation was induced by the water-annealing of the membranes in a vacuum oven at -80 kPa with ~100 mL water (beaker) for 6 hours at room temperature (25 ºC). The permeability of fibroin membranes has been previously examined using a horizontal diffusion cell using 3 model molecules (Bray et al., 2011).

3.3.3 Cell culture of human RPE cell line, ARPE-19

ARPE-19 cells were routinely cultured using the Miller's medium formulation (Maminishkis et al., 2006); minimum essential medium, alpha modification (MEM-α, M-4526) supplemented with N1 supplement (N-6530), glutamine-penicillin-streptomycin (G-1146), non-essential amino acids (M-7145), taurine (T-0625), hydrocortisone (H-0396) and triiodo-thyronin (T-5516). All these components were purchased from Sigma Aldrich. This medium formulation allows RPE cultures to be incubated at 37 °C using a standard level of 5 % CO_2 air. Cultures were established in the presence of 10 % FBS, and after 24 hours this serum level was decreased to 1 %. Stock cultures were fed two to three times per week, and passaged routinely using Versene (15040-066, Life Technologies) and TrypLE™ (12563-011, Life Technologies), between passages number 23 and 28. An independent STR profile analysis of our working stocks by the Garvan Institute of Medical Research revealed a 100 % match with reference ARPE-19 cell line CRL-2302.

3.3.4 Using ultrathin fibroin membranes in Teflon® chambers for cell culture

Discs of ultrathin fibroin membrane (16-mm diameter) were inserted into custom-made chambers designed by our group, which are manufactured from interlocking Telfon® rings specifically for cell culture use (Fig. 3.1). The combined membrane and chamber were sterilised together by immersion in 70 % ethanol for 1 hour at room temperature, air-dried and washed thoroughly with phosphate buffered

solution (PBS) prior to use. The custom-made chamber suspends the fibroin membrane (reminiscent of the commercially available Transwell® insert system) creating an apical compartment (upper chamber) and a basal compartment (lower chamber) on either side of the membrane (Fig. 3.1). This culture setup is required for the development of a polarised epithelial culture.

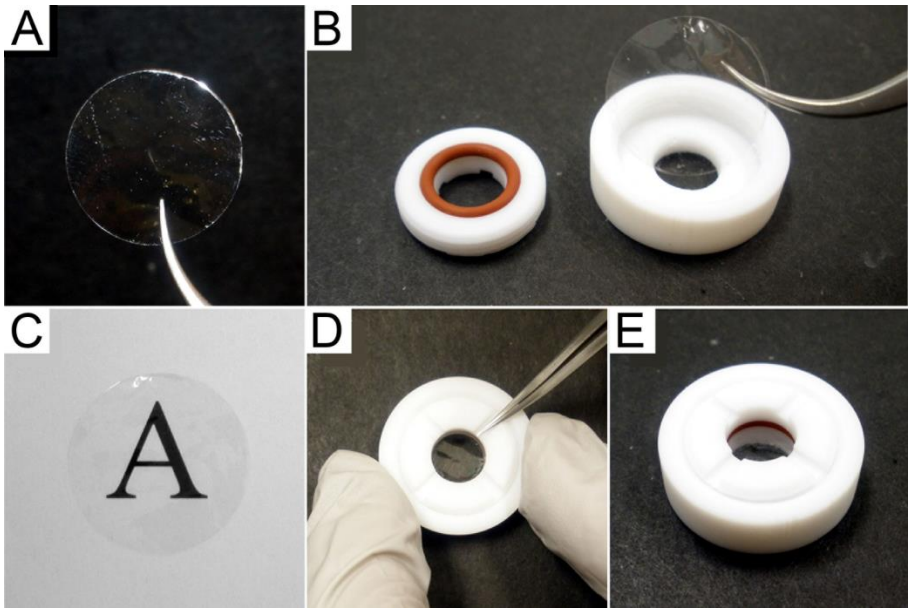

Figure 3.1. Appearance and assembly of fibroin membranes into cell culture chamber. (A and C) Appearance of fibroin membrane (16-mm diameter discs) as photographed while being held up to light or placed over letter of printed text. (B, D and E) Stages of membrane assembly into custom-made cell culture chambers consisting of two interlocking Teflon® rings and silicon o-ring. A locking mechanism is achieved by manufacturing the upper chamber piece to screw down into the base.

3.3.5 Culture of ARPE-19 on ultrathin fibroin membranes and commercial Transwell® permeable membrane inserts

ARPE-19 cells were seeded onto the apical surface of, ultrathin fibroin membranes in chambers, or, polyester membrane in Transwell® inserts (12 mm diameter, with 0.4 µm pores, 10 µm thickness. #3460, Corning Inc.) at a density of 10,000 cells/cm^2. Both membrane types were pre-coated with a commercial ECM blend obtained from human placenta (66 µg/mL, #354237, BD Biosciences) diluted in Hank's buffered salt solution (HBSS). Cultures were incubated at 37 °C and 5 % CO_2, and were fed twice weekly, with Miller's medium used in both the apical and basal compartments. Cultures were analysed for maturity after four months in culture. Cultures were fixed in 3.7 % formaldehyde (for immunocytochemistry) or 3 % glutaraldehyde (for electron microscopy). Membranes of both types (fibroin and

commercial inserts) without cells were used as negative controls for TER studies. Measurements of TER were taken over the culture period using the methodology outlined by Sonoda et al. (2009) and an epithelial voltohmmeter ($EVOM^2$) with the STX3 chopstick electrode set (World Precision Instruments).

3.3.6 Immunocytochemistry

Cultures were fixed in 3.7 % formaldehyde, blocked in 2 % normal goat serum in PBS, permeabilised with 0.5 % Triton X-100 in 100 mM HEPES buffer (pH 7.2), and stained with rhodamine phalloidin (R415, Life Technologies) and Hoechst nuclear dye (H1399, Life Technologies). Primary monoclonal antibodies to zona occludens-1 (ZO-1, 1:100, 33-9100, Clone ZO1-1A12, Life Technologies), ezrin (1:100, 35-7300, Clone 3C12, Life Technologies), cytokeratin pair 8/18 (1:10, DM189, Clone 5D3, Acris Antibodies), RPE-65 (1:50, ab13826, Clone 401.8B11.3D9, Abcam), and sodium potassium ATPase (Na^+/K^+-ATPase, 1:100, ab7671, Clone 464.6, Abcam) were used to highlight functional markers. The secondary antibody used was an Alexa 488-conjugated goat-anti-mouse IgG (Molecular Probes®, Life Technologies). Negative control for immunostaining used the secondary antibody only. Confocal laser scanning microscopy (Nikon A1R) was used to image immunofluorescence.

3.3.7 Electron microscopy

Electron microscopy was used to visualise the formation of ultrastructural features of RPE cells; cuboidal morphology, apical microvilli, basal infoldings, and junctional complexes. Representative cultures were selected for sampling and were fixed with a 3 % glutaraldehyde solution. Samples for scanning electron microscopy (SEM) were washed with 0.1 M cacodylate buffer, post-fixed in 1 % osmium tetroxide in cacodylate buffer for 1 hour, prior to dehydration through sequential graded series of ethanol (50 % to 100 %). Finally, samples were immersed in hexamethyldisilazane (HMDS) for 1 hour, air dried, mounted on an aluminium stub and gold coated. Samples were observed with a FEI Quanta 200 SEM operating at 10 kV. Samples for transmission electron microscopy (TEM) were washed with 0.1 M cacodylate buffer, post-fixed in 1 % osmium tetroxide and 1 % uranyl acetate, and dehydrated through a sequential graded series of ethanol. Samples were then infiltrated and embedded in Spurr epoxy resin. Ultrathin sections (50 nm to 100 nm) were cut, and uranyl acetate and lead citrate stains were applied prior to examination

and photography using a JEOL 1400 Transmission Electron Microscope operating at 80 kV.

3.3.8 Selective phagocytosis assay

The phagocytic function of mature RPE cultures was tested by quantifying the uptake of highly fluorescent vitronectin-coated polystyrene microspheres (2 µm, FluoSpheres, Molecular Probes®, Life Technologies). The assay is an established protocol (Ainscough et al., 2009) that was designed in our laboratory to exploit the known role of the apical transmembrane integrin, $\alpha_V\beta_5$, which interacts with vitronectin to initiate phagocytosis by RPE cells (Nandrot et al., 2006). Briefly, the microspheres were treated with vitronectin (20 µg/mL) in 20 mM HEPES binding buffer (HBB) and incubated for 1 hour at 37 °C, and blocked with 0.1 % bovine serum albumin (BSA, A-7030, Sigma Aldrich) in HBB, incubated for a further hour at 37 °C. Fluorescent microspheres treated with 0.1 % BSA in HBB only for the two incubation times were used as a negative control. Coated microspheres were exposed to representative culture samples for 24 hours at 37 °C. Cultures were then washed, fixed in 3.7 % formaldehyde in PBS, stained with Hoechst nuclear dye and imaged with confocal laser scanning microscopy (Nikon A1R).

3.3.9 Growth factor secretion

The secretion of growth factors by mature cultures was examined using a standard ELISA approach. Briefly, the culture medium from the apical and basal compartments of representative culture samples was collected 24 hours after replacement of media. Commercial ELISA kits for PEDF (#CYT420, Merck Millipore), and VEGF (#DY293B, R&D Systems) were used to quantify growth factor secretion in culture medium volumes. Five cultures for each membrane type were tested using both ELISA kits (samples tested in duplicate). Basal volumes were concentrated using centrifugal filters (Amicon® Ultra-4, Ultracel® 10K MW, regenerated cellulose, Merck Millipore) to reduce the final sample volume to be comparable to the apical volume, and for the sample to be concentrated enough for the sensitivity range of the commercial ELISA assay kits.

3.3.10 Statistical analyses

The ELISA results for growth factor secretion into the apical and basal compartment and the apical-basal growth factor ratio for each membrane type were

analyzed for statistical significance using a two-way ANOVA followed by a Tukey's multiple comparisons test (GraphPad Prism, V 6).

3.4 RESULTS

3.4.1 Cultivation of RPE cells on fibroin membranes

Long-term cultivation (16 weeks) of ARPE-19 cells on fibroin membranes in Miller's medium produced a confluent layer of tightly packed cobblestoned cells (Fig. 3.2 A). Approximately 25-50 % of cells displayed pigmentation after 12 weeks in culture. The distribution of F-actin filaments after 16 weeks was mostly at cell boundaries, but some stress fibres were occasionally seen (Fig. 3.2 C). The distribution of ZO-1 was very similar to the localization of F-actin at the epithelial cell boundaries (Fig. 3.2 D). Immunostaining for ezrin generally revealed a homogenous distribution for this protein, however, relatively intense staining was observed adjacent to the apical surface (Fig. 3.2 E). Positive immunostaining for the cytokeratin pair 8/18 (Fig. 3.2 F), RPE-65 (Fig. 3.2 G) and Na^+/K^+-ATPase (Fig. 3.2 H) was also observed, with varying levels of intensity depending upon the Z-level of confocal sectioning.

Analysis of parallel cultures prepared on commercial polyester membranes (Fig. 3.3) revealed similar results to those for cultures grown on fibroin membranes. Once again, cultures developed into a cobblestoned morphology and pigmentation was evident within a similar time frame (by approximately 12 weeks) (Fig. 3.3 A). Markers of cell structure (F-actin, ZO-1, ezrin, and cytokeratin pair 8/18) were generally similar in distribution to those observed in cultures grown on fibroin (Fig. 3.3 C, D and G respectively). Fewer stress fibres, however, were observed and staining for ZO-1 was less intense at cell boundaries than was observed using fibroin membranes. Confocal sectioning in the Z-axis once again revealed most intense staining for ezrin at the apical surface (Fig. 3.3 E). Positive staining was also confirmed for the metabolic markers RPE-65 and Na^+/K^+-ATPase (Fig 3.3 panels G and H). The distribution patterns for these markers were noticeably more homogenous than for cultures grown on fibroin membrane.

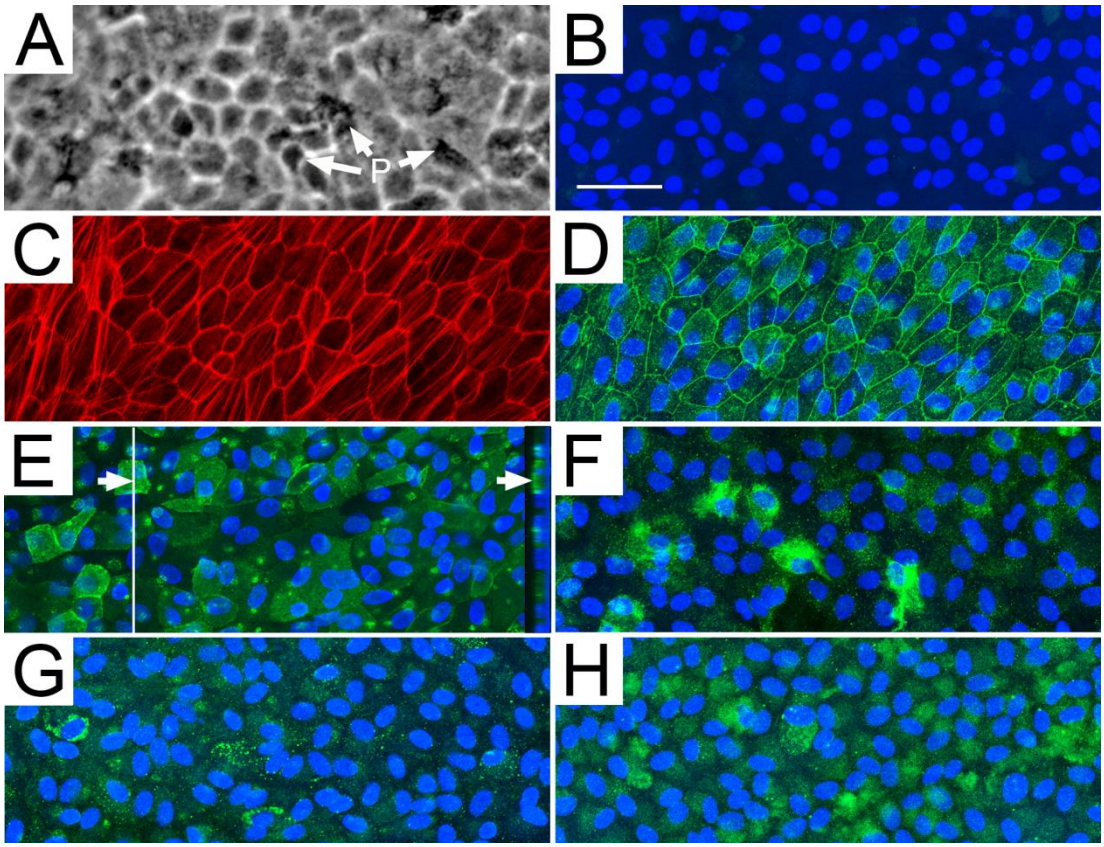

Figure 3.2. Morphology of RPE cells (ARPE-19) after 16 weeks cultivation on fibroin membranes. (A) A cobblestoned morphology accompanied by pigmentation (labelled by arrows; P) was evident within 12 weeks. Assessment of fixed cultures after 16 weeks revealed: a mostly circumferential arrangement of F-actin with occasional stress fibres (C; stained with rhodamine phalloidin). Positive immunostaining (relative to negative control; B), for ZO-1 (D), ezrin (E), cytokeratin pair 8/18 (F), RPE-65 (G) and Na^{+}/K^{+}-ATPase (H) was evident. The distribution for ZO-1 staining resembled the circumferential distribution for F-actin (with C and D displaying identical field of cells). The most intense staining for ezrin was observed at the apical cell surface (refer Z-Y panel at right of panel E). Hoechst nuclear dye is displayed as the blue counter-stain in panel B and panels D to H. The scale bar represents 100 µm and applied to all images.

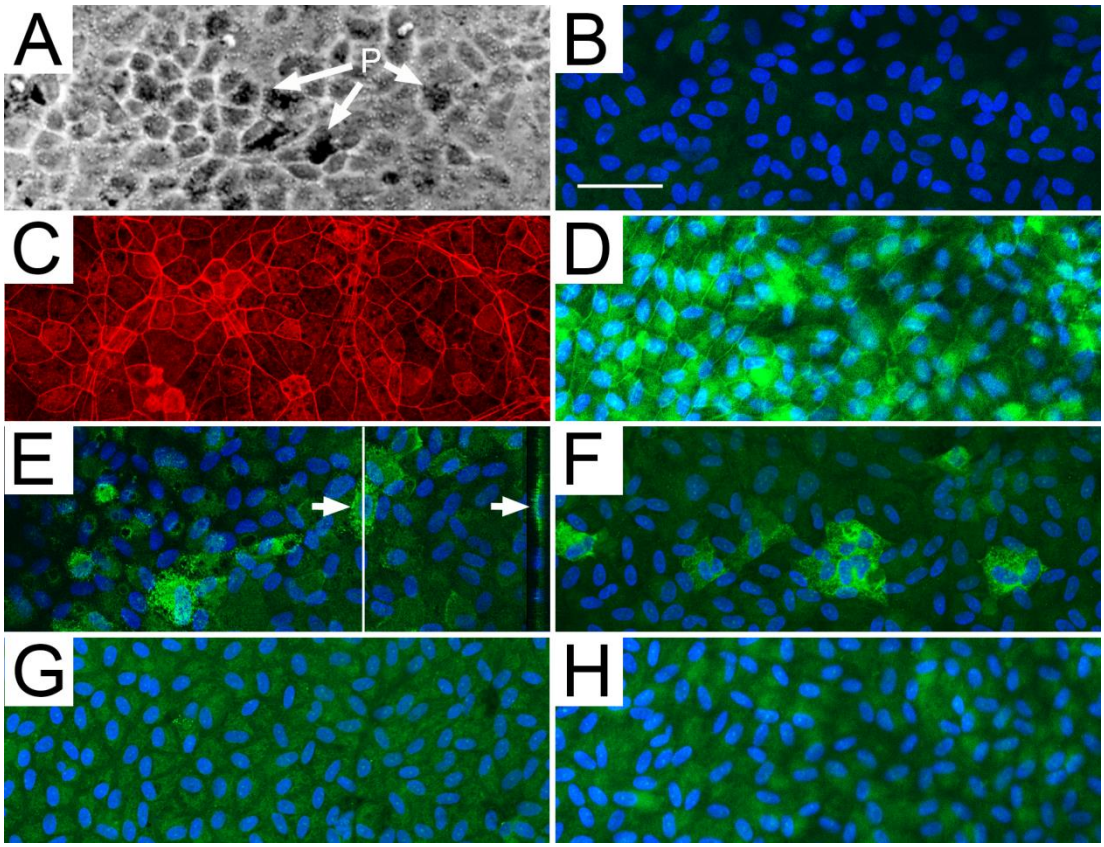

Figure 3.3. Morphology of RPE cells (ARPE-19) after 16 weeks cultivation on commercial polyester membranes (Transwell®). (A) A cobblestoned morphology accompanied by pigmentation (labelled by arrows; P) was evident within 12 weeks. Assessment of fixed cultures after 16 weeks revealed: a mostly circumferential arrangement of F-actin with less evidence of stress fibres (C; stained with rhodamine phalloidin). Positive immunostaining (relative to negative control; B), was again observed for ZO-1 (D), ezrin (E), cytokeratin 8/18 (F), RPE-65 (G) and Na^+/K^+-ATPase (H). As for cultures grown on fibroin, the distribution for ZO-1 staining resembled the circumferential distribution for F-actin (with C and D displaying identical field of cells). The most intense staining for ezrin observed at the apical cell surface (refer Z-Y panel at right of panel E). While staining for cytokeratin pair 8/18 varied according to Z-axis within each cell (F), a more homogenous distribution was observed for RPE-65 and Na^+/K^+-ATPase (G and H respectively). Hoechst nuclear dye is displayed as the blue counter-stain in panel B and panels D to H. The scale bar represents 100 µm and applied to all images.

3.4.2 Ultrastructure of RPE cells established on fibroin membrane

In parallel with the above studies, several replicate cultures established on each type of membrane were processed for scanning and transmission electron microscopy (Fig. 3.4). SEM revealed numerous projections of the cell surface for cultures established on both membrane types (Fig. 3.4 A to D). The projections emanating from cultures grown on polyester membranes were less dense and the surface of the culture generally displayed a flatter profile with cell margins being less well defined (Fig. 3.4 panels B and D). This flatter profile for cultures grown on polyester membranes was confirmed by TEM (Fig. 3.4 F), however, differences in apical cell projections were less apparent when viewed from this angle. Despite these subtle variations, the general ultrastructure of cultures grown on either membrane was generally similar. Importantly, high magnification examination of cultures grown on fibroin membranes revealed the existence of electron dense material near the apical cell borders akin to junctional complexes (Fig. 3.4 G). Examination of the basal cell surface revealed numerous infolding (Fig. 3.4 H). The basal surface of the cells grown on either membrane was separated from the substrate by a layer of extracellular matrix components approximately 1 μm thick (Fig. 3.4 panels F and H).

3.4.3 Examination of trans-epithelial resistance

Throughout the 16 weeks of study, cultures established on both membrane types were routinely assessed for evidence of developing increased TER. Membranes maintained under culture conditions but without cells were also routinely measured as controls. Fibroin membranes alone set up in our custom-designed Teflon® chambers displayed an endogenous level of TER between 250-300 Ohms per cm^2 (Ωcm^2) throughout the 16 weeks of study. In contrast, the TER for polyester membranes fluctuated between 170-250 Ωcm^2. No significant change in TER was detected for ARPE-19 cultivated on either membrane type over time.

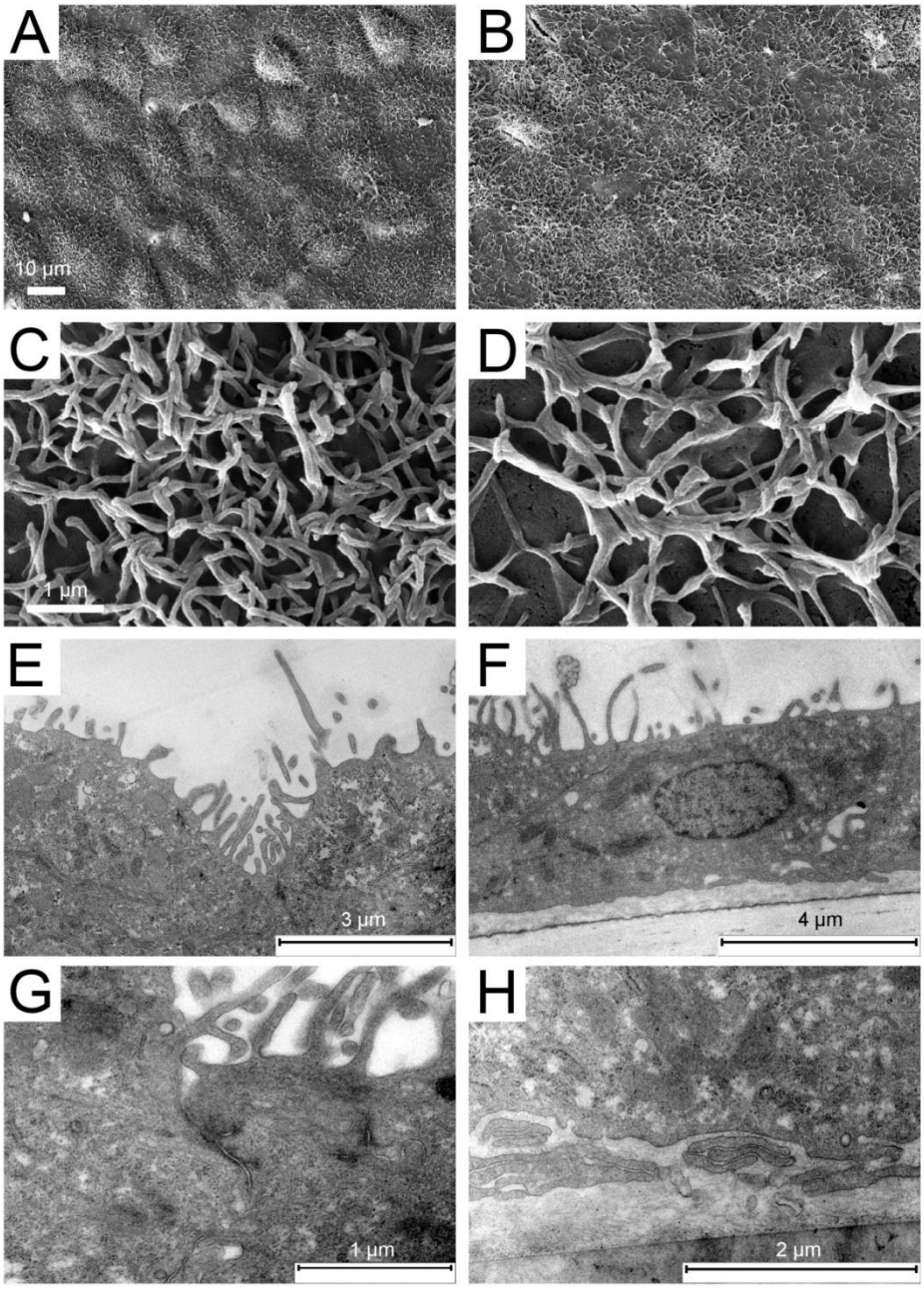

Figure 3.4. Electron micrographs of RPE cells grown on membranes fabricated from fibroin (A and C), or polyester (B and D). Scanning electron micrographs after 16 weeks in culture show cells that display a surface morphology indicative of normal RPE cells. Tight, cobblestoned morphology with dense microvilli-like projections can be visualised and uniformly cover the apical surface of the RPE cells grown on either material (A and B). Differences in density can be seen when comparing the microvilli at 50K magnification (C and D). Transmission electron micrographs show morphological features consistent with biological functioning (E-H). Cross-sections of apical microvilli-like projections in cultures grown on fibroin membranes (E and G), and polyester (F). Electron-dense regions along the plasma membranes of adjacent cells are consistent with development of tight junctional complexes (G), and the basal surface of cells grown on polyester (F) and fibroin (H) show features of membrane infolding and the deposition of material between the cell surface and the membrane.

3.4.4 Examination of phagocytosis

Sixteen week-old cultures of ARPE-19 cells grown on either membrane type both displayed a marked response to fluorescent polystyrene microspheres coated with vitronectin (followed by BSA) (Fig. 3.5). Internalisation of the vitronectin-coated microspheres was confirmed by confocal laser scanning microscopy (refer X-Z and Z-Y axis profiles in Fig. 3.5 panels A and B). In sharp contrast, neither culture displayed an affinity for microspheres coated with BSA alone and those few microspheres that were retained after washing were typically located near the cell surface (Fig. 3.5 panels C and D).

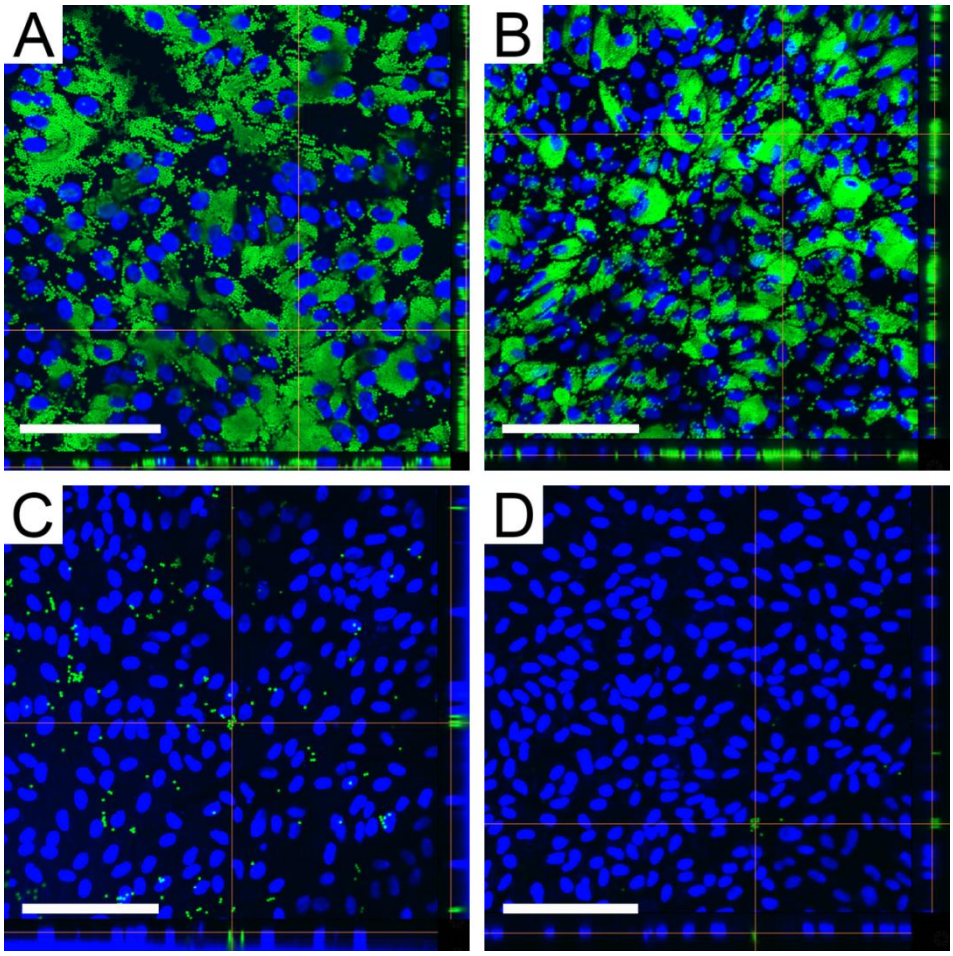

Figure 3.5. Selective phagocytosis by mature RPE cells (ARPE-19) grown on membranes fabricated from fibroin (A and C), and polyester (B and D). Fluorescent microspheres (green) were treated and then exposed to mature RPE cultures 24 hours prior to fixation. (A and B) Microspheres were treated with vitronectin, and blocked with bovine serum albumin (BSA). (C and D) For control purposes, fluorescent microspheres were treated with BSA only. Cultures were imaged using confocal laser scanning microscopy, with the side profiles confirming bead engulfment. Nuclei are stained with Hoechst nuclear dye (blue). Scale bar represents 100 µm.

3.4.5 Examination of growth factor secretion

Cultures grown on either membrane type secreted significant quantities of VEGF and PEDF (Fig. 3.6). In both cases the quantity of PEDF secreted by ARPE-19 cells was approximately 10 to 50-fold higher than for VEGF (1-5.5 ng/cm^2 PEDF versus 50-100 pg/cm^2 for VEGF; $p < 0.0001$). While higher concentrations of PEDF were consistently observed in the apical compartments (above the membrane) compared to the basal compartments (below the membrane), this was not found to be statistically significant. Similar levels of VEGF were observed in both compartments for cultures grown on fibroin membrane. A slight but significantly higher ($p < 0.01$) concentration of VEGF was observed in the basal compartment (compared to the apical compartment) for cultures grown on polyester membrane. Based on this data, the apical-basal ratio of growth factor secretion was calculated for the two substrate types. ARPE-19 cells grown on fibroin membranes had a $[PEDF/VEGF]_{Ap}$ ratio = 53.5, and a $[PEDF/VEGF]_{Ba}$ ratio = 9.8 ($p < 0.05$). ARPE-19 cells grown on polyester membranes had a $[PEDF/VEGF]_{Ap}$ ratio = 70.6, and $[PEDF/VEGF]_{Ba}$ ratio = 25.1 ($p < 0.05$). There was no significant difference between the values for $[PEDF/VEGF]_{Ap}$ ratio or $[PEDF/VEGF]_{Ba}$ ratio when comparing the substrate types.

3.5 DISCUSSION

A variety of different materials have been proposed as a potential vehicle for RPE cell implants, but an optimal candidate has yet to be identified. We have previously proposed evaluation of *Bombyx mori* silk fibroin based on this material's long history of prior clinical use (in the form of silk sutures), favourable mechanical properties and amenability to simple manufacturing techniques. We presently demonstrate that mature cultures of RPE cells (derived from ARPE-19 cells) grown on fibroin membranes, display similar morphological features to those grown in parallel on commercial cell culture membranes constructed from porous polyester. Moreover, we have demonstrated similarities in key RPE functions when cells are grown on either type of material. While minor differences in RPE morphology and function were observed when cultures grown on fibroin or polyester membranes were compared, we consider that the performance of fibroin is sufficient to warrant advancement to pre-clinical studies of this material as a vehicle for RPE cell implantation.

The ARPE-19 cell line is widely used as a model of human RPE cell function, however, it is seldom grown using best current standard practices, i.e. with the use of defined media formulations, porous supports permitting separation of apical and basal compartments, and extended culture periods for maturation (Pfeffer & Philp, 2014). In our previous studies we utilised a growth medium as recommended by the original authors (Dunn et al., 1996), however, it has since become apparent that a

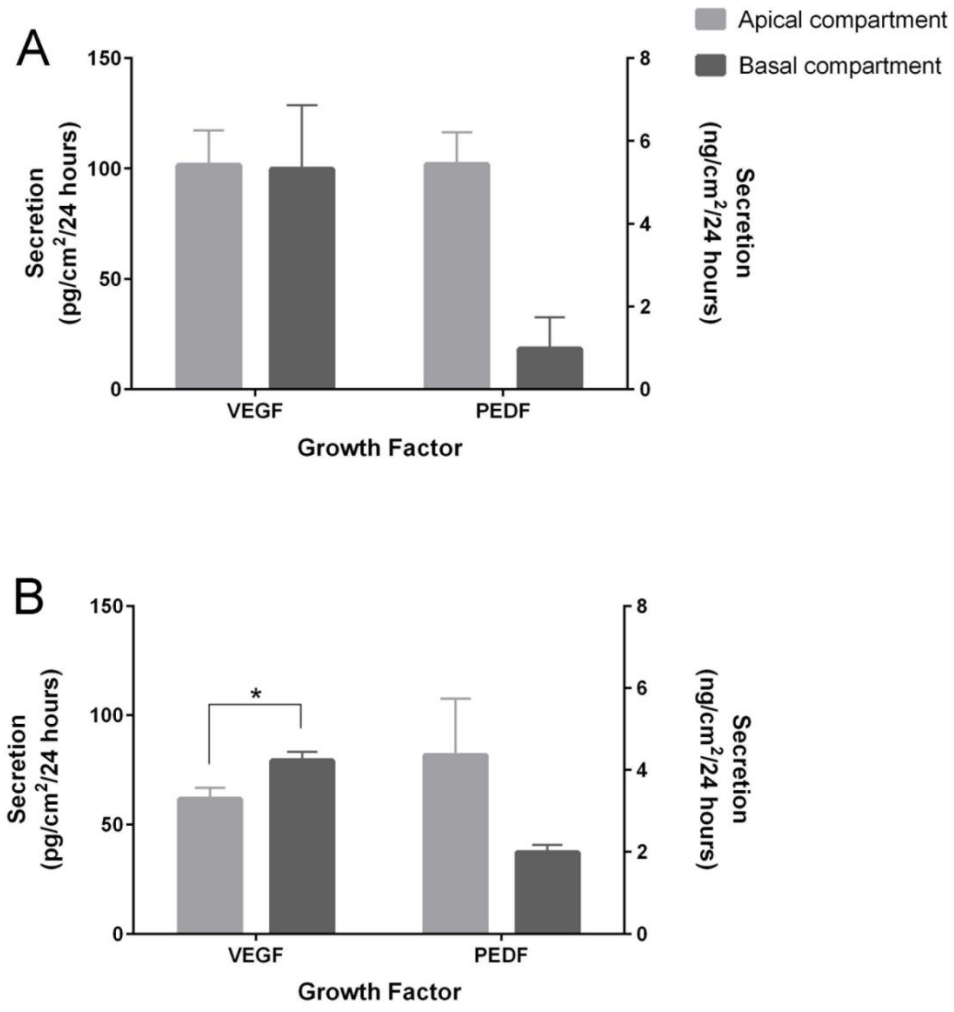

Figure 3.6. Growth factor secretion by mature RPE cells (ARPE-19) grown on membranes fabricated from fibroin (A), and polyester (B). Commercial ELISA kits (for VEGF and PEDF) were used to quantify the concentration of growth factors secreted in culture medium collected from the apical and basal compartments 24 hours after media replacement. Five cultures for each membrane type were tested using both ELISA kits (samples tested in duplicate). Data presented is mean (+ standard error of mean) with VEGF data on left axis and PEDF data corresponding to right axis. Significant difference in growth factor concentration comparing 'VEGF vs PEDF' for both membranes ($p < 0.0001$). Significant difference between apical and basal compartment found for 'VEGF + polyester membrane' only (*p =0.0084).

different medium (as described in detail by Maminishkis et al., 2006) is required to assure a mature RPE morphology using conventional cell culture incubator settings. Using this approach we have demonstrated clear evidence of mature RPE morphology for cultures grown on fibroin membranes coated with extracellular matrix components extracted from human placenta. In a sense, the fibroin membrane is therefore being exploited for its mechanical properties as a tissue scaffold rather than a material intended to directly interact with the cells, i.e. it is used as a Bruch's membrane prosthesis.

Measurement of TER using a voltohmmeter is regularly performed to assess the maturity and function of RPE cells. The principle behind these measurements is that the electrical resistance of RPE cultures increases during the development of tight junctions between neighbouring cells (Sonoda et al., 2009). While ARPE-19 cells lack the full complement of proteins required to produce mature tight junctions (Luo et al., 2006), the distribution of F-actin filaments and ZO-1 observed in our cultures indicates that a similar degree of partial-tight junction formation is observed when cultures grown on fibroin or polyester membranes were compared. As expected, we were unable to detect significant increases in TER for cultures grown on either test material. Interestingly, the endogenous TER for fibroin membrane (no cells) was only marginally higher than the endogenous TER recorded for the polyester membrane (no cells).

Despite the above limitations, the long term cultures of ARPE-19 cells grown on fibroin membranes demonstrated multiple features associated with normal mature RPE cell morphology and function including development of pigmentation and apical-basal polarity (demonstrated by apical staining for ezrin and development of microvilli-like structures). The functionality of the apical surface is demonstrated by the marked phagocytic response to the synthetic fluorescent microparticles coated with vitronectin. This assay is based upon the fact that phagocytosis of photoreceptor outer segments (POS) *in vivo* is initiated via binding to the vitronectin receptor $\alpha v\beta 5$ integrin. While there are limitations with using materials other than actual POS, this approach does have the advantage of enabling inclusion of a negative control (particles coated only with BSA). In any case, future studies of RPE cell function when grown on fibroin membranes should include an analysis of POS uptake.

Secretion of pro- and anti- angiogenic growth factors is vital to maintaining a healthy outer blood-retinal barrier. The RPE normally contributes to this balance by secreting the pro-angiogenic factor VEGF and the antiangiogenic factor PEDF (Strauss, 2005). While the secretion of VEGF across Bruch's membrane is considered important for maintaining a normal choriocapillaris, apical secretion of PEDF discourages aberrant growth of blood vessels into the subretinal space (a neuroprotective component of PEDF also nourishes the sensory retina) (Kay et al., 2013). It is therefore significant to note that mature RPE cultures established on fibroin membrane secrete higher amounts of PEDF than VEGF and that the former tends to be preferentially released into the apical compartment. Moreover, while the polyester membranes appear to be more permeable to VEGF, the fibroin membranes supported sufficient diffusion of this angiogenic factor into the basal compartment to produce an apparent equilibrium with the apical compartment. The apical-basal ratio of growth factor secretion by ARPE-19 cells grown on both substrate types, are similar to values that have been reported previously (Maminishkis et al., 2006). On this basis, we predict that the balance of VEGF and PEDF secreted by RPE cells grown on fibroin membrane would be consistent with the requirements of a healthy outer blood-retinal barrier following implantation.

Notwithstanding the positive considerations above, there remain opportunities to improve the formulation of fibroin membranes as a vehicle for RPE cell implantation. Human recombinant tropoelastin has recently been shown to alter the elastic properties of fibroin membranes when the two proteins are blended together in solution (Hu et al., 2011; Hu et al., 2010). Moreover, since elastin fibers are a prominent feature of the inner Bruch's membrane structure, a tri-layered structure consisting of fibroin-tropoelastin-fibroin might better replicate the functional requirements of a prosthetic Bruch's membrane. The outer coating of fibroin membranes also presents opportunities for optimization. For example, since fibroin is a protein, peptides of desired design could be readily conjugated to the surface of membranes using relatively simple chemical methods including reaction with terminal amine groups. Indeed, each side of the fibroin membrane could be specifically tailored to encourage attachment and growth of RPE cells and choroidal cell types respectively.

3.6 CONCLUSIONS

In summary, we conclude that the behaviour of mature RPE cell cultures established on fibroin membranes is essentially equivalent to that displayed by best practice cultures grown on porous polyester membranes. Unlike the latter research material, however, fibroin membranes are fabricated entirely from a protein with low immunogenicity and at a thickness comparable to healthy Bruch's membrane, which makes this material an attractive choice of vehicle for RPE cell implantation. Future refinements in the performance of fibroin membranes should also be possible through the replacement of crude ECM coatings, as used presently, with desired combinations of medical grade proteins or synthetic peptide analogues. Ultimately, the potential of fibroin membranes as a vehicle for RPE cell implants will need to be examined *in vivo*. To this end, the present data encourages advancement to a preclinical study of fibroin safety and feasibility as a vehicle for RPE implantation into the subretinal space.

Chapter 4: Research Study Two

Incorporation of human recombinant tropoelastin into silk fibroin membranes with the view to repairing Bruch's membrane

4.1 ABSTRACT

Bombyx mori silk fibroin membranes provide a potential delivery vehicle for both cells and ECM components into diseased or injured tissues. We have previously demonstrated the feasibility of growing RPE cells on fibroin membranes with the view to repairing the retina of patients afflicted with AMD. The goal of the present study was to investigate the feasibility of incorporating the ECM component elastin, in the form of human recombinant tropoelastin, into these same membranes. Two basic strategies were explored: (1) membranes prepared from blended solutions of fibroin and tropoelastin, and (2) layered constructs prepared from sequentially cast solutions of fibroin, tropoelastin and fibroin. Optimal conditions for RPE attachment were achieved using a tropoelastin-fibroin blend ratio of 10 to 90 parts by weight. Retention of tropoelastin within blend and layered constructs was confirmed by immunolabelling and Fourier-transform infrared spectroscopy (FTIR). In the layered constructs, the bulk of tropoelastin was apparently absorbed into the initially cast fibroin layer. Blend membranes displayed higher elastic modulus, percentage elongation and tensile strength ($p < 0.01$) when compared to the layered constructs. RPE cell response to fibroin membranes was not affected by the presence of tropoelastin. These findings support the potential use of fibroin membranes for the co-delivery of RPE cells and tropoelastin.

4.2 INTRODUCTION

While strategies for tissue regeneration are often based upon the replacement of lost cells, such efforts often ignore the significant contribution of ECM components to tissue structure and function. A good example of this problem is illustrated through the attempts to treat AMD of the retina. In short, although the pathology of AMD involves significant changes to both cellular and ECM components, most efforts to date have been largely focused on replacing only the cellular components and especially RPE cells (Binder et al., 2007; da Cruz et al., 2007; Jha & Bharti, 2015; Lee & Maclaren, 2011). In doing so healthy RPE cells are ultimately delivered into sites containing an abnormal composition and arrangement of ECM components. In order to address this issue, a number of groups have explored the potential of a variety of biomaterials as temporary ECM substitutes to

support the RPE cells during cultivation and implantation (Binder, 2011; Hynes & Lavik, 2010). In our case, we have focused on the development of a substitute prepared from the silk structural protein, fibroin (Harkin et al., 2011; Shadforth et al., 2012). Using this strategy, we have demonstrated the feasibility of establishing functional monolayers of RPE cells grown on fibroin membranes (Chapter 3). These RPE monolayers share several important features with those found within the healthy retina including apical-basal polarity, patterns of growth factor secretion and phagocytic function. As such, fibroin membranes have potential as a vehicle for implanting cultured RPE cells into AMD patients. Since the fibroin membranes will eventually degrade, the incorporation of ECM components, or their precursors, within the fabricated membranes may further facilitate subsequent development of a more permanent ECM. The aim of the present study, therefore, was to examine the feasibility of incorporating ECM components found naturally within the outer retina. More specifically, we have examined the incorporation of the precursor protein from which elastin fibres are produced, tropoelastin (Wise et al., 2009).

Our focus on tropoelastin arises from considering the composition of the ECM that resides immediately posterior to the RPE, a structure known as Bruch's membrane. A functional, native Bruch's membrane contains an elastin fibre-rich core that is thought to facilitate tissue compliance during cycles of tissue expansion and recoil as blood flows through the adjacent capillaries of the choriocapillaris (Booij et al., 2010). The elastic properties of Bruch's membrane may also serve to protect the delicate connections that exist between RPE cells and the adjacent photoreceptor cells (Leure-duPree, 1968). However, age-related changes, such as the accumulation of abnormal deposits referred to as drusen, disrupt the biochemical and mechanical properties of Bruch's membrane (Booij et al., 2010). Moreover, an aged Bruch's membrane deters the survival of both endogenous as well as implanted RPE cells (Bhutto & Lutty, 2012; Sugino et al., 2011; Tezel et al., 1999; Tezel & Del Priore, 1997, 1999). Importantly, RPE cells have been shown to produce microfibrils, and lysyl oxidase, the enzyme responsible for converting tropoelastin into elastin fibres (Wachi et al., 2005). Thus, by implanting RPE cells in conjunction with tropoelastin it may be possible to regenerate the core element of a functional, native Bruch's membrane following degradation of the fibroin-based delivery template. In addition, since tropoelastin shares similar elastic properties with elastin (Wise et al., 2009), it

may also be possible to create fibroin-tropoelastin constructs with physical and mechanical properties that are more favorable for establishing and implanting RPE cell cultures than constructs based solely on fibroin.

Two strategies for incorporating tropoelastin into fibroin membranes were examined in this study. Membranes were produced from fibroin solutions supplemented with recombinant human tropoelastin (fibroin-tropoelastin blend) or prepared from alternating cast solutions of fibroin and tropoelastin (layered approach). In the case of the blend, we commenced by optimizing the amount of tropoelastin that can be added to fibroin solution without negatively impacting on the attachment of RPE cells to the resulting membranes. Freestanding membranes were subsequently produced from the optimal blend formulation, and by using the layered approach. The two types of biomaterial membrane were subsequently compared in parallel with standard fibroin membranes using a variety of criteria including morphology (scanning electron microscopy), secondary structure (Fourier-transform infrared spectroscopy-attenuated total reflectance, FTIR-ATR), the distribution of tropoelastin (immunofluorescence), the cultivation of RPE cells, and mechanical properties. These studies led to some unexpected findings, especially in regard to how tropoelastin in solution interacts with cast fibroin membranes.

4.3 MATERIALS AND METHODS

4.3.1 Production of aqueous solutions of fibroin

The procedure has been previously described in detail by our group (Chirila et al., 2008). Briefly, dried *Bombyx mori* silkworm cocoons (Tajima Shoji Co. Ltd., Yokohama, Japan) were boiled in a solution of sodium carbonate containing 0.85 g of salt for each gram of cocoon material. This procedure removed the sericin outer coat from the core fibroin protein. The resulting fibrous material was washed and dried, and then dissolved (at 60 °C for 4 hours) in a concentrated solution of lithium bromide (9.3 M) to obtain a silk concentration of approximately 10 % wt./vol. The fibroin solution was subsequently filtered using syringe filters in succession with pore size 0.7 μm and 0.2 μm. This step is performed slowly to avoid shearing forces that could promote spontaneous gelation. The filtrate was dialyzed against water using a dialysis cassette with a molecular mass cut-off of 3.5 kDa (Slide-A-Lyzer,

Pierce Biotechnology) using 6 changes of water over 3 days. The resulting fibroin solution was filtered again as above and used to produce fibroin membranes.

4.3.2 Preparation of films cast in TCP wells: fibroin and tropoelastin solutions blended in different ratios

Films of fibroin and tropoelastin were prepared by the method reported by (Hu et al., 2011) with some modifications. Briefly, tropoelastin (freeze-dried powder) was dissolved in cold MilliQ water (4ºC) to make the concentration of 1.78 %, and kept in an ice bath for 2-3 hours with occasional vortex mixing. The low temperature is required to prevent coacervation of the solution (self-aggregation of hydrophobic domains). The tropoelastin solution was slowly added to a cold fibroin solution (1.78%) by a pipet, and mixed by inverting the tube slowly. The volume ratio of the fibroin solution to the tropoelastin solution was mixed over the range 90:10, 75:25, and 50:50. The mixture solutions were cast into wells of 24-well TCP plates and dried in a fan-driven oven for 12 hours at room temperature. For structural stabilization of fibroin with tropoelastin, β-sheet formation was induced by water annealing the plates in a vacuum oven at 60 ºC, -80 kPa with ~100 mL water in a beaker, for 12 hours, followed by drying in a fan-driven oven for 12 hours at room temperature.

4.3.3 Cell culture of human RPE cell line, ARPE-19

ARPE-19 cells were routinely cultured using the Miller's medium formulation (Maminishkis et al., 2006); minimum essential medium, alpha modification (MEM-α, M-4526) supplemented with N1 supplement (N-6530), glutamine-penicillin-streptomycin (G-1146), non-essential amino acids (M-7145), taurine (T-0625), hydrocortisone (H-0396) and triiodo-thyronin (T-5516). All these components were purchased from Sigma Aldrich. This medium formulation allows RPE cultures to be incubated at 37 °C using a standard level of 5 % CO_2 air. Cultures were established in the presence of 10 % FBS, and after 24 hours this serum level was decreased to 1 %. Stock cultures were fed two to three times per week, and passaged routinely using Versene (15040-066, Life Technologies) and TrypLE™ (12563-011, Life Technologies), between passages number 23 and 28. An independent STR profile analysis of our working stocks by the Garvan Institute of Medical Research revealed a 100 % match with reference ARPE-19 cell line CRL-2302.

4.3.4 Testing the attachment of RPE cells on films of fibroin and tropoelastin blended in different ratios

The cell attachment was quantified on films prepared by blending solutions of fibroin and tropoelastin (section 4.3.2). RPE cells (ARPE-19) were seeded at a density of 40,000 cells/cm^2 and incubated at 37 °C, 5 % CO_2 for 4 hours using Miller's medium without serum. Fibroin films and TCP (used with and without serum) were used as control substrates for ARPE-19 cell attachment. Each substrate type was tested in triplicate, with the experiment performed in triplicate and quantified using the Quant-iT PicoGreen® dsDNA kit (Molecular Probes™, Life Technologies).

4.3.5 Preparation of fibroin membranes

Fibroin membranes were cast using a custom-made casting table as described previously by our group (Bray et al., 2011). The thickness of fibroin membranes was measured using an upright micrometer and only areas of membrane 3 μm ± 1 μm thick were used. For structural stabilisation of fibroin membranes, β-sheet formation was induced by the water-annealing of the membranes in a vacuum oven at -80 kPa with ~100 mL water (beaker) for 6 hours at room temperature (25 ºC). The permeability of fibroin membranes has been previously examined using a horizontal diffusion cell using 3 model molecules (Bray et al., 2011).

4.3.6 Preparation of freestanding membranes of fibroin and tropoelastin, proteins blended in 90:10 solution ratio

Freestanding membranes of fibroin and tropoelastin blend were prepared by the method outlined above (section 4.3.2), except that only the 90:10 volume ratio of the fibroin solution to the tropoelastin solution was used. For casting, 45-mm Petri dishes were first coated with a Topas® (a commercial hydrophobic cyclic olefin copolymer) film (1 mL of a 7 % solution) by the evaporation from a solution in cyclohexane. The Topas® solution forms a hydrophobic film on the glass, facilitating easy removal of the membranes from the dishes later. The mixture solution (1.78 %, 1 ml) was poured into the dish, and dried in a fan-driven oven for 12 hours at room temperature. For structural stabilisation of fibroin with tropoelastin, the blend membranes were water annealed using a vacuum oven with a container of water and kept at -80 kPa at 60 ºC for 12 hours, followed by drying in a fan-driven oven for 12 hours at room temperature. The membranes were peeled from the Topas® film and

used for cell culture and mechanical testing. The thickness of the membranes used was 2-3 µm.

4.3.7 Preparation of freestanding layered (fibroin-tropoelastin-fibroin) membranes

Layered membranes were fabricated using separate aqueous solutions of fibroin and tropoelastin, layered in sequence and followed by stabilisation after each layer. Before casting any protein solutions, 45-mm Petri dishes were first coated with a Topas® film. The layered membrane was prepared as following. Firstly, 1 mL of 0.59 % fibroin solution was cast and dried in a fan-driven oven at room temperature overnight, followed by water annealing in a vacuum oven with a beaker of water at -80 kPa at room temperature, for 6 hours. Then 1 mL of 0.59 % tropoelastin solution was cast and dried at 4˚C for 4 days. The tropoelastin layer was stabilized by treatment with methanol (5 mL) for 24 hours at room temperature. Finally, 1 mL of 0.59 % fibroin solution was cast on top of the tropoelastin layer, and stabilized by water annealing as above. The volumes used were calculated to generate 1 µm-thick layers of each protein, which would result in a 3 µm-thick layered membrane. A 1 µm-thick membrane of tropoelastin was cast and was not treated with methanol (untreated) as a comparison for FTIR-ATR studies.

4.3.8 Suspension of the membranes in custom-made Teflon® chambers

Discs (16-mm diameter) of biomaterial membrane were inserted into custom-made chambers designed by our group, which are manufactured from interlocking Telfon® rings specifically for cell culture use (Fig. 3.1). The combined membrane and chamber were sterilised together by immersion in 70 % ethanol for 1 hour at room temperature, air-dried and washed thoroughly with PBS. The custom-made chamber suspends the biomaterial membrane (reminiscent of the commercially available Transwell® insert system) creating an apical compartment (upper chamber) and a basal compartment (lower chamber) on either side of the membrane. This culture setup is required for the development of a polarised epithelial culture.

4.3.9 Visualization of tropoelastin within the membranes using immunofluorescence

Samples of fibroin, blend, and layered membranes were incubated with a primary monoclonal antibody to tropoelastin (BA4, 1:50, ab21599, Abcam). The secondary antibody used was an Alexa 488-conjugated goat-anti-mouse IgG

(Molecular Probes®, Life Technologies). Negative controls for immunostaining were incubated with the secondary antibody only. Confocal laser scanning microscopy (Nikon A1R) was used to image immunofluorescence.

4.3.10 Testing cell growth of RPE cells on the membranes

Cell growth on the fibroin, blend, and layered membranes was compared and quantified. RPE (ARPE-19) cells were seeded (4,000 cells/cm^2) on the discs (6-mm diameter) of different biomaterial membranes and evaluated for total cell numbers, 72 hours after seeding using the Quant-iT PicoGreen® dsDNA kit (Molecular Probes™, Life Technologies). This experiment was performed in triplicate using discs of freestanding biomaterial membrane (samples tested in triplicate) held down rubber o-rings in the wells of 96-well plates.

4.3.11 Extended culture of RPE cells on the membranes

RPE (ARPE-19) cells were seeded (10,000 cells/cm^2) onto the apical surface of biomaterial membranes suspended in Teflon® chambers (section 3.8). All membrane types; fibroin, blend, and layered membranes, were precoated with a commercial Collagen I solution obtained from porcine origin (0.3 mg/mL, Cellmatrix®, Nitta Gelatin Inc., Osaka, Japan) diluted in MilliQ water. Cultures were incubated at 37 °C and 5 % CO_2, and culture media was changed twice weekly. Phase contrast light microscopy was used to examine the cultures over a two month culture period.

4.3.12 Fourier-transform infrared spectroscopy of the membranes

The FTIR-ATR spectra of the membranes (fibroin, blend, and layered) and tropoelastin were collected using a Nicolet FTIR spectrometer (Thermo Electron Corp, Waltham, MA, USA), equipped with a Nicolet Smart Endurance diamond ATR accessory. Each spectrum was obtained by co-adding 64 scans over the range of 4,000 to 525 cm–1 at a resolution of 8 cm–1. The OMNIC 7 software package (Thermo Electron Corp, Waltham, MA, USA) was used to analyze and plot the spectra.

4.3.13 Mechanical testing of the membranes

Strips (1×3 cm) were cut from each membrane type and subjected to tensile measurements in an Instron 5848 micrometer, equipped with a 5 N load cell and a set gauge distance of 14 mm. The membranes were mounted in pneumatic grips and submersed in PBS at 37 ºC in a BioPulsTM unit for 5 minutes prior to testing. Stress-

strain plots were recorded, and the Young's moduli were computed in the linear region. The mean values were calculated from results generated by 4-6 measurements for each specimen. In addition, cyclic tensile loading/unloading testing was carried out to evaluate recovery behaviour. The testing experiments were set up as above. However, the following method profile was used: the repeated cyclic loading/unloading was performed at strain of 20 % in the stress-strain curve, which is the linear region, with ± 5% strain of loading/unloading and the rate of 14 mm/min. The number of cycles performed was 200 cycles. Four measurements were performed for each specimen. From stress-strain plots, the areas under the curve of cycles 10 and 200 were calculated and used to evaluate deformation using the following equation:

Deformation (%) = ((Area cycle 10 –Area cycle 200)/ Area cycle 10)□100

4.3.14 Statistical analyses

Results from cell attachment and growth assays were analyzed for statistical significance using a two-way ANOVA followed by a Tukey's multiple comparisons test (with the two variables being either "substrate and serum" or "substrate and time"). Mechanical testing data were analyzed using a one-way ANOVA with Tukey's test comparing membrane types (with the variable being "membrane type"). Recoil testing data for fibroin and blend membranes were analyzed using an unpaired t test (since comparing only two independent samples). All statistical analyses was performed using GraphPad Prism, V 6.

4.4 RESULTS AND DISCUSSION

4.4.1 Properties of fibroin and tropoelastin solutions

During their extraction from silkworm cocoons (Wray et al., 2011), a significant proportion of the native fibroin proteins (heavy chain 350 kDa and light chain 26 kDa) were cleaved into fragments of varying molecular weights (Fig. 4.1). In contrast, human tropoelastin produced via recombinant DNA technology (Martin et al., 1995) displayed a single band by gel electrophoresis, at approximately 55 kDa (Fig. 4.1). The aqueous solutions of fibroin and tropoelastin mixed readily with increasing ratios of up to 50% tropoelastin by weight. Phase separation was observed when combining solutions at 10 % tropoelastin by weight (resulting in a cloudy

solution), however the resulting dried films were transparent and smooth when cast in plastic (polystyrene) tissue culture dishes.

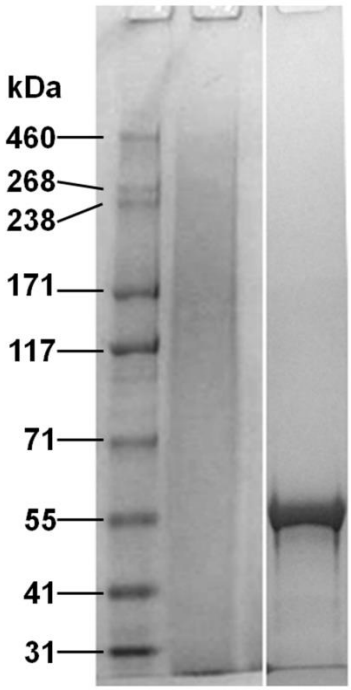

Figure 4.1. Relative molecular weight distribution for purified native *Bombyx mori* silk fibroin (middle lane) and recombinant human tropoelastin (right lane) as displayed by gel electrophoresis. While the extracted fibroin proteins present as a broad range of peptide fragments, recombinant human tropoelastin has a defined molecular weight of approximately 55 kDa. The left hand lane shows a selection of molecular weight markers.

4.4.2 Effect of tropoelastin on RPE cell attachment to fibroin

Since fibroin supports the attachment and growth of RPE cells (Shadforth et al., 2012) and tropoelastin has also been shown to positively influence cell attachment (Hu et al., 2011, 2010), we examined different blend ratios of fibroin and tropoelastin with the goal of identifying an optimal formulation for the resulting blend membrane. As demonstrated in Fig. 4.2, a consistent trend was observed towards an optimal RPE cell attachment (as defined by DNA content), in either the presence or absence of serum (10% v/v), using a tropoelastin-fibroin ratio of 10 to 90 parts by weight. This result was consistent with prior reports (Hu et al., 2011) and has been explained as the optimal ratio between the two proteins.

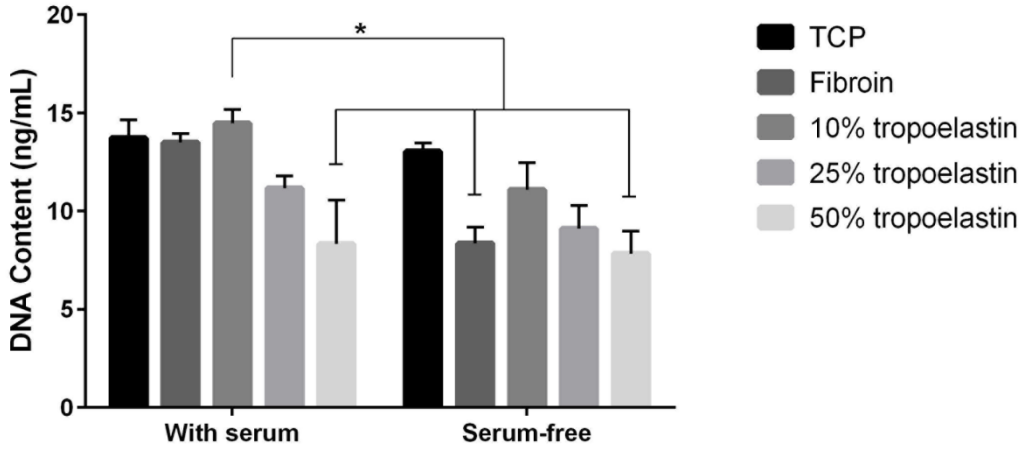

Figure 4.2. Comparison of cell attachment of retinal pigment epithelial cell line (ARPE-19) on tissue culture plastic (TCP) coated with either fibroin solution, or fibroin mixed with increasing concentrations of tropoelastin (proteins blended in solution before coating TCP). Evidence of cell attachment was examined after 4 hours in either the presence or absence of 10 % (v/v) fetal bovine serum (with washing prior to measurement). Each substrate was tested in triplicate. Bars represent mean values (+ standard error of the mean) from three experiments. The difference between fibroin with 10 % tropoelastin used in the presence of serum and the other identified bars was statistically significant ($p < 0.05$).

4.4.3 Gross morphology of the freestanding membranes

Having established the optimal blend ratio of fibroin to tropoelastin for RPE cells, we proceeded to test the feasibility of producing freestanding membranes from the optimal blend, as well as layered constructs produced by sequential addition and drying/stabilization of aqueous solutions containing each protein (fibroin followed by tropoelastin, then fibroin again). Both types of membrane were prepared in glass Petri dishes coated with Topas® polymer as described previously (Bray et al., 2013). In brief, the Topas® coating facilitated the subsequent removal of fibroin-based membranes from the glass Petri dishes and was itself delaminated easily leaving behind the protein membranes. The membranes produced from the optimal blend (Fig. 4.3 B) or by layering (Fig. 4.3 C) were physically comparable to the standard fibroin membranes produced routinely in our laboratory (Fig. 4.3 A). All membranes were transparent and could be cut into the 16-mm diameter discs required for our custom-designed Teflon® cell culture chambers (Fig. 3.1). Nevertheless, the layered membranes (Fig. 4.3 C) were noticeably more brittle during excision resulting in discs with uneven edges (Fig. 4.3 C). While no layers were evident within the membranes examined by scanning electron microscopy (SEM) following freeze

fracture (Fig. 4.3 D to F), a distinct band of positive immunolabelling for tropoelastin was observed within the layered construct by confocal fluorescence microscopy (Fig. 4.3 I). In contrast, an uneven distribution of staining for tropoelastin was observed within the blend membrane (Fig. 4.3 H). Unexpectedly, only a single band of fibroin autofluorescence was observed within the layered constructs (Fig. 4.3 I). This result initially suggested to us that perhaps one of the fibroin layers had detached during handling, but repeated attempts using multiple samples revealed the same result. Moreover, no evidence of a detached fibroin sheet was observed in any sample mounted for confocal microscopy. We therefore embarked upon an FTIR analysis of the layered composites to determine the fate of the apparently "missing" third layer.

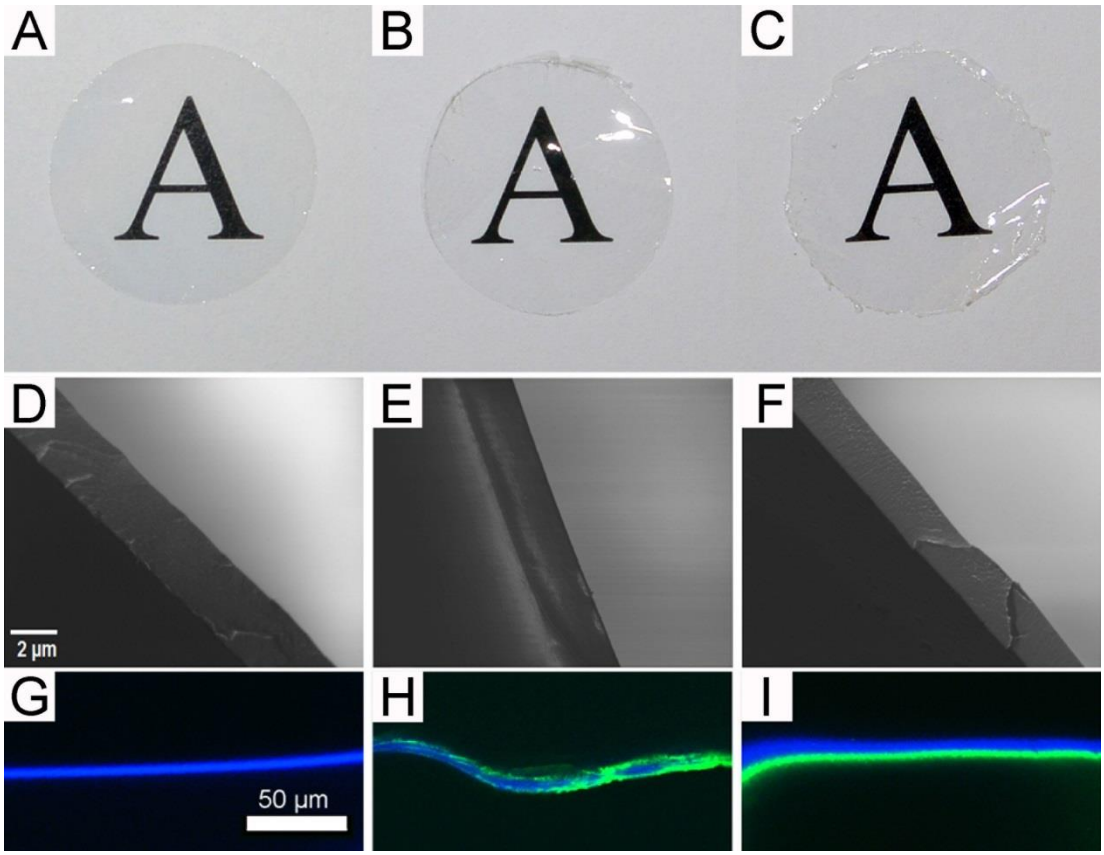

Figure 4.3. Physical appearance of membranes prepared from either fibroin alone (A, D and G), tropoelastin-fibroin blend (10:90 ratio) (B, E and H), and layered solutions of fibroin and tropoelastin (C, F and I). (A-C): gross appearance of each membrane when placed over printed text (16-mm diameter discs). (D-F): internal structures revealed by scanning electron microscopy following freeze-fracture. (G-I) Visualization of tropoelastin (green) by immunolabelling and confocal fluorescence microscopy (the presence of fibroin revealed as blue autofluorescence).

4.4.4 Analysis of membrane structure by Fourier-transform infrared spectroscopy-attenuated total reflectance, "FTIR-ATR"

The FTIR-ATR spectra in the range of 1800-950 cm-1 were used to examine the surface structure of the different biomaterial membranes (Fig. 4.4 A). The amide I region between 1720 and 1580 cm-1 is traditionally used for analysis of the secondary structure in proteins, and this region has been well described for fibroin (Hu et al., 2006). In the spectrum of the standard fibroin membrane (water-annealed for 6 h at 25 °C) (Fig. 4.4 A, A1), both the amide I band shape and its peak maximum at 1640 cm-1 indicate a significant amount of random coil component. The fibroin (Fig. 4.4 A, A2) and blend (Fig. 4.4 A, A3), membranes that were water annealed for 12 h at 60 °C, revealed a strong band at 1621 cm-1 and a shoulder at 1700 cm-1, corresponding to β-sheet structures and their aggregates (Hu et al., 2006). If the layered (fibroin-tropoelastin-fibroin) membrane truly had three layers as expected, both surface spectra should reveal a similar fibroin signature. One side of the layered membrane (Fig. 4.4 A, A4) did reveal a fibroin signature similar to those described above, however, the other side (Fig. 4.4 A, A5) revealed more pronounced β-sheet bands. This may be a result of the additional methanol treatment of the initial fibroin layer after tropoelastin was added. The other side (Fig. 4.4 A, A5) also revealed two weak bands at 1200 and 1135 cm-1 (indicative of tropoelastin) (Fig. 4.4 A, A6), suggesting that one side of the layered membrane consists of a mixture of fibroin and tropoelastin near the surface. The possibility that the methanol treatment might be removing some of the tropoelastin layer was also considered. The tropoelastin bands were used to investigate the stability of tropoelastin in two-layered (fibroin-tropoelastin) membranes before and after methanol treatment (Fig. 4.4 B). The spectrum for the tropoelastin side before methanol treatment (Fig. 4.4 B, B2) presented two bands at 1200 and 1135 cm-1 which correspond to the spectrum of the untreated tropoelastin membrane (Fig. 4.4 B, B5). After methanol treatment these tropoelastin bands had dramatically decreased (Fig. 4.4 B, B4). Indeed, a thin membrane (thickness of ~1 μm) of tropoelastin was readily soluble in pure methanol which was demonstrated in a separate investigation to confirm FTIR results.

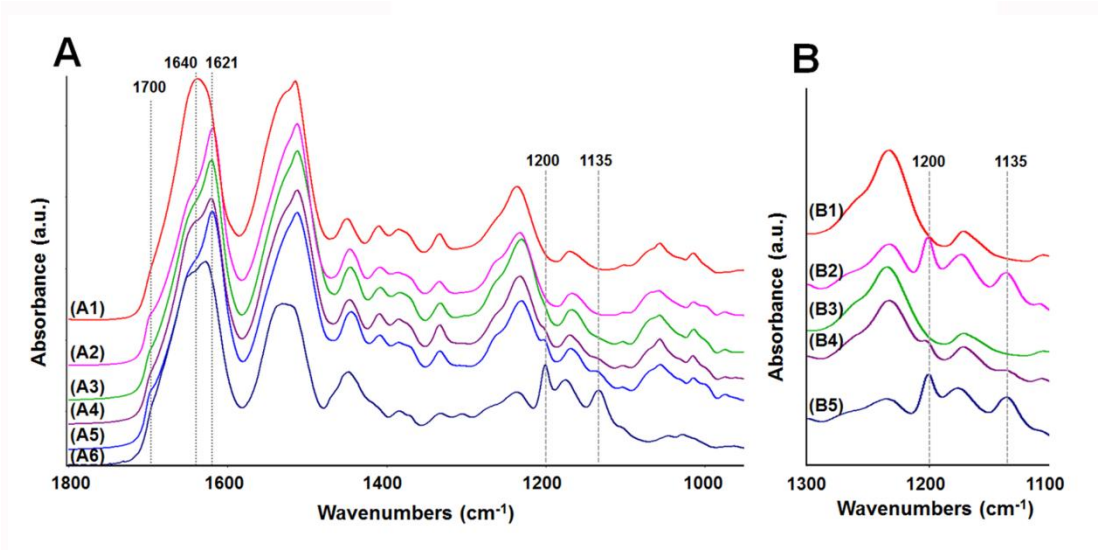

Figure 4.4. FTIR-ATR spectra of membranes. A (in the range of 1800-950 cm-1): (A1) fibroin membrane (water annealed at 25 °C, 6 h), (A2) fibroin membrane (water annealed at 60 °C, 12 h), (A3) blend membrane (fibroin:tropoelastin = 90:10), (A4) three-layered membrane – side 1, (A5) three-layered membrane – side 2, (A6) tropoelastin membrane (untreated). B (in the range of 1300-1100 cm-1): (B1) two-layered membrane (untreated) - fibroin side, (B2) two-layered membrane (untreated) – tropoelastin side, (B3) two-layered membrane (methanol treated) – fibroin side, (B4) two-layered membrane (methanol treated) – tropoelastin side, (B5) tropoelastin membrane (untreated).

In considering the differences in relative molecular weight distributions for fibroin and tropoelastin (Fig. 4.1) and our previous studies of fibroin membrane permeability (≤70 kDa using FITC-dextran) (Bray et al., 2011), the following explanation for the "missing layer" was devised (Fig. 4.5). When tropoelastin solution was cast onto the first fibroin layer it is proposed that some tropoelastin penetrated through the loosely stabilized fibroin hydrogel network. These tropoelastin molecules were subsequently trapped within the fibroin network by drying and treatment with methanol. Hence the first fibroin layer had a well-distributed content of tropoelastin as demonstrated by immunofluorescence. A small proportion of tropoelastin remaining on top of the first fibroin layer is also likely to have been washed away by methanol treatment. The final layer applied (second fibroin layer) would then appear as a single blue layer by autofluorescence.

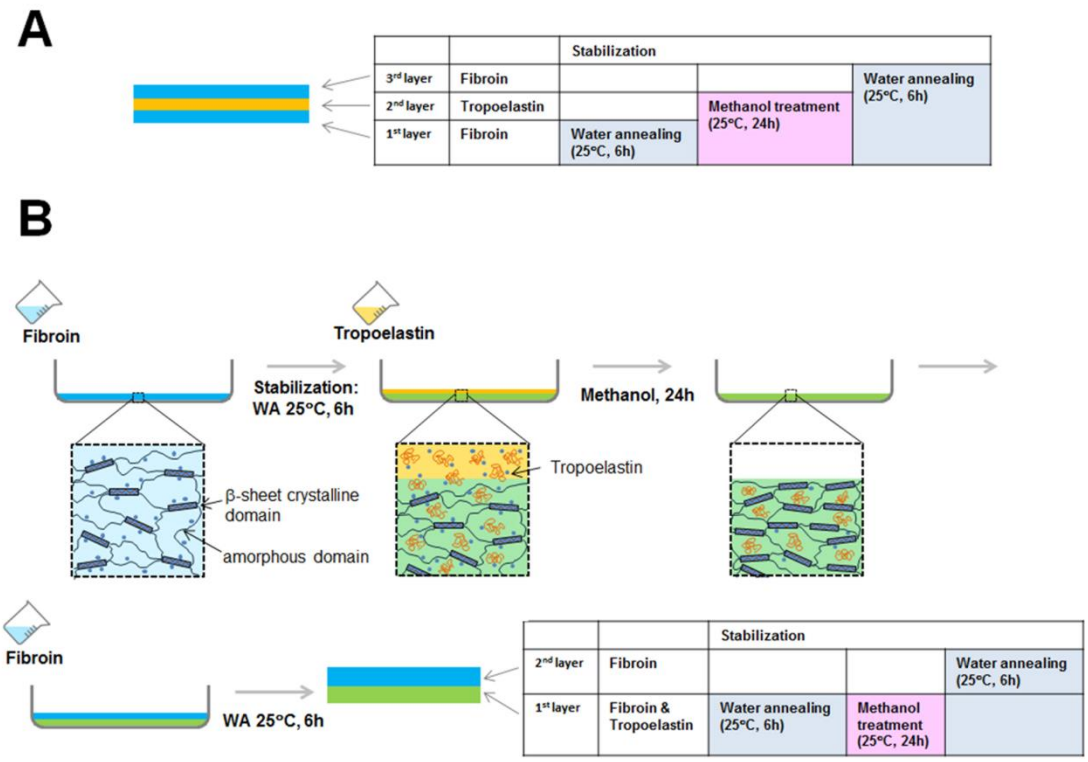

Figure 4.5. Schematic scenario of the predicted (A) and actual (B) outcomes achieved during the creation of a layered membrane of fibroin and tropoelastin. Based upon FTIR-ATR data, we propose that the bulk of applied tropoelastin is absorbed and subsequently trapped within the initially created fibroin membrane. Therefore, only two main layers are detected by immunofluorescence/microscopy.

4.4.5 Cytocompatibility of the membranes

The cytocompatibility of the fibroin, blend and layered membranes was examined over an extended culture period using current best practice culture conditions (Pfeffer & Philp, 2014). An assessment of cell numbers after three days culture (Fig. 4.6 A) was quantified using the PicoGreen® assay (DNA content provides an indication of cell numbers). There was no statistically significant difference in the number of cells attached across the three biomaterial membrane types, and when compared to the TCP control substrate. The RPE cells seeded on each membrane type showed a similar appropriate morphology over the extended culture period (Fig. 4.6 B to D).

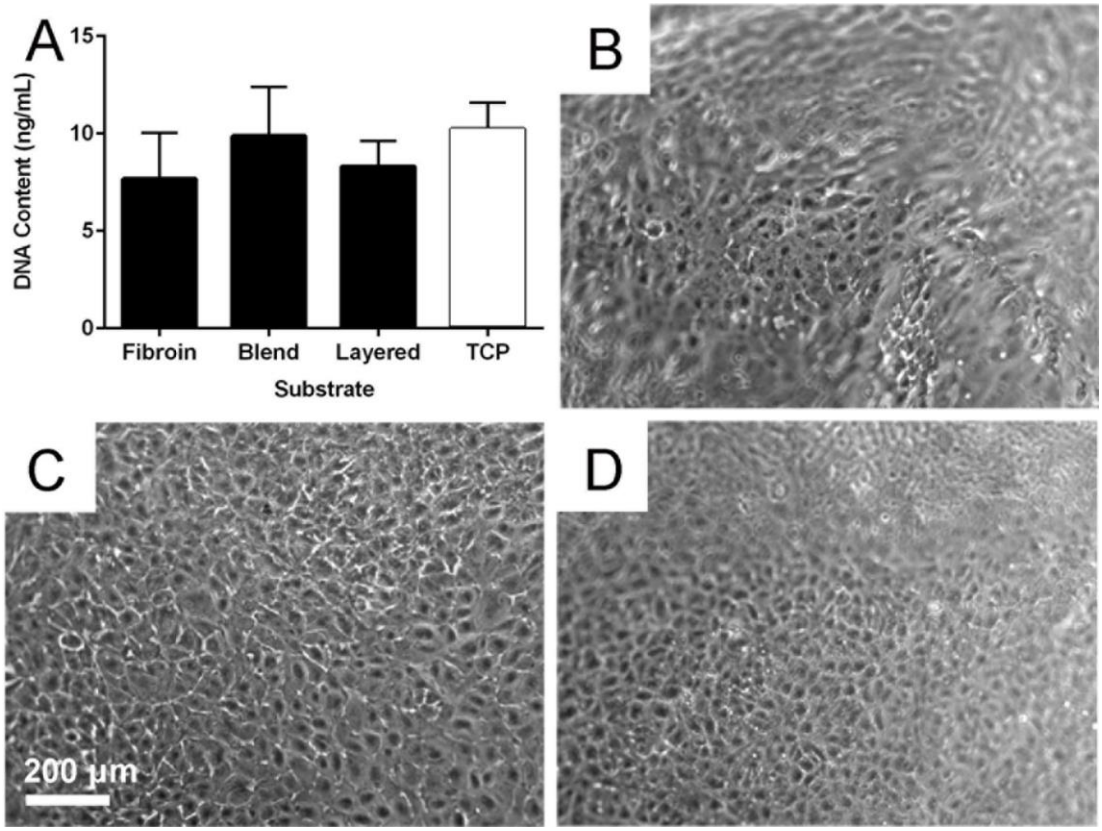

Figure 4.6. Retinal pigment epithelial (RPE) cell behaviour on biomaterial membranes. Quantification of RPE cell numbers (A) using the PicoGreen® assay after 3 days culture on fibroin, blend, and layered membranes. Tissue culture plastic (TCP) was included as control substrate. Data presented is mean (+ standard error of mean) from three experiments. Phase contrast micrographs of RPE cells after 21 days of growth on fibroin (B), blend (C), and layered (D) membranes. The undulating nature of the suspended membranes is the reason some areas of panels (B) and (D) are out of focus. The scale bar represents 200 µm and applied to the micrographs.

4.4.6 Mechanical properties of the membranes

While our primary goal is to use fibroin as a delivery vehicle for tropoelastin, it is possible that combining the two proteins may produce changes in mechanical properties that impact upon their handling during RPE cell culture and surgical implantation. As a consequence we compared the mechanical properties of standard fibroin membranes to those displayed by the blend and layered constructs. The results (Fig. 4.7) revealed significant differences between the membranes. The layered membranes, while considerably thicker than the other membranes (data presented as mean values ± standard error of the mean; layered membranes 16.667 ± 0.639 µm, compared to fibroin membranes water-annealed at 25 °C 3.610 ± 0.369 µm, fibroin membranes water-annealed at 60 °C 4.612 ± 0.540 µm, and blend membranes 6.112 ± 0.362 µm), were also more brittle (Fig. 4.7 B). In contrast,

membranes prepared using a 10 % tropoelastin by weight blend with fibroin were the stiffest (Fig. 4.7 A), however they were also strong (Fig. 4.7 B) and elastic (Fig. 4.7 C). The most interesting results were seen in the standard fibroin membranes that were water-annealed at 25 ºC. There was no statistical difference between these membranes and the fibroin membranes water-annealed at 60 ºC, however they did show different properties. The former were the only membranes that had a Young's modulus (Fig. 4.7 A) within the range of native Bruch's membrane (7-19 MPa; (Curcio & Johnson, 2013) and a useful combination of maximum tensile strength (Fig. 4.7 B) and elongation properties. This is especially clear when considering there was no difference in elongation at break when compared to the blend membrane (Fig. 4.7 C). There was also no statistical difference in recoil capacity of the fibroin (water-annealed at 25 ºC) and blend membranes after 200 cycles (Fig. 4.7 D) of stretching.

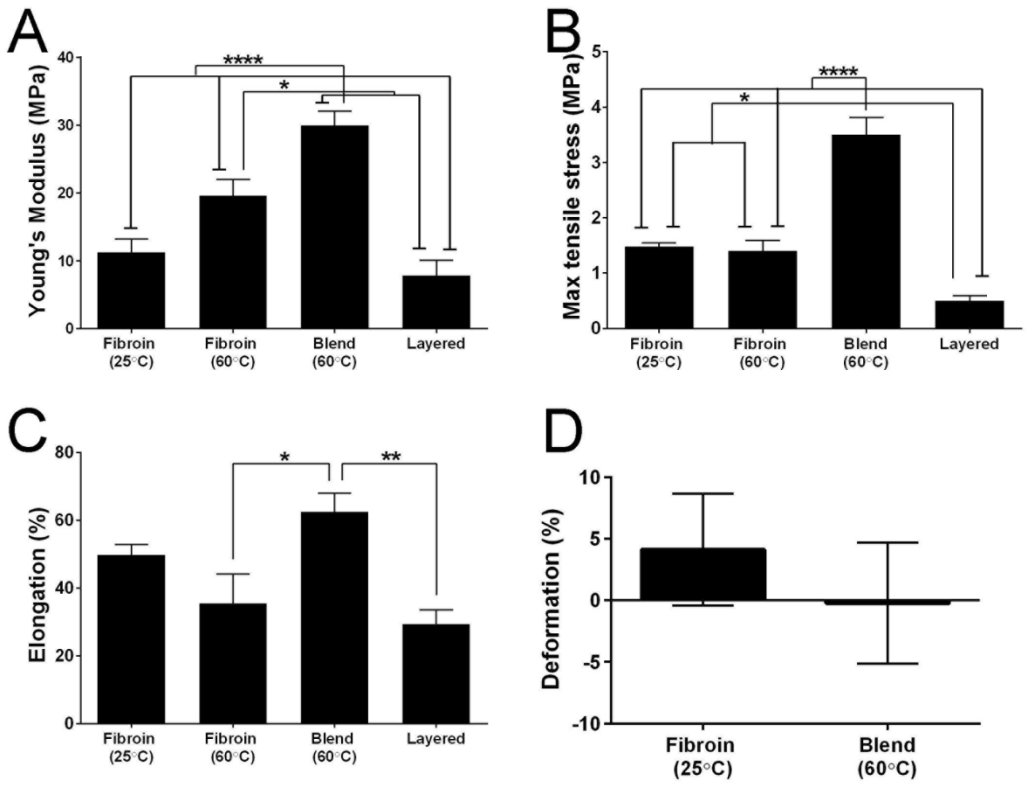

Figure 4.7. Quantitative comparison of the tensile properties of biomaterial membranes. (A) Young's modulus, (B) maximum tensile strength, (C) elongation to break, and (D) deformation/recoil capacity after 200 cycles. Bars represent mean values ± standard error of the mean. Asterisks indicate differences are statistically significant (*$p < 0.05$, **$p < 0.01$, ****$p < 0.0001$).

4.5 GENERAL DISCUSSION AND CONCLUSIONS

AMD is a leading cause of permanent vision loss in the elderly. Significant efforts are therefore underway in countries with ageing populations to address this disease. Consideration of the underlying histopathology indicates that therapies based upon the replacement of both cellular (e.g. RPE cells) as well as extracellular tissue components may well be required. To this end, we have previously demonstrated that freestanding membranes prepared from fibroin provide a potential vehicle for delivering RPE cells into the subretinal space (Chapter 3). The present study builds upon this research by examining the feasibility of incorporating elastin (in the form of tropoelastin) into these same fibroin membranes. In doing so, we have proposed that fibroin membranes may provide a vehicle for co-delivering RPE cells and tropoelastin to the subretinal space. Moreover, since tropoelastin displays similar elastic properties to elastin, we considered that the mechanical properties of fibroin membranes may be significantly altered when combined with tropoelastin.

With regard to our first aim, our data confirms the feasibility of incorporating human recombinant tropoelastin into fibroin membranes. Varying results, however, are achieved according to the methods used. In short, membranes prepared from blended solutions of the two proteins displayed a more heterogeneous composition than those produced using a sequential layering method. We propose that the patchy distribution most likely results from either phase separation or specific molecular interactions between the two proteins when present together in solution. By comparison, our subsequent analyses by FTIR suggest that the more homogenous distribution of tropoelastin achieved using the layering approach is due to absorption and subsequent fixation of this protein within the originally cast fibroin membrane (by treatment with methanol). This result suggests that membranes prepared via the absorption/fixation method should theoretically support a more even profile of tropoelastin delivery following implantation to the subretinal space. Nevertheless, the choice of technique is also likely to be influenced by consideration of membrane mechanical properties.

Our study of the effects of tropoelastin on the mechanical properties of fibroin membranes, when blended, led to some unexpected results. While others have reported reduced stiffness of fibroin membranes following inclusion of tropoelastin (Hu et al., 2011, 2010), we have presently reported the opposite result. On the

surface, this conflicting data seems quite difficult to resolve. A close comparison of the methods used, however, reveals several significant variations including the source of cocoons, fibroin isolation protocol, water annealing temperature and the thickness of membranes used. In our experience, any one of the parameters alone can have significant effects on the properties of fibroin membranes. Thus in combination, the differing processes could well have been responsible for the variations in response to the tropoelastin observed between each study.

A comparison of blended versus "layered" strategies for incorporating fibroin and tropoelastin is also an interesting exercise. On the basis of their superior strength and elasticity, it could be concluded that the blended membranes are superior to the more brittle "layered" constructs. Nevertheless, a revised formulation whereby the tropoelastin is simply absorbed and trapped, without an additional fibroin layer being deposited, is worthy of investigation. In any case, the key comparison to make is how closely each membrane resembles the mechanical properties of Bruch's membrane. It is thus significant that fibroin membranes water-annealed at 25 °C and membranes prepared using the layered approach are closest to native Bruch's membrane in terms of Young's modulus (Curcio & Johnson, 2013). Therefore on this basis, and in combination with the more uniform distribution of tropoelastin, we propose that the layered membranes are at present the better option to pursue in order to address both issues of ECM delivery as well as matching the desired mechanical properties.

Reconstructing both the cellular and ECM components of diseased and injured tissues is an important area of tissue engineering and regenerative medicine. The incorporation of a tropoelastin component in fibroin membranes, while maybe not bestowing benefits to mechanical properties, offers a potential vehicle for the delivery of RPE cells and Bruch's membrane ECM components into the subretinal environment of patients with AMD. Future studies will need to investigate the suitability of these membranes in a pre-clinical animal model.

Chapter 5: Research Study Three

Development of a cultured tissue substitute for repairing Ruysch's complex

5.1 INTRODUCTION

The previous chapters have shown that fibroin membranes can mimic some properties of Bruch's membrane, including thickness, and mechanical properties. They can also support the establishment of a functional monolayer of human RPE cells, and also show potential as a vehicle to deliver native ECM components of Bruch's membrane into the subretinal environment.

The transplantation of RPE cells, and their survival in the subretinal space, has long been established in animal models as a viable way to prevent or slow photoreceptor degeneration (Binder et al., 2007; da Cruz et al., 2007). However, a similar application to human patients is yet to be resolved. Due to the complexity of the macula and complications of human ageing, considerations in relation to the precise location and placement of the implant as well as consideration for the surgical trauma are of vital importance in the development, evaluation and use of a viable cell-based therapy (Gouras, 1998).

A novel approach was proposed by Binder et al. in 2007, outlining how a bioengineered complex could be developed with similar considerations. The proposed complex would include a functioning monolayer of RPE, a suitable biomaterial substitute for Bruch's membrane (thin, yet mechanically strong and permeable) and choroidal vascular endothelial cells that could anastomose with the patient's vasculature, helping to anchor the complex upon implantation. This hypothesis is supported by the relative success of RPE-choroid patch transplantation approaches, however allowing the potential to use of a fresh source of RPE cells, such as pluripotent stem cell-derived RPE cells or adult RPE stem cells.

Choroidal vascular endothelial cells and RPE cells have been grown together in culture previously and the interaction was described by Sakamoto et al. (1995). This group highlighted the heterogeneity and organ-specificity of vascular endothelial cells, and showed that vessel formation by choroidal-derived vascular endothelial cells *in vitro* is modulated by RPE cells. Both cell types used in this study were

isolated from bovine tissue. The presence of the RPE cells promoted angiogenesis of the vascular endothelial cells within the collagen type I gel. Unfortunately the culture system did not use a substitute for Bruch's membrane, and there was no physical barrier (other than the 50-300 μm collagen gel) between the two cell types. Therefore it was not truly representative of the subretinal architecture.

An alternative RPE-choroidal endothelial cell co-culture model was established and described by Fan et al. (2002). The authors put special emphasis on co-culturing the cell types with a definite interface between them. Fan and colleagues were able to show functional interactions between co-cultured ARPE-19 cells and human primary choroidal-derived endothelial cells. Nevertheless their co-culture setup allows these interactions to be studied primarily as an *in vitro* model only, with no ability to use it in an *in vivo* application. The co-cultures were assembled by placing cultures of ARPE-19 cells grown on Transwell® filters over human primary choroidal-derived endothelial cells sandwiched within a collagen gel coating the TCP surface below. There was a functional interface between the two cell types however the complex was essentially two parts grown closely together. By this definition, their construct cannot be considered as a reconstruction of Ruysch's complex with a Bruch's membrane substitute.

A simpler model of the RPE-Bruch's membrane-choriocapillaris complex was established and described by Hamilton et al. (2007). This *in vitro* model used ARPE-19 cells, denuded human amniotic membrane, and human umbilical vein endothelial cells (HUVECs) to replicate the three *in vivo* layers. Results from this group show their trilayer culture is a promising model; however, the use of amnion and HUVECs pose several problems. Amnion, like any allogenically derived material, could be a source of infection and disease transmission to the eventual patient. More importantly, the thickness of amniotic membrane at 60-100 μm is not an appropriate substitute for the much thinner native Bruch's membrane (3 μm). Human amniotic membrane has also been found to be a source of growth factors (Shao et al., 2004) that could potentially alter the critical balance of growth factors required for normal retinal structure and function. Finally, HUVECs, derived from the vein of the umbilical cord, are a macrovascular cell type and may well lack the specific features required to replicate the distinct and small capillary vessels of the choriocapillaris. A microvascular endothelial cell line or specifically choroidal-

derived endothelial cells like the ones described by Sakamoto et al. (1995) and Fan et al. (2002) would be a better representation of the *in vivo* environment.

The goal of the present study was therefore to investigate the feasibility of incorporating a vascular endothelial cell component to the RPE-fibroin membrane complex. In an attempt to accurately replicate the subretinal architecture, choroidal vascular endothelial cells were suspended within a collagen gel to create a 3D matrix on one side of the fibroin membrane. The effect of mature RPE cells on the behaviour of the choroidal vascular endothelial cells was subsequently examined.

5.2 MATERIALS AND METHODS

5.2.1 Production of aqueous solutions of fibroin

The procedure has been previously described in detail by our group (Chirila et al., 2008). Briefly, dried *Bombyx mori* silkworm cocoons (Tajima Shoji Co. Ltd., Yokohama, Japan) were boiled in a solution of sodium carbonate containing 0.85 g of salt for each gram of cocoon material. This procedure removed the sericin outer coat from the core fibroin protein. The resulting fibrous material was washed and dried, and then dissolved (at 60 °C for 4 hours) in a concentrated solution of lithium bromide (9.3 M) to obtain a silk concentration of approximately 10 % wt./vol. The fibroin solution was subsequently filtered using syringe filters in succession with pore size 0.7 μm and 0.2 μm. This step is performed slowly to avoid shearing forces that could promote spontaneous gelation. The filtrate was dialyzed against water using a dialysis cassette with a molecular mass cut-off of 3.5 kDa (Slide-A-Lyzer, Pierce Biotechnology) using 6 changes of water over 3 days. The resulting fibroin solution was filtered again as above and used to produce fibroin membranes.

5.2.2 Preparation of fibroin membranes

Fibroin membranes were cast using a custom-made casting table as described previously by our group (Bray et al., 2011). The thickness of fibroin membranes was measured using an upright micrometer and only areas of membrane 3 μm ± 1 μm thick were used. For structural stabilisation of fibroin membranes, β-sheet formation was induced by the water-annealing of the membranes in a vacuum oven at -80 kPa with ~100 mL water (beaker) for 6 hours at room temperature (25 ºC). The permeability of fibroin membranes has been previously examined using a horizontal diffusion cell using 3 model molecules (Bray et al., 2011).

5.2.3 Routine RF6A culture

The microvascular endothelial cell line, RF6A (CRL-1780™, ATCC®) was derived from fetal rhesus monkey (*Macaca mulatta*). It was used for this study because it is a choroidal derived vascular endothelial cell source. The culture medium, 'Endothelial medium', used with these cells is MCDB 131 Base media (Life Technologies) supplemented with 1% glutamine, 1 % penicillin and streptomycin, 0.08 % hydrocortisone, 0.1 % EGF, 0.1% heparin, 0.1 % FGF and 10 % FBS (Gillies et al., 2015). Stock cultures are grown on Attachment Factor (AF, Life Technologies).

5.2.4 Examining RF6A cell attachment and growth on fibroin

Cell attachment and growth of microvascular endothelial cells on fibroin coated with Attachment Factor (AF, Life Technologies) or Collagen I (0.3 mg/mL, Cellmatrix®, Nitta Gelatin Inc.) was compared and quantified. The microvascular endothelial cell line, RF6A cells were seeded at a density of 25,000 cells/cm^2 and incubated at 37 °C, 5 % CO_2 for 4 hours using Endothelial medium without serum, or for 72 hours using full Endothelial medium (i.e. with 10 % serum). Uncoated fibroin and tissue culture plastic were used as control substrates. Both experiments were performed in triplicate, with each substrate type tested in triplicate. Relative cell numbers were quantified using the Quant-iT PicoGreen dsDNA kit (Molecular Probes, Invitrogen, Life Technologies).

5.2.5 Preparation of Collagen I gel

The collagen type I solution was polymerised into a gel using the correct pH, temperature and physiological solutions as per manufacturer's instructions. Ice-cold collagen type I solution (pH 3.0) was mixed with a 10X sodium chloride solution and a Buffer Solution (50 mM sodium hydroxide, 260 mM sodium bicarbonate and 200 mM HEPES, pH 8.0). Solutions were mixed in a ratio of 8:1:1, and kept ice-cold before and after mixing. The collagen gel polymerised when the combined solution was transferred to 37 ºC. Collagen fibres were labelled with fluorescein isothiocyanate (FITC) by adding a 1 mg/mL concentration of FITC to the Buffer Solution. The collagen type I gel solution was then diluted 1:1 with culture medium containing the appropriate concentration of cells. Once transferred to 37 °C, the cells were suspended within the polymerising collagen gel.

5.2.6 Cell culture of human RPE cell line, ARPE-19

ARPE-19 cells were routinely cultured using the Miller's medium formulation (Maminishkis et al., 2006); minimum essential medium, alpha modification (MEM-α, M-4526) supplemented with N1 supplement (N-6530), glutamine-penicillin-streptomycin (G-1146), non-essential amino acids (M-7145), taurine (T-0625), hydrocortisone (H-0396) and triiodo-thyronin (T-5516). All these components were purchased from Sigma Aldrich. This medium formulation allows RPE cultures to be incubated at 37 °C using a standard level of 5 % CO_2 air. Cultures were established in the presence of 10 % FBS, and after 24 hours this serum level was decreased to 1 %. Stock cultures were fed two to three times per week, and passaged routinely using Versene (15040-066, Life Technologies) and TrypLE™ (12563-011, Life Technologies), between passages number 23 and 28. An independent STR profile analysis of our working stocks by the Garvan Institute of Medical Research revealed a 100 % match with reference ARPE-19 cell line CRL-2302.

5.2.7 Using fibroin membranes in Teflon® chambers for cell culture

Discs of ultrathin fibroin membrane (16-mm diameter) were inserted into custom-made chambers designed by our group, which are manufactured from interlocking Telfon® rings specifically for cell culture use (Fig. 3.1). The combined membrane and chamber were sterilised together by immersion in 70 % ethanol for 1 hour at room temperature, air-dried and washed thoroughly with PBS prior to use. The custom-made chamber suspends the fibroin membrane (reminiscent of the commercially available Transwell® insert system) creating an apical compartment (upper chamber) and a basal compartment (lower chamber) on either side of the membrane (Fig. 3.1). This culture setup is required for the development of a polarised epithelial culture.

5.2.8 Longterm culture of ARPE-19 cells on ultrathin fibroin membranes

ARPE-19 cells were seeded onto the apical surface of ultrathin fibroin membranes in chambers at a density of 10,000 cells/cm^2. Membranes were precoated on both sides with the collagen type I solution diluted (1 in 10) in MilliQ water. The membranes are coated with the diluted collagen solution and incubated at room temperature for 1 hour. The excess solution is removed and membranes are dried at room temperature. Membranes are washed twice with culture medium before cell

seeding. ARPE-19 cultures were incubated at 37°C and 5% CO_2, and were fed twice weekly, with Miller medium used in both the apical and basal compartments.

5.2.9 Co-culture of ARPE-19 cells, RF6As in collagen gel on either side of fibroin membrane

Collagen gel solution was prepared as per section 5.2.5. The mature RPE monolayers (established in section 5.2.8) were grown for 2 months before co-cultures were attempted. In order for culture conditions to be consistent all chambers were inverted. This meant the mature RPE monolayer would now be "underneath" the fibroin membrane, facing into the basal compartment of the Teflon® chamber. This chamber orientation would allow the RF6A cells in collagen gel to be added to the top of the fibroin membrane, and easy monitoring of the collagen gel over the culture period. The co-cultures were established using two seeding patterns in an attempt to reconstruct choriocapillaris morphology. The first attempt mixed approximately 4,700 cells in 62.5 µL of culture medium with an equal volume of collagen type I gel solution (which equates to 40,000 cells/mL or 25,000 cells/cm^2 as used in section 5.3.2).This total volume (125 µL) was added to the apical side of the fibroin membrane. The second experimental seeding pattern used 2,500 cells (5,000 cells/cm^2) seeded as a monolayer on the apical surface of the fibroin membrane, and 3,000 cells in a total volume of 62.5 µL (1:1 ratio of culture medium and collagen gel solution equalling 48,000 cells/mL or 30,000 cells/cm^2) was added after a 2.5 hour attachment time. Control cultures were established for both experimental seeding patterns, with the same volumes of RF6A cells with collagen gel solution added to the apical side of fibroin membranes that did not have a mature RPE monolayer on the underside. The diameter of the collagen gel was monitored over the culture period, and the maximum time in co-culture was 8 days.

5.2.10 Confocal microscopy

Confocal microscopy (Nikon A1R) was used to visualise the three dimensional cultures (DIC40X, oil immersion, 1.000 µm steps, 1.0 AU pinhole). Samples were stained with Rhodamine Phalloidin (R415, Life Technologies) and Hoechst nuclear dye (H1399, Life Technologies) for 1 hour at 37 °C, and mounted on glass slides that had been built up so the collagen gel was not squashed. The three dimensional structure of the cultures were imaged and visualised using Nikon NIS-Elements software.

5.2.11 Statistical analyses

The cell attachment and proliferation data results were analyzed for statistical significance using a one-way ANOVA followed by a Tukey's multiple comparisons test comparing substrate type. Statistical analyses were performed using GraphPad Prism, V 6.

5.3 RESULTS

5.3.1 Cytocompatability of choroidal vascular endothelial cells on fibroin

The attachment and growth of choroidal vascular endothelial cells (RF6A) on fibroin was evaluated, and the effect of different extracellular matrix coatings on the fibroin were compared (Fig. 5.1). At 4 hours in serum-free conditions, the attachment of cells to fibroin alone, and fibroin coated with AF or collagen type I was significantly lower than the attachment to TCP (Fig. 5.1 A). However, after 72 hours in the presence of serum, this trend had reversed and the relative total cell numbers (relative to the measurement of DNA content) measured on fibroin coated with AF or collagen type I was significantly higher than the growth on TCP (Fig. 5.1 B). There was no difference in growth between AF and collagen type I, both ECM coatings supported similar cell numbers.

The morphology of the RF6A cells seeded on the different culture substrates was visualised by phase contrast microscopy over the time period (Fig 5.2). There was no obvious difference in morphology when comparing the different culture substrates after 4 hours attachment (Fig. 5.2 A to D). The cells exhibited similar stellate morphology with the extension of pseudopodia. Nevertheless, there were less rounded cells with halos on TCP (Fig. 5.2 A), which indicates that more cells have attached and started to spread out on TCP at this time point in comparison to the fibroin alone and coated fibroin substrates (Fig. 5.2 B to D). This result supports the relative cell number values recorded (via measurement of DNA content) on the different substrates at 4 hours (Fig 5.1 A). The morphology of the cultures at 72 hours (Fig. 5.2 E to H) also seems to support the relative cell number values (Fig. 5.1 B). The morphology and density of cells on the fibroin alone, and coated fibroin substrates (Fig. 5.2 F to H) were different to the cells on TCP (Fig. 5.2 E). There were more spherical cells with halos on the TCP substrate, and the TCP surface was

evident between cells. There was no obvious difference in morphology between AF and collagen type I coated fibroin substrates (Fig. 5.2 G and H).

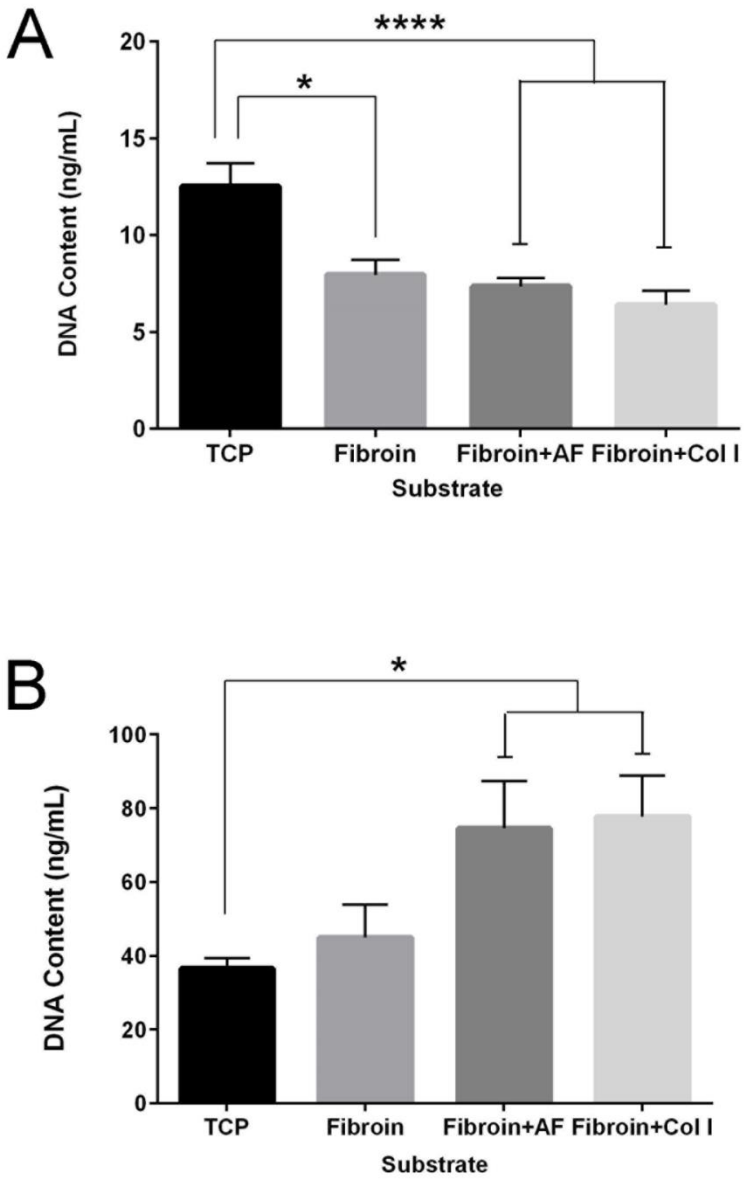

Figure 5.1. Comparison of choroidal vascular endothelial cell (RF6A) attachment and growth on either fibroin, fibroin coated with Attachment Factor (+AF), or fibroin coated with collagen I (+Col I). Cultures of RF6A were evaluated for (A) cell attachment after 4 hours in serum free conditions (with washing prior to measurement), and (B) total cell numbers after 72 hours in the presence of 10 % (v/v) serum. Tissue culture plastic (TCP) was used as a control substrate. Each substrate was tested in triplicate for each time point. DNA content was measured using the Picogreen® assay to provide an indication of cell numbers. Bars represent the mean values (+ standard error of the mean) from three experiments. Statistical difference in means indicated (*p< 0.05, ****p<0.0001).

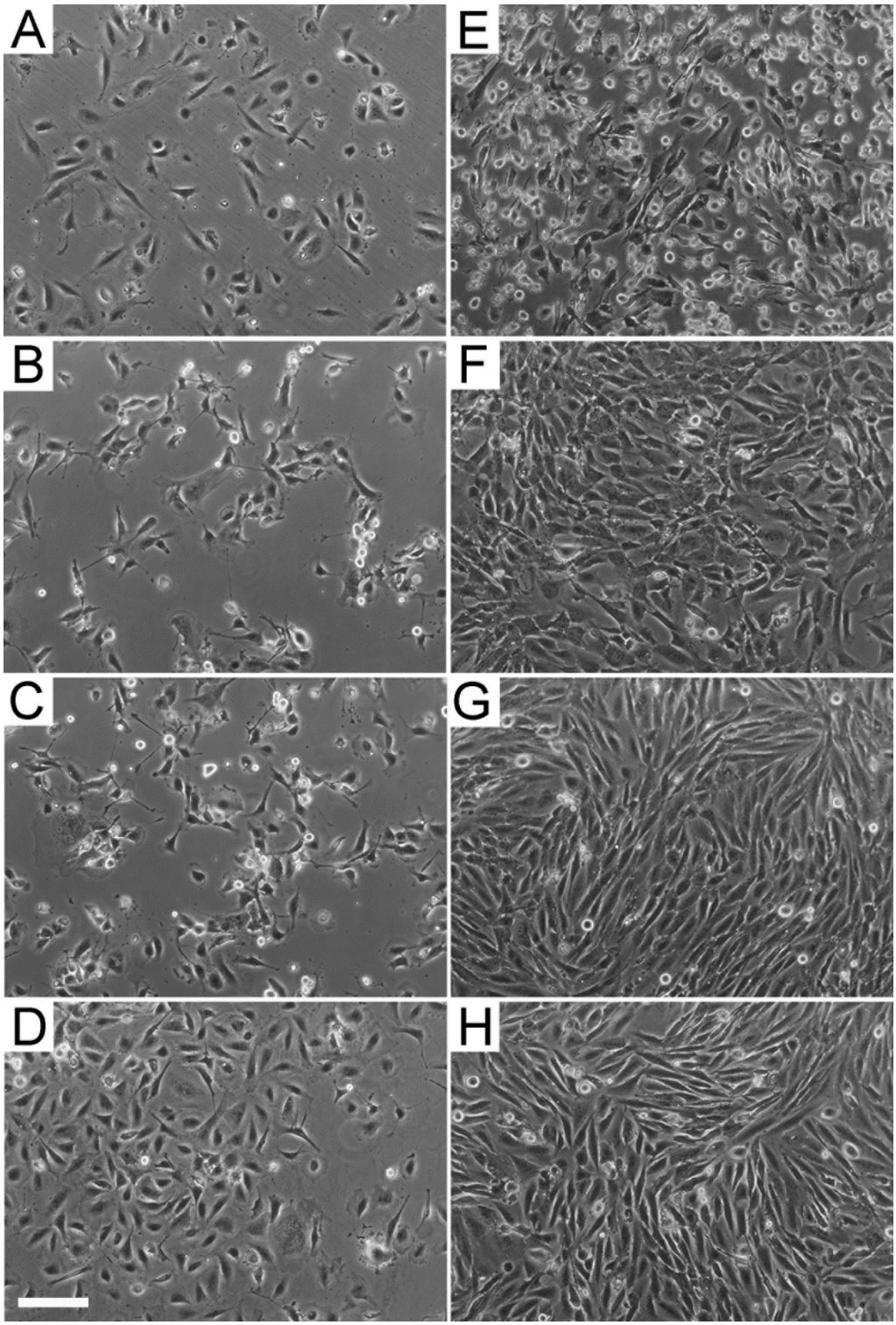

Figure 5.2. Comparison of choroidal vascular endothelial cell (RF6A) attachment and growth on either (A and E) tissue culture plastic (TCP), (B and F) fibroin, (C and G) fibroin coated with Attachment Factor, or (D and H) fibroin coated with collagen I. Cultures of RF6A were grown without serum for 4 hours (A to D) or 72 hours in the presence of 10 % (v/v) serum (E to H). Panel D shows a particularly dense cluster of cells however this density was not uniform across the culture substrate. All micrographs taken at 20X magnification using phase contrast microscopy. Scale bar represents 200 µm and applies to all panels.

5.3.2 Morphology of choroidal vascular endothelial cells seeded within a collagen type I gel

Optimisation of choroidal vascular endothelial cells (RF6A) seeding density within the collagen gel 3-D matrix was evaluated by comparing the morphology of cells with increasing cell density (Fig. 5.3). The higher the initial seeding density, the more the collagen gel contracted over 2 weeks in culture (Fig. 5.3 A). As expected, when optically sectioned using confocal microscopy, cell numbers increased proportionately with the increase in initial seeding density (Fig. 5.3 B to D). Although evidence of cell-cell contacts and branching was observed, it was difficult to identify specific interactions between the collagen matrix and the cells.

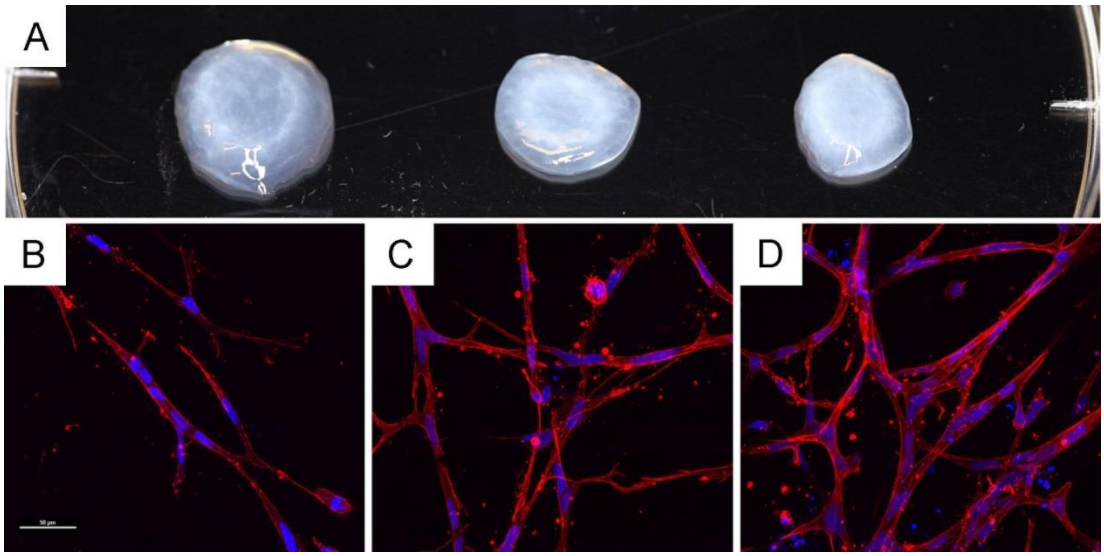

Figure 5.3. Choroidal vascular endothelial cells (RF6A) grown in collagen gel. (A) Photograph of three collagen gels in 90-mm diameter petri dish. Each gel in (A) corresponds to the micrograph directly below. (B to D) Morphology of vascular endothelial cells (RF6A) seeded within collagen gels. (B) Seeded with 25,000 cells/cm^2, (C) seeded with 50,000 cells/cm^2, (D) seeded with 100,000 cells/cm^2. Red is F-actin stained with rhodamine phalloidin, and blue is nuclei stained with Hoechst nuclear dye. Scale bar represents 50 µm and applies to panels B to D.

5.3.3 Labelling the collagen type I gels with fluorescein isothiocyanate (FITC)

The self-assembly process of collagen fibril formation in vitro was exploited by adding a 1 mg/mL FITC solution to the buffer (pH 8.0) solution combined with the collagen type I solution. As the gel polymerised the FITC was incorporated into the collagen fibrils. When examined using confocal microscopy the gels fluoresced green using a 488 nm laser (Fig. 5.4). The addition of FITC did not appear to adversely affect cell morphology, and allowed the visualisation of tracks made by migrating cells (data not shown) and the interaction of the cells with their three dimensional environment.

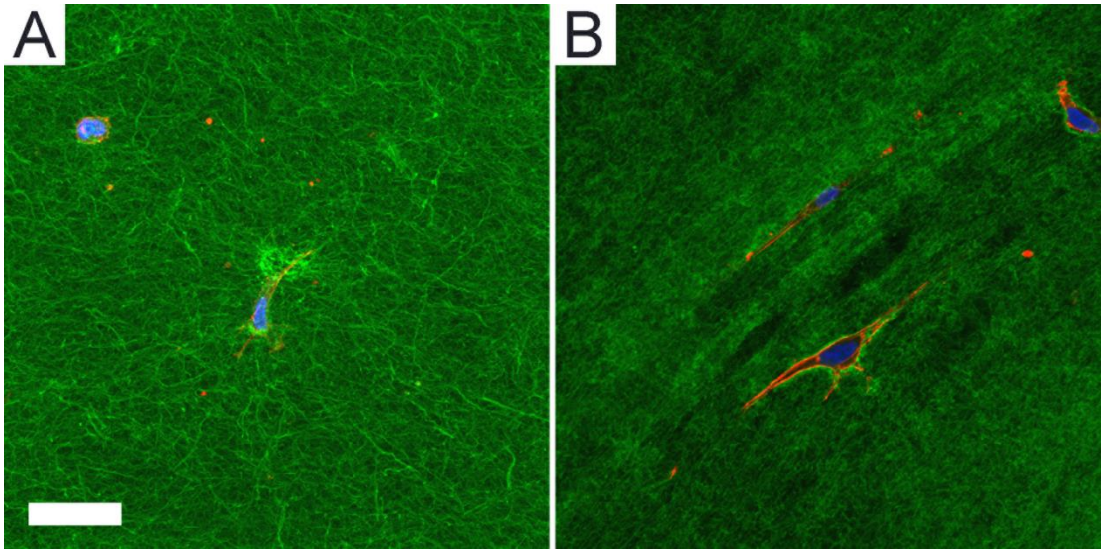

Figure 5.4. Micrographs (imaged using confocal scanning laser microscopy) of collagen I gels that have been labelled with fluorescein isothiocyanate (FITC). (A) The collagen fibers are clearly identified with FITC labelling (green). (B) The processing of this sample has changed the presentation of the collagen fibers, however, it has allowed the visualisation of the choroidal vascular endothelial cells that have been incorporated into the gel during polymerisation. Red is F-actin stained with rhodamine phalloidin, and blue is nuclei stained with Hoechst nuclear dye. Cells had been in culture for 3 days. The scale bar represents 50 µm and applies to both images.

5.3.4 Effect of mature RPE cells on choroidal vascular endothelial cell behaviour

The establishment of the co-cultures was relatively simple, and the fibroin membranes acted as a physical barrier between the two cell types. Interestingly, when a collagen gel seeded with RF6A cells was polymerised onto a fibroin membrane with a monolayer of mature RPE cells on the other side, the collagen gel did not contract over 8 days (Fig. 5.5 B and D). In contrast, when the collagen gel with RF6A cells was cultured without a RPE monolayer, it contracted after a few days and was significantly smaller by 8 days (Fig. 5.5 A and C). This result is consistent with earlier experiments (Fig. 5.3). As shown in Fig. 5.6, the difference in diameter of the collagen gels with and without a RPE monolayer was statistically significant. The morphology of the RF6A cells was also different between treatment groups. Specifically, in the presence of the mature RPE monolayer (Fig. 5.7), cells exhibited an elongated morphology, and a network of cells had formed parallel to the fibroin membrane (Fig. 5.7 B). Without the presence of a mature RPE monolayer, however, the RF6A cells clumped together with the collagen fibres localised around these cells (Fig. 5.7 A).

A three dimensional reconstruction (Fig. 5.8) of the co-culture (same culture as Fig. 5.7 B), shows the monolayer of RPE cells on the fibroin membrane. Vascular endothelial cells, which formed elongated branching networks of cells parallel to the fibroin membrane, were observed on the underside of the membrane.

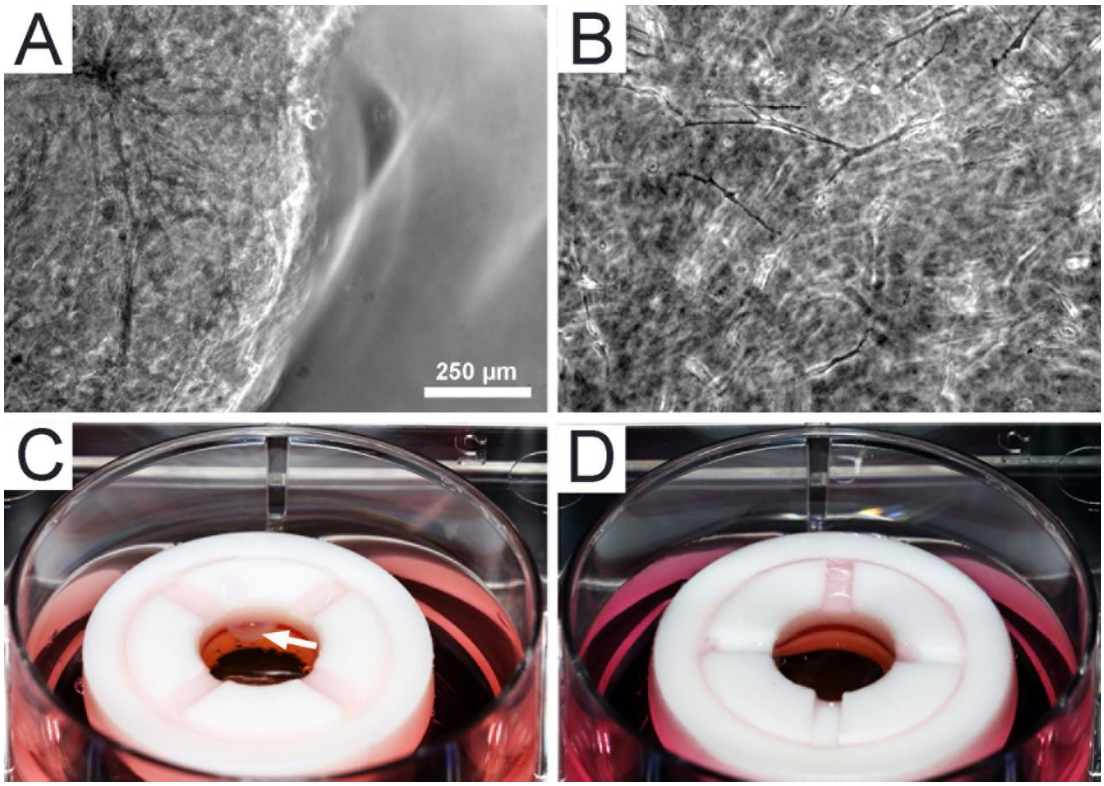

Figure 5.5. Comparison of choroidal vascular endothelial cell (RF6A) morphology and collagen gel contraction after 8 days in the presence or absence of a monolayer of mature RPE cells. An ultrathin fibroin membrane was suspended inside the custom-made Teflon chambers. (A and C) A collagen gel seeded with RF6A cells polymerised onto fibroin membrane. (B and D) A collagen gel seeded with RF6A cells polymerised onto fibroin membrane that had a monolayer of mature RPE cells (ARPE-19) on the underside. (A and C) After 8 days the collagen gel has contracted. The edge of the collagen gel with cells can be seen in panel A, and the contracted gel within the chamber is highlighted by arrow in panel C. (B and D) In the presence of a mature monolayer of ARPE-19 cells the collagen gel has not contracted. The collagen gel still fills the majority of the apical compartment (above the fibroin membrane). The collagen gels were seeded with the exact same number of cells and the only difference is the presence or absence of RPE cells. The first study was performed in triplicate for each culture set up arrangement. The scale bar represents 250 µm and applies to panels A and B.

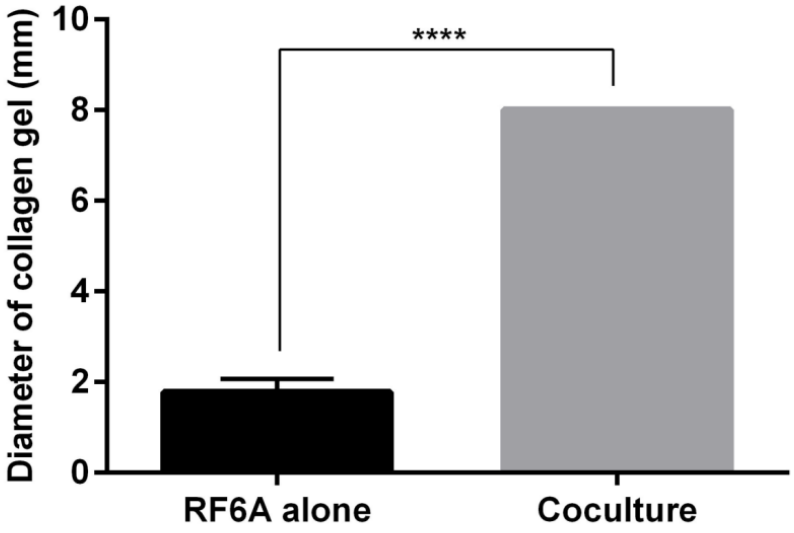

Figure 5.6. Difference in diameter of collagen gels with and without the presence of a mature RPE monolayer after 8 days in culture (****$p < 0.0001$). Data presented represents mean (+ standard error of mean) from 5 samples for each culture condition.

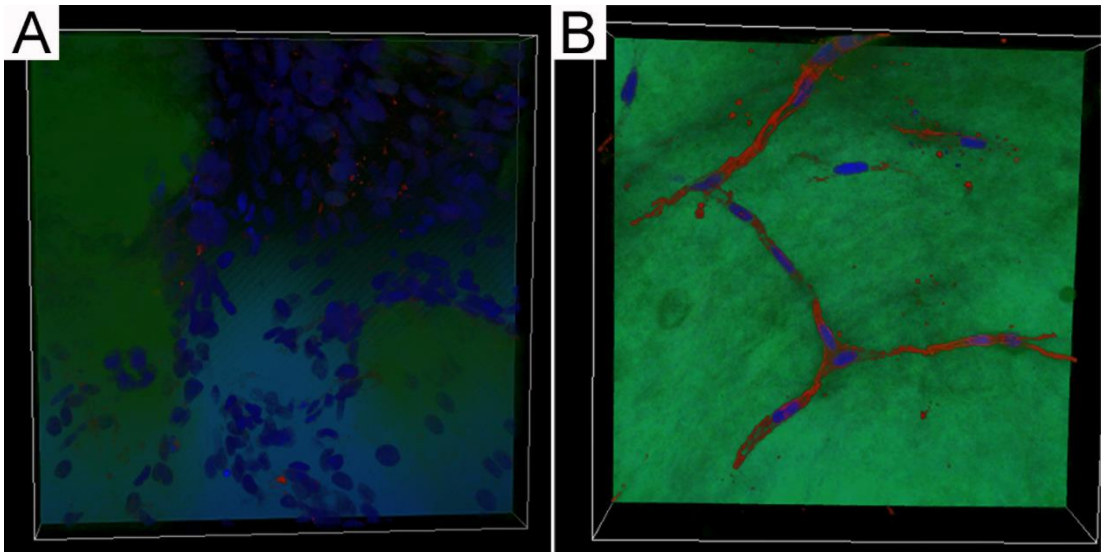

Figure 5.7. Comparison of RF6A cell morphology when grown for 8 days in a collagen gel on a fibroin membrane, with or without the presence of a mature RPE monolayer. (A) RF6A cells (nuclei; blue) are clumped together with very little cytoskeletal morphology seen (F-actin; red), and the collagen gel (green) has been pulled tightly around the cells. (B) RF6A cells seeded within collagen gel in the presence of a mature RPE monolayer exhibit a relaxed, elongated morphology, making connections with neighbouring cells. Area of sample represents 318.20 μm^2.

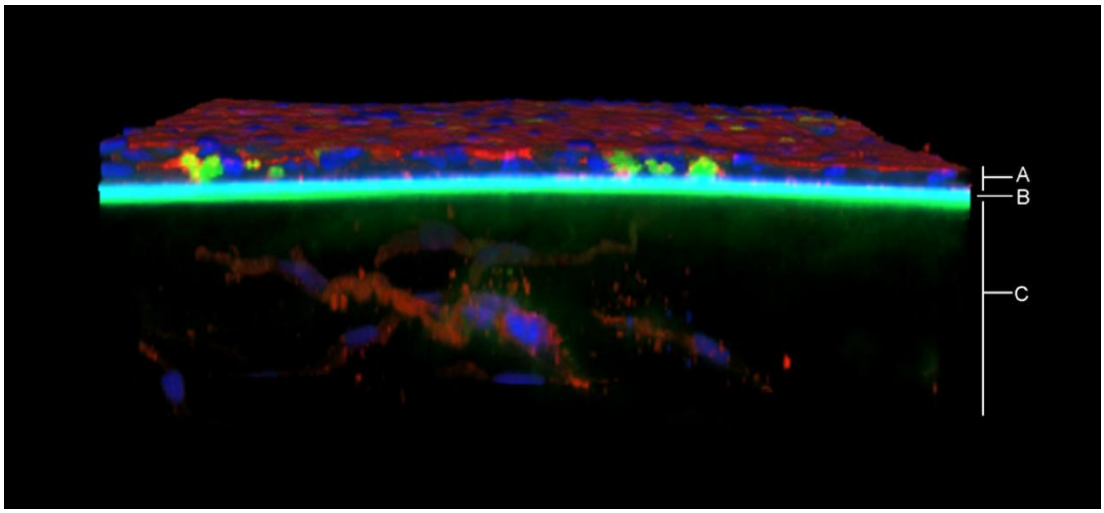

Figure 5.8. A three-dimensional projection of a mature RPE monolayer (A), grown on a fibroin membrane (B, pale blue), with RF6A cells growing within a collagen gel underneath (C, green is FITC staining of collagen fibres). Both cell types have F-actin (red) and nuclei (dark blue) staining. The RPE have taken up some loose FITC which can be seen as clumps of green in the cytoplasm of the cells. Area of sample equals 318.20 μm^2 x 120 µm Depth.

5.4 DISCUSSION

The structural and functional changes that occur in Ruysch's complex with age significantly affect the viability and survival of photoreceptors, and ultimately vision. Surgical replacement of this complex has shown promise, however issues continue to arise in relation to surgical trauma, graft rejection and the persistent pathogenesis and natural history of AMD.

The aim of this study was based on the "bioprosthesis" proposed by Binder et al (2007), the development of a cell-based complex that is representative of Ruysch's complex *in vivo*. We used a fibroin membrane, as a substitute for Bruch's membrane. The fibroin membrane has been shown to have characteristics of a functioning, native Bruch's membrane, including appropriate thickness, permeability and mechanical strength, and can also support a functioning monolayer of mature RPE cells. In this chapter we demonstrated that the fibroin membrane can support a culture of choroidal-derived vascular endothelial cells contained within a collagen type I gel. We demonstrated that the fibroin membrane facilitates movement of modulating factors between the mature monolayer of the RPE cells and the choroidal vascular endothelial cells while keeping a physical barrier between the two cell types.

In our study we utilised a choroidal vascular endothelial cell line (RF6A) derived from Rhesus monkeys. This cell line was selected for preliminary feasibility testing prior to extending the study to human primary cells. As with all vascular endothelial cells, the RF6A cell cultures benefit from an ECM coating to improve attachment and proliferation on the scaffold material. A standard ECM coating is a solution called Attachment Factor (AF) which is a proprietary blend of proteins containing gelatin which enhances the growth of microvascular endothelial cells. In order for the co-culture to be representative of the subretinal architecture, a three dimensional gel was used similar to previous studies (Fan et al., 2002; Sakamoto et al., 1995).

A commercial collagen type I (Cellmatrix®, Nitta Gelatin Inc.) solution (which can be polymerised into a gel) was shown to support microvascular endothelial cell growth comparable to AF. When grown in the presence of serum there was no difference in total cell numbers after 72 hours when comparing the two ECM coatings, and there were no obvious differences in cell morphology. An appropriate

morphology was also seen in cells that were suspended within a collagen type I gel. The co-cultures created in this study displayed longevity as a three dimensional structure throughout the culture period and during processing for confocal microscopy. The fibroin membrane acted as a physical barrier between the two cell types, yet was able to facilitate some form of communication between the two cell types, which was evidenced by the difference in contraction of the collagen gel matrix with and without the presence of the mature RPE monolayer. The collagen gels were seeded with the same initial number of RF6A cells, however, without the presence of a mature monolayer of RPE the collagen gel matrix contracted significantly over the 8 day culture period.

Future studies could investigate the mechanisms and causes for this variation. In the presence of a mature RPE monolayer, the RF6A cells may be establishing in a more polarised environment and therefore lumen formation is being encouraged (Montaño et al., 2010). The RPE secrete both pro- and anti-angiogenic factors, and therefore the difference in morphology and collagen matrix contraction may be a direct effect of modulating factors being released by the mature RPE monolayer. Previous studies have shown RPE cells can mediate effects on choroidal vascular endothelial cells (Fan et al., 2002; Sakamoto et al., 1995) which can be inhibited by blocking the specific factors. The difference in contraction could be primarily due to a difference in RF6A proliferation rate under the two culture conditions, and therefore digestion of the collagen gel matrix and quantification of DNA content using a Picogreen assay could give a representation of the total cell numbers at different time points. This difference would still be modulated by the presence of the RPE cells, and further studies could elucidate the cause.

It would also be interesting to examine the benefits that might be conferred to the RPE cells in the co-culture system. Examining the functionality of the RPE cells with and without the presence of vascular endothelial cells would give further insight to the interactions that occur in Ruysch's complex and, potentially, the progression of disease. In the presence of the vascular endothelial cells there may be a difference in protein expression and cellular polarisation of the RPE cells. There may also be differences in levels of growth factor secretion and phagocytic ability. A functioning Ruysch's complex relies on communication between the RPE and the choroidal

blood supply and issues start to arise and the progression of natural history of AMD is often triggered by this communication breakdown.

The future evaluation of fibroin membranes in a co-culture complex will need to utilise human primary cell sources for both cell types. Currently a fetal source is the gold standard RPE cell type (Sonoda et al., 2009; Maminishkis et al., 2006), and adult vascular endothelial cells can be isolated and grown in culture using MACS® sorting, selective cell surface markers, and specialised culture medium (Gillies et al., 2015). These cell types would provide a more robust evaluation of fibroin membranes and allow quantification of the morphological and functional changes that occur to human choroidal-derived vascular endothelial cells in the presence of RPE cells.

Ultimately this complex has been designed as a cell-based therapy that with further investigation and modification could be used as a graft implant. In evaluating its ability to function as an *in vivo* complex, this co-culture could be used to model elements of AMD disease. This could be done by modifying growth factor concentrations on either side of the membrane, by introducing toxic substances that can cause oxidative damage, and by potentially making changes to the fibroin membranes themselves to better represent an aged Bruch's membrane and study the cellular changes that might occur in response. This could be done by increasing membrane thickness, reducing membrane permeability, and maybe even by adding a lipid component to the fibroin protein.

5.5 CONCLUSIONS

In the current study we have shown that fibroin membranes support the co-culture of RPE cells and choroidal-derived vascular endothelial cells and therefore demonstrate potential as a Bruch's membranes substitute. Significantly, we demonstrated that there was a difference in morphology of the choroidal-derived vascular endothelial cells when co-cultured in the presence of a mature monolayer of RPE cells, and that while the fibroin membranes formed a physical barrier between the two cell types, there was evidence of some form of cell-cell communication. Future studies will need to employ primary cell sources to confirm and quantify these results. If successful, the potential of fibroin membranes as a vehicle for RPE and choroidal vascular endothelial cell implants could then be determined *in vivo*.

Chapter 6: Summary and Future Directions

Many biomaterials have been proposed as a vehicle for RPE cell implantation, and as a material for repairing Bruch's membrane. None of these biomaterials, however, currently fulfil the range of specific structural and functional criteria of Bruch's membrane. The purpose of this project was therefore to evaluate fibroin as a possible Bruch's membrane substitute. In an effort to engineer a tissue construct that resembles the three tissue layers of Ruysch's complex, this project was designed with three separate but closely linked studies. I evaluated the functionality of RPE cells grown on fibroin membranes, evaluated the feasibility of modifying fibroin membranes to include ECM components vital to the native structure of Bruch's membrane, and established a co-culture model of Ruysch's complex *in vitro.*

6.1 FUNCTIONALITY OF RPE CELLS ON FIBROIN MEMBRANES

The first study represents the first time the growth of mature cultures of RPE cells on fibroin and commercial polyester membranes have been directly compared. My findings demonstrate that RPE cells can develop functionality on fibroin comparable to the commercial polyester membranes. Specifically, cultures established on either material developed a cobblestoned morphology with partial pigmentation within 12 weeks, and evaluation after 16 weeks in culture revealed that the cultures grown on fibroin displayed a rounder apical surface with a more dense distribution of microvilli-like projections. RPE cultures grown on either membrane were able to demonstrate appropriate localisation of RPE specific cytoplasmic and membrane-bound protein distribution, selective phagocytosis and polarised growth factor secretion. The morphology and functionality of the RPE cells that has been achieved in this study suggest that fibroin may be an appropriate substitute for Bruch's membrane.

A major limitation of this study, however, is the use of the immortalised RPE cell line, ARPE-19, which cannot be used in human transplantation. Compounding this issue is the contradictory results that have been reported using this cell source. Most reported results for ARPE-19 cells have been collected from immature cultures often before they reached confluency, let alone maturation. This problem has been

multiplied when culture medium formulations have been used in combination with inappropriate levels of CO_2 in cell culture incubators, and by not employing suspended culture substrates that allow an apical-basal polarisation of the culture (Pfeffer & Philp, 2014). It is acknowledged that there are distinct differences in ARPE-19 cells when compared to native RPE cells, for example, the inability to complete the formation of functioning tight junction complexes (Luo et al., 2006), however, if the cells are grown with best standard practice, ARPE-19 cultures can be useful in evaluating approximate RPE morphology and functionality. Nevertheless, a more appropriate source of human RPE cells, such as primary fetal RPE cells, or iPS-derived RPE cells will need to be used to further evaluate the potential of fibroin membranes.

Looking to the future, the implantation of fibroin membranes into the subretinal space of an animal model to study safety, efficacy and surgical handling is necessary. Understanding the immunogenicity and degradation rate of fibroin membranes in the subretinal space are of vital importance for advancement to a pre-clinical study in combination with RPE cells. The commercial polyester membranes have supported the implantation of human RPE cells into the subretinal space of a rabbit model (Stanzel et al., 2014), however, the permeability, rigidity, and perhaps thickness of the polyester membranes resulted in the death of the overlying host photoreceptor cells, regardless of implanted RPE cell survival. It was suggested that the transport of nutrients and waste with the underlying choroidal blood supply was interrupted by the presence of the polyester membrane. Theoretically the fibroin membrane should be well tolerated in the subretinal space as it is immunologically inert, and silk sutures have been used in the human body for centuries. Eventually the implantation of fibroin membranes with a monolayer of RPE cells, under the macula, with and without removing the equivalent areas of host tissue will be the ultimate test of viability.

6.2 INCORPORATING AN ELASTIN COMPONENT IN FIBROIN MEMBRANES

Considering the elastin-rich core of Bruch's membrane I proposed that fibroin membranes may provide a vehicle for co-delivering RPE cells as well as ECM components to the subretinal space. The feasibility of incorporating recombinant human tropoelastin, which displays similar elastic properties to elastin, into the

fibroin membranes was confirmed, and RPE cell responses (attachment and growth) to fibroin membranes was not affected by the presence of tropoelastin. Membranes prepared using a sequential layering method (fibroin-tropoelastin-fibroin) achieved a homogenous distribution of tropoelastin and fibroin. It was subsequently proposed that this result was due to absorption and subsequent fixation (by treatment with methanol) of tropoelastin within the originally cast fibroin membrane. In comparison, membranes prepared from blended solutions of the two proteins displayed a more heterogeneous composition, with the patchy distribution most likely resulting from either phase separation or specific molecular interactions between the two proteins when present together in solution.

While others have reported reduced stiffness of fibroin membranes following inclusion of tropoelastin (via blending in solution) (Hu et al., 2011, 2010), we reported the opposite result. A close comparison of the methods used, however, revealed several significant variations including the source of cocoons, fibroin protein isolation protocol, water annealing temperature and the thickness of membranes used. In our experience, any one of the parameters alone can have significant effects on the properties of fibroin membranes. Thus in combination, the differing processes could well have been responsible for the variations in response to the tropoelastin observed between each study. It is thus significant that our standard fibroin membranes and membranes prepared using the layered approach are closest to native Bruch's membrane in terms of Young's modulus (Curcio & Johnson, 2013).

While loading of tropoelastin into fibroin membranes has been demonstrated, it remains to be seen if the tropoelastin will be released and converted to elastin by the RPE cells. An *in vitro* model of the elastic fiber assembly process demonstrated that RPE cells are able of converting tropoelastin into elastic fibers, using endogenous microfibrils and lysyl oxidase (Wachi et al., 2005). Although, this study used semi-confluent ARPE-19 cells, it was quite clear that the integration of exogenous tropoelastin provided to the cells via the culture medium was actively incorporated into the ECM of the RPE cultures. It is unknown if the tropoelastin provided to the RPE cells within the fibroin membranes will be converted in a similar way. It is also unknown if processing of the tropoelastin by methanol treatment will reduce its bioavailability to the elastic fiber assembly process. Regardless, further studies may elucidate new understanding of the interaction between the two proteins, and the

mechanisms of the apparent absorption of the tropoelastin protein into the initially cast fibroin layer. Modifying the layered approach and testing new methods of stabilising the tropoelastin protein (other than methanol "fixation") may improve the mechanical properties, and potentially, the conversion of tropoelastin. Further studies would also need to examine the differences in degradation rate, and whether the presence of the tropoelastin will alter this turnover and perhaps promote the development of a new native Bruch's membrane structure, when compared to the fibroin membranes alone (George et al., 2013).

A further consideration when using recombinant human tropoelastin is the cost of the protein, which is in stark contrast to the relatively cheap isolation of the fibroin protein. Without the kind gift of the tropoelastin protein from our collaborator, Professor Tony Weiss, this study would have been prohibitively expensive. Preliminary studies were performed using a cheaper elastin protein from a bovine source, however, the resulting membranes were extremely fragile and unsuitable for further evaluation. It is unknown whether the theoretical benefits of including ECM components in the RPE-fibroin membrane complex, and therefore in the subretinal space upon implantation, would offset this significant additional cost of production.

6.3 CO-CULTURE OF RPE AND CHOROIDAL VASCULAR ENDOTHELIAL CELLS EITHER SIDE OF FIBROIN MEMBRANE

Due to the complexity of the macula and complications of human ageing, surgical replacement of RPE cells and reconstruction of the subretinal architecture is yet to be resolved in humans. The inspiration for the final study was the novel approach proposed by Binder et al. (2007) in which they described a complex that would be most like the native structure of Ruysch's complex, and could potentially anchor into the patient's vasculature upon implantation. The main goal was to evaluate the ability to use fibroin membranes as a substitute for Bruch's membrane in the creation of a co-culture complex of RPE cells and choroidal-derived vascular endothelial cells. I was able to demonstrate that the fibroin membrane acted as a physical barrier between the two cell types, while facilitating communication between the mature monolayer of RPE cells and the choroidal-derived vascular endothelial cells as demonstrated by differences in vascular endothelial cell morphology. The fibroin membrane, suspended in our custom-designed culture chamber, was able to support a three-dimensional collagen gel for the entirety of the

culture period and the co-culture complex could be described as being an *in vitro* representation of the subretinal architecture. Within the timeframe of this doctoral project, the mechanisms of interaction between the two cell types and their interaction with the fibroin membrane were not elucidated. Regardless, as only cell line cultures were used and a primate vascular endothelial cell line at that, this complex would need to be recreated with primary human cell sources before proceeding with further investigation.

Future investigations of this co-culture complex should focus on refinement of the culture system and measuring cell function and mechanisms of cell to cell interaction. The use of this co-culture complex as a model of AMD disease will likely be the ultimate test of function, prior to pre-clinical trials. It is possible this co-culture complex might also provide enlightenment on the potential regeneration of a new Bruch's membrane *in vivo*. It is known that both the RPE cells and the choroidal vasculature are able to produce individual components of Bruch's membrane and during embryonic development the ECM structure is formed between these two cell layers (Booij et al., 2010). However, to the best of my knowledge this process has not been demonstrated *in vitro*, and certainly not *in vivo* postnatal. The theoretical potential of implanted RPE cells to reconstruct a Bruch's membrane structure in an aged patient is a cornerstone of most RPE transplantation ideas. Further refinement and development of this co-culture complex could provide insights into the contribution of the RPE and choroidal vascular endothelial cells in the re-creation of Bruch's membrane, with the fibroin membrane acting as a tissue framework, and the presence of tropoelastin perhaps providing an advantage.

6.4 CONCLUSION

In this PhD project, I have investigated the potential of using fibroin membranes as a Bruch's membrane substitute in the context of RPE cell transplantation. This project demonstrated the functionality of RPE cells grown on fibroin membranes, the feasibility of incorporating a native Bruch's membrane ECM component in the fibroin membranes, and the effect of co-culturing vascular cells in this system. The tissue engineered complex is in many ways comparable to Ruysch's complex, however considerable future efforts will be required to create an implant suitable for human patients. The outcomes of this thesis provide a foundation for the

use of fibroin membranes as a Bruch's membrane substitute and offer a stepping stone for future studies in RPE transplantation.

References

Ainscough, S. L., Feigl, B., Malda, J., & Harkin, D. G. (2009). Discovery and characterization of IGFBP-mediated endocytosis in the human retinal pigment epithelial cell line ARPE-19. *Experimental Eye Research*, *89*(5), 629–37.

Algvere, P. V., Berglin, L., Gouras, P., & Sheng, Y. (1994). Transplantation of fetal retinal pigment epithelium in age-related macular degeneration with subfoveal neovascularization. *Graefe's Archive for Clinical and Experimental Ophthalmology*, *232*(12), 707–16.

Algvere, P. V., Gouras, P., & Kopp, E. D. (1999). Long-term outcome of RPE allografts in non-immunosuppressed patients with AMD. *European Journal of Ophthalmology*, *9*, 217–30.

Altman, G. H., Diaz, F., Jakuba, C., Calabro, T., Horan, R. L., Chen, J., … Kaplan, D. L. (2003). Silk-based biomaterials. *Biomaterials*, *24*(3), 401–16.

Bhatt, N. S., Newsome, D. A., Fenech, T., Hessburg, T. P., Diamond, J. G., Miceli, M. V., … Oliver, P. D. (1994). Experimental transplantation of human retinal pigment epithelial cells on collagen substrates. *American Journal of Ophthalmology*, *117*, 214–21.

Bhutto, I., & Lutty, G. (2012). Understanding age-related macular degeneration (AMD): relationships between the photoreceptor/retinal pigment epithelium/Bruch's membrane/choriocapillaris complex. *Molecular Aspects of Medicine*, *33*(4), 295–317.

Binder, S. (2011). Scaffolds for retinal pigment epithelium (RPE) replacement therapy. *The British Journal of Ophthalmology*, *95*(4), 441–42.

Binder, S., Stanzel, B. V., Krebs, I., & Glittenberg, C. (2007). Transplantation of the RPE in AMD. *Progress in Retinal and Eye Research*, *26*(5), 516–54.

Binder, S., Stolba, U., Krebs, I., Kellner, L., Jahn, C., Feichtinger, H., … Krugluger, W. (2002). Transplantation of autologous retinal pigment epithelium in eyes with foveal neovascularization resulting from age-related macular degeneration: a pilot study. *American Journal of Ophthalmology*, *133*(2), 215–25.

Blenkinsop, T. A., Salero, E., Stern, J. H., & Temple, S. (2013). The culture and maintenane of functional retinal pigment epithelial monolayers from adult human eye. In S. H. Randell & M. L. Fulcher (Eds.), *Epithelial Cell Culture Protocols Methods of Molecular Biology* (Vol. 945, pp. 45–65). Totowa, NJ: Humana Press.

Bodnar, R. J. (2014). Anti-Angiogenic Drugs: Involvement in Cutaneous Side

Effects and Wound-Healing Complication. *Advances in Wound Care*, *3*(10), 635–46.

Bonilha, V. L. (2008). Age and disease-related structural changes in the retinal pigment epithelium. *Clinical Ophthalmology (Auckland, N.Z.)*, *2*(2), 413–24.

Booij, J. C., Baas, D. C., Beisekeeva, J., Gorgels, T. G. M. F., & Bergen, A. A. B. (2010). The dynamic nature of Bruch's membrane. *Progress in Retinal and Eye Research*, *29*(1), 1–18.

Boron, W. F., & Boulpaep, E. L. (Eds.). (2009). *Medical Physiology*. Philadelphia: Saunders/Elsevier.

Borooah, S., Phillips, M. J., Bilican, B., Wright, A. F., Wilmut, I., Chandran, S., … Dhillon, B. (2013). Using human induced pluripotent stem cells to treat retinal disease. *Progress in Retinal and Eye Research*, *37*, 163–81.

Boulton, M. (1998). Melanin and the RPE. In M. F. Marmor & T. F. Wolfsenberger (Eds.), *The Retinal Pigment Epithelium: Function and Disease* (pp. 68–85). Oxford University Press.

Bray, L. J., George, K. A., Ainscough, S. L., Hutmacher, D. W., Chirila, T. V., & Harkin, D. G. (2011). Human corneal epithelial equivalents constructed on Bombyx mori silk fibroin membranes. *Biomaterials*, *32*(22), 5086–91.

Bray, L. J., George, K. A., Hutmacher, D. W., Chirila, T. V., & Harkin, D. G. (2012). A dual-layer silk fibroin scaffold for reconstructing the human corneal limbus. *Biomaterials*, *33*(13), 3529–3538.

Bray, L. J., George, K. A., Suzuki, S., Chirila, T. V., & Harkin, D. G. (2013). Fabrication of a corneal-limbal tissue substitute using silk fibroin. In B. Wright & C. J. Connon (Eds.), *Corneal Regenerative Medicine: Methods and Protocols* (Vol. 1014, pp. 131–39). New York: Springer Science+Business Media.

Bray, L. J., Suzuki, S., Harkin, D. G., & Chirila, T. V. (2013). Incorporation of exogenous RGD peptide and inter-species blending as strategies for enhancing human corneal limbal epithelial cell growth on Bombyx mori silk fibroin membranes. *Journal of Functional Biomaterials*, *4*(2), 74–88.

Campochiaro, P. A., Jerdon, J. A., & Glaser, B. M. (1986). The extracellular matrix of human retinal pigment epithelial cells in vivo and its synthesis in vitro. *Investigative Ophthalmology & Visual Science*, *27*(11), 1615–21.

Chen, F. K., Patel, P. J., Uppal, G. S., Rubin, G. S., Coffey, P. J., Aylward, G. W., & Da Cruz, L. (2009). A comparison of macular translocation with patch graft in neovascular age-related macular degeneration. *Investigative Ophthalmology & Visual Science*, *50*(4), 1848–55.

Chirila, T. V., Barnard, Z., Harkin, D. G., Schwab, I. R., & Hirst, L. W. (2008).

Bombyx mori silk fibroin membranes as potential substrata for epithelial constructs used in the management of ocular surface disorders. *Tissue Engineering Part A*, *14*(7), 1203–11.

Crafoord, S., Geng, L., Seregard, S., & Algvere, P. V. (2002). Photoreceptor survival in transplantation of autologous iris pigment epithelial cells to the subretinal space. *Acta Ophthalmologica Scandinavica*, *80*(4), 387–94.

Curcio, C. A., & Johnson, M. (2013). Structure, function, and pathology of Bruch's membrane. In S. J. Ryan, A. P. Schachat, C. P. Wilkinson, D. R. Hinton, S. Sadda, & P. Wiedemann (Eds.), *Retina* (5th ed., Vol. 1, pp. 465–81). London: Elsevier.

Curcio, C., Messinger, J., Sloan, K., McGwin, G., Medeiros, N., & Spaide, R. (2013). Subretinal drusenoid deposits in non neovascular age-related macular degeneration: morphology, prevalence, topography, and biogenesis model. *Retina*, *33*, 265–76.

Curcio, C., Presley, J., Medeiros, N., Avery, D., & Kruth, H. (2005). Esterified and unesterified cholesterol in drusen and basal deposits of eyes with age-related maculopathy. *Experimental Eye Research*, *81*, 731–41.

Cyranoski, D. (2014). Japanese woman is first recipient of next - generation stem cells. *Nature News*, 2–4. doi:10.1038/nature.2014.15915

da Cruz, L., Chen, F. K., Ahmado, A., Greenwood, J., & Coffey, P. (2007). RPE transplantation and its role in retinal disease. *Progress in Retinal and Eye Research*, *26*(6), 598–635.

de Jong, P. T. V. M. (2006). Mechanisms of Disease: age-related macular degeneration. *The New England Journal of Medicine*, *355*, 1474–86.

de Juan, E., & Machemer, R. (1988). Vitreous surgery for hemorrhagic and fibrous complications of age-related macular degeneration. *American Journal of Ophthalmology*, *105*, 25–28.

Diniz, B., Thomas, P., Thomas, B., Ribeiro, R., Hu, Y., Brant, R., … Humayun, M. S. (2013). Subretinal implantation of retinal pigment epithelial cells derived from human embryonic stem cells: improved survival when implanted as a monolayer. *Investigative Ophthalmology & Visual Science*, *54*(7), 5087–96.

Dunn, K. C., Aotaki-Keen, A. E., Putkey, F. R., & Hjelmeland, L. M. (1996). ARPE-19, a human retinal pigment epithelial cell line with differentiated properties. *Experimental Eye Research*, *62*, 155–69.

Falavarjani, K. G., & Nguyen, Q. D. (2013). Adverse events and complications associated with intravitreal injection of anti-VEGF agents: a review of literature. *Eye (London, England)*, *27*(7), 787–94.

Fan, W., Zheng, J. J., & McLaughlin, B. J. (2002). An in vitro model of the back of the eye for studying retinal pigment ... *In Vitro Cellular & Developmental Biology - Animal*, *38*(April), 228–34.

Fariss, R. N., Apte, S. S., Olsen, B. R., Iwata, K., & Milam, A. H. (1997). Tissue inhibitor of metalloproteinases-3 is a component of Bruch's membrane of the eye. *The American Journal of Pathology*, *150*(1), 323–28.

Feeney, L. (1978). Lipofuscin and melanin of human retinal pigment epithelium. Fluorescence, enzyme cytochemical and ultrastructural studies. *Investigative Ophthalmology and Visual Science*, *17*, 583–600.

Feeney-Burns, L., Hilderbrand, E., & Eldridge, S. (1984). Aging human RPE: Morphometric analysis of macular, equatorial, and peripheral cells. *Investigative Ophthalmology and Visual Science*, *25*, 195–200.

Gal, A., Li, Y., Thompson, D. A., Weir, J., Orth, U., Jacobson, S. G., … Vollrath, D. (2000). Mutations in MERTK, the human orthologue of the RCS rat retinal dystrophy gene, cause retinitis pigmentosa. *Nature Genetics*, *26*(3), 270–71.

Gamm, D. M., Phillips, M. J., & Singh, R. (2013). Modeling retinal degenerative diseases with human iPS-derived cells: current status and future implications. *Expert Review of Ophthalmology*, *8*(3), 213–16.

George, K. A., Shadforth, A. M. A., Chirila, T. V., Laurent, M. J., Stephenson, S.-A., Edwards, G. A., … Harkin, D. G. (2013). Effect of the sterilization method on the properties of Bombyx mori silk fibroin films. *Materials Science and Engineering: C*, *33*, 668–74.

Gil, E., Panilaitis, B., Bellas, E., & Kaplan, D. (2013). Functionalized silk biomaterials for wound healing. *Advanced Healthcare Materials*, *2*, 206–17.

Gillies, P. J., Bray, L. J., Richardson, N. A., Chirila, T. V., & Harkin, D. G. (2015). Isolation of microvascular endothelial cells from cadaveric corneal limbus. *Experimental Eye Research*, *131*, 20–28.

Gordois, A., Cutler, H., Pezzullo, L., Gordon, K., Cruess, A., Winyard, S., … Chua, K. (2012). An estimation of the worldwide economic and health burden of visual impairment. *Global Public Health*, *7*(5), 465–81.

Gouras, P. (1998). Transplantation of retinal pigment epithelium. In M. F. Marmor & T. F. Wolfsenberger (Eds.), *The Retinal Pigment Epithelium: Function and Disease* (pp. 492–507). Oxford University Press.

Guymer, R., Luthert, P., & Bird, A. (1998). Changes in Bruch's Membrane and Related Structures with Age. *Progress in Retinal and Eye Research*, *18*(1), 59–90.

Hakimi, O., Knight, D., Vollrath, F., & Vadgama, P. (2007). Spider and mulberry

silkworm silks as compatible biomaterials. *Composites*, *38*, 324–37.

Hamilton, R. D., Foss, A. J., & Leach, L. (2007). Establishment of a human in vitro model of the outer blood-retinal barrier. *Journal of Anatomy*, *211*(6), 707–16.

Harkin, D. G., George, K. A., Madden, P. W., Schwab, I. R., Hutmacher, D. W., & Chirila, T. V. (2011). Silk fibroin in ocular tissue reconstruction. *Biomaterials*, *32*(10), 2445–58.

Harman, A. M., Fleming, P. A., Hoskins, R. V, & Moore, S. R. (1997). Development and aging of cell topography in the human retinal pigment epithelium. *Investigative Ophthalmology & Visual Science*, *38*(10), 2016–26.

Hayden, E. C. (2011). The growing pains of pluripotency. *Nature*, *473*, 272–74.

Hiscott, P., & Sheridan, C. (1998). The retinal pigment epithelium, epiretinal membranes and proliferative vitreoretinopathy. In *Retinal pigment epithelium—current aspects of function and disease* (pp. 478–91). Cambridge: Harvard University Press.

Hogerheyde, T. A., Suzuki, S., Stephenson, S. A., Richardson, N. A., Chirila, T. V., Harkin, D. G., & Bray, L. J. (2014). Assessment of freestanding membranes prepared from Antheraea pernyi silk fibroin as a potential vehicle for corneal epithelial cell transplantation. *Biomedical Materials (Bristol, England)*, *9*(2), 025016.

Hollburn, M., Stathopoulos, C., Steffen, A., Wiedemann, P., Kohan, L., Bringmann, A., … Bringmann, A. (2007). Positive feedback regulation between MMP-9 and VEGF in human RPE cells. *Investigative Ophthalmology & Visual Science*, *48*(9), 4360–67.

Hong, T., Mitchell, P., Rochtchina, E., Fong, C. S., Chia, E.-M., & Wang, J. J. (2013). Long-term changes in visual acuity in an older population over a 15-year period: the Blue Mountains Eye Study. *Ophthalmology*, *120*(10), 2091–99.

Hu, X., Kaplan, D., & Cebe, P. (2006). Determining beta-sheet crystallinity in fibrous proteins by thermal analysis and infrared spectroscopy. *Macromolecules*, *39*(18), 6161–70.

Hu, X., Park, S.-H., Gil, E. S., Xia, X.-X., Weiss, A. S., & Kaplan, D. L. (2011). The influence of elasticity and surface roughness on myogenic and osteogenic-differentiation of cells on silk-elastin biomaterials. *Biomaterials*, *32*(34), 8979–89.

Hu, X., Shmelev, K., Sun, L., Gil, E., Park, S., Cebe, P., & Kaplan, D. (2011). Regulation of silk material structure by temperature-controlled water vapor annealing. *Biomacromolecules*, *12*(5), 1686–96.

Hu, X., Wang, X., Rnjak, J., Weiss, A. S., & Kaplan, D. L. (2010). Biomaterials

derived from silk-tropoelastin protein systems. *Biomaterials*, *31*(32), 8121–31.

Hu, Y., Liu, L., Lu, B., Zhu, D., Ribeiro, R., Diniz, B., … Humayun, M. S. (2012). A novel approach for subretinal implantation of ultrathin substrates containing stem cell-derived retinal pigment epithelium monolayer. *Ophthalmic Research*, *48*(4), 186–91.

Hynes, S. R., & Lavik, E. B. (2010). A tissue-engineered approach towards retinal repair: scaffolds for cell transplantation to the subretinal space. *Graefe's Archive for Clinical and Experimental Ophthalmology*, *248*(6), 763–78.

Jha, B. S., & Bharti, K. (2015). Regenerating retinal pigment epithelial cells to cure blindness: a road towards personalized artificial tissue. *Current Stem Cell Reports*, *1*(2), 79–91.

Kamao, H., Mandai, M., Okamoto, S., Sakai, N., Suga, A., Sugita, S., … Takahashi, M. (2014). Characterization of human induced pluripotent stem cell-derived retinal pigment epithelium cell sheets aiming for clinical application. *Stem Cell Reports*, *2*(2), 205–18.

Kamei, M., & Hollyfield, J. G. (1999). TIMP-3 in Bruch's membrane: Changes during aging and in Age-Related Macular Degeneration. *Investigative Ophthalmology & Visual Science*, *40*, 2367–75.

Kay, P., Yang, Y. C., & Paraoan, L. (2013). Directional protein secretion by the retinal pigment epithelium: Roles in retinal health and the development of age-related macular degeneration. *Journal of Cellular and Molecular Medicine*, *17*(7), 833–43.

Klenotic, P., Munier, F., Marmorstein, L., & Anand-Apte, B. (2004). Tissue inhibitor of metalloproteinases-3 (TIMP-3) is a binding partner of epithelial growth factor-containing fibulin-like extracellular matrix protein 1 (EFEMP1). Implications for macular degenerations. *The Journal of Biological Chemistry*, *279*, 30469–73.

Köberlein, J., Beifus, K., Schaffert, C., & Finger, R. P. (2013). The economic burden of visual impairment and blindness: a systematic review. *BMJ Open*, *3*(11), e003471.

Kokkinaki, M., Sahibzada, N., & Golestaneh, N. (2011). Human induced pluripotent stem-derived retinal pigment epithelium (RPE) cells exhibit ion transport, membrane potential, polarized vascular endothelial growth factor secretion, and gene expression pattern similar to native RPE. *Stem Cells (Dayton, Ohio)*, *29*(5), 825–35.

Kozel, B. A., Ciliberto, C. H., & Mecham, R. P. (2004). Deposition of tropoelastin into the extracellular matrix requires a competent elastic fiber scaffold but not live cells. *Matrix Biology : Journal of the International Society for Matrix*

Biology, *23*(1), 23–34.

Kwan, A. S., Chirila, T. V, & Cheng S. (2010). Development of tissue-engineered membranes for the culture and transplantation of retinal pigment epithelial cells. In T. V. Chirila (Ed.), *Biomaterials and Regenerative Medicine in Ophthalmology* (pp. 390–408). Cambridge, UK: Woodhead Publishing Limited.

Lanzetta, P., Mitchell, P., Wolf, S., & Veritti, D. (2013). Different antivascular endothelial growth factor treatments and regimens and their outcomes in neovascular age-related macular degeneration: a literature review. *The British Journal of Ophthalmology*, *97*(12), 1497–507.

Lee, E., & Maclaren, R. E. (2011). Sources of retinal pigment epithelium (RPE) for replacement therapy. *The British Journal of Ophthalmology*, *95*(4), 445–49.

Leure-duPree, A. (1968). Ultrastructure of the retinal pigment epithelium in domestic sheep. *American Journal of Ophthalmology*, *65*, 383–98.

Li, L. X., & Turner, J. E. (1988). Inherited retinal dystrophy in the RCS rat: prevention of photoreceptor degeneration by pigment epithelial cell transplantation. *Experimental Eye Research*, *47*(6), 911–17.

Lu, B., Zhu, D., Hinton, D., Humayun, M. S., & Tai, Y.-C. (2012). Mesh-supported submicron parylene-C membranes for culturing retinal pigment epithelial cells. *Biomedical Microdevices*, *14*(4), 659–67.

Luo, Y., Zhuo, Y., Fukuhara, M., & Rizzolo, L. J. (2006). Effects of culture conditions on heterogeneity and the apical junctional complex of the ARPE-19 cell line. *Investigative Ophthalmology and Visual Science*, *47*(8), 3644–55.

Madden, P. W., Lai, J. N. X., George, K. A., Giovenco, T., Harkin, D. G., & Chirila, T. V. (2011). Human corneal endothelial cell growth on a silk fibroin membrane. *Biomaterials*, *32*(17), 4076–84.

Maminishkis, A., Chen, S., Jalickee, S., Banzon, T., Shi, G., Wang, F. E., … Miller, S. S. (2006). Confluent monolayers of cultured human fetal retinal pigment epithelium exhibit morphology and physiology of native tissue. *Investigative Ophthalmology & Visual Science*, *47*(8), 3612–24.

Marmor, M. F. (1998). Structure, Function and Disease of the RPE. In M. F. Marmor & T. F. Wolfsenberger (Eds.), *The Retinal Pigment Epithelium: Function and Disease* (pp. 3–9). Oxford University Press.

Marmor, M. F., & Wolfsenberger, T. J. (Eds.). (1998). *The retinal pigment epithelium: function and disease.* Oxford University Press.

Marshall, J., Hussain, A. A., Starita, C., Moore, D. J., & Patmore, A. L. (1998). Ageing and Bruch's membrane. In M. F. Marmor & T. F. Wolfsenberger (Eds.), *The Retinal Pigment Epithelium: Function and Disease* (pp. 669–92). Oxford

University Press.

Martin, S. L., Vrhovski, B., & Weiss, A. S. (1995). Total synthesis and expression in Escherichia coli of a gene encoding human tropoelastin. *Gene*, *154*(2), 159–66.

Meinel, L., Hofmann, S., Karageorgiou, V., Kirker-Head, C., McCool, J., Gronowicz, G., & Kaplan, D. L. (2005). The inflammatory responses to silk films in vitro and in vivo. *Biomaterials*, *26*(2), 147–55.

Melville, H., Carpiniello, M., Hollis, K., Staffaroni, A., & Golestaneh, N. (2013). Stem cells: a new paradigm for disease modeling and developing therapies for age-related macular degeneration. *Journal of Translational Medicine*, *11*(1), 53.

Montaño, I., Schiestl, C., Schneider, J., Pontiggia, L., Luginbühl, J., Biedermann, T., … Reichmann, E. (2010). Formation of human capillaries in vitro: the engineering of prevascularized matrices. *Tissue Engineering. Part A*, *16*(1), 269–82.

Murphy, A., & Kaplan, D. (2009). Biomedical applications of chemically-modified silk fibroin. *Journal of Materials Chemistry*, *19*, 6443–50.

Nandrot, E. F., Anand, M., Sircar, M., & Finnemann, S. C. (2006). Novel role for alpha v beta 5 -integrin in retinal adhesion and its diurnal peak. *American Journal of Physiology Cell Physiology*, *290*(4), 1256–62.

Nicolini, J., Kiilgaard, J. F., Wiencke, a K., Heegaard, S., Scherfig, E., Prause, J. U., & la Cour, M. (2000). The anterior lens capsule used as support material in RPE cell-transplantation. *Acta Ophthalmologica Scandinavica*, *78*(5), 527–31.

Nita, M., Strzalka-Mrozik, B., Grzybowski, A., Mazurek, U., & Romaniuk, W. (2014). Age-related macular degeneration and changes in the extracellular matrix. *Medical Science Monitor*, *20*, 1003–16.

Panda-Jones, S., Jonas, J. B., & Jakobczyk-Zmilja, M. (1996). Retinal pigment epithelial cell count, distribution, and correlations in normal human eyes. *American Journal of Ophthalmology*, *121*(2), 181–89.

Pastor, J. C., De La Rúa, E. R., & Martín, F. (2002). Proliferative vitreoretinopathy: Risk factors and pathobiology. *Progress in Retinal and Eye Research*, *21*(1), 127–44.

Pearl, J. I., Lee, A. S., Leveson-Gower, D. B., Sun, N., Ghosh, Z., Lan, F., … Wu, J. C. (2011). Short-term immunosuppression promotes engraftment of embryonic and induced pluripotent stem cells. *Cell Stem Cell*, *8*(3), 309–17.

Peyman, G. A., Blinder, K. J., Paris, C. L., Alturki, W., Nelson, N. C., & Desai, U. (1991). A Technique for Retinal Pigment Epithelium Transplantation for Age-Related macular Degeneration Secondary to Extensive Subfoveal Scarring. *Ophthalmic Surgery*, *22*(2), 102–108.

Pfeffer, B. A., & Philp, N. J. (2014). Cell culture of retinal pigment epithelium: Special Issue. *Experimental Eye Research*, *126*, 1–4.

Ramrattan, R. S., van der Schaft, T. L., Mooy, C. M., de Bruijn, W. C., Mulder, P. G. H., & de Jong, P. T. V. M. (1994). Morphometric Analysis of Bruch's Membrane, the Choriocapillaris, and the Choroid in Aging. *Investigative Ophthalmology & Visual Science*, *35*(6), 2857–64.

Reardon, S., & Cyranoski, D. (2014). Japan stem-cell trial stirs envy. *Nature*, *513*, 287–88.

Ribeiro, R. M., Oregon, A., Diniz, B., Fernandes, R. B., Koss, M. J., Charafeddin, W., … Humayun, M. S. (2013). In vivo detection of hESC-RPE cells via confocal near-infrared fundus reflectance. *Ophthalmic Surgery, Lasers & Imaging Retina*, *44*(4), 380–84.

Rizzolo, L. J. (1997). Polarity and development of the outer blood retinal barrier. *Histology and Histopathology*, *12*, 1057–67.

Rong, Z., Wang, M., Hu, Z., Stradner, M., Zhu, S., Kong, H., … Fu, X. (2014). An effective approach to prevent immune rejection of human ESC-derived allografts. *Cell Stem Cell*, *14*(1), 121–30.

Rowland, T., Buchholz, D., & DO Clegg. (2012). Pluripotent human stem cells for the treatment of retinal disease. *Journal of Cell Physiology*, *227*, 457–66.

Sakamoto, T., Sakamoto, H., Murphy, T. L., Spee, C., Soriano, D., Ishibashi, T., … Ryan, S. J. (1995). Vessel Formation by Choroidal Endothelial Cells In Vitro Is Modulated by Retinal Pigment Epithelial Cells. *Archives of Ophthalmology*, *113*, 512–20.

Salero, E., Blenkinsop, T. A., Corneo, B., Harris, A., Rabin, D., Stern, J. H., & Temple, S. (2012). Adult Human RPE Can Be Activated into a Multipotent Stem Cell that Produces Mesenchymal Derivatives. *Cell Stem Cell*, *10 Suppl*(1), 88–95.

Schwartz, S. D., Hubschman, J.-P., Heilwell, G., Franco-Cardenas, V., Pan, C. K., Ostrick, R. M., … Lanza, R. (2012). Embryonic stem cell trials for macular degeneration: a preliminary report. *Lancet*, *379*(9817), 713–20.

Schwartz, S. D., Regillo, C. D., Lam, B. L., Eliott, D., Rosenfeld, P. J., Gregori, N. Z., … Lanza, R. (2014). Human embryonic stem cell-derived retinal pigment epithelium in patients with age-related macular degeneration and Stargardt's macular dystrophy : follow-up of two open-label phase 1/2 studies. *The Lancet*, *6736*(14), 1–8.

Shadforth, A. M. A., George, K. A., Kwan, A. S., Chirila, T. V., & Harkin, D. G. (2012). The cultivation of human retinal pigment epithelial cells on Bombyx

mori silk fibroin. *Biomaterials*, *33*(16), 4110–17.

Shao, C., Sima, J., Zhang, S. X., Jin, J., Reinach, P., Wang, Z., & Ma, J. X. (2004). Suppression of corneal neovascularization by PEDF release from human amniotic membranes. *Investigative Ophthalmology and Visual Science*, *45*(6), 1758–62.

Sivaprasad, S., Webster, A., Egan, C., Bird, A., & Tufail, A. (2008). Clinical course and treatment outcomes of Sorsby fundus dystrophy. *American Journal of Ophthalmology*, *146*, 228–34.

Sonoda, S., Spee, C., Barron, E., Ryan, S. J., Kannan, R., & Hinton, D. R. (2009). A protocol for the culture and differentiation of highly polarized human retinal pigment epithelial cells. *Nature Protocols*, *4*(5), 662–73.

Stanzel, B. V., Liu, Z., Somboonthanakij, S., Wongsawad, W., Brinken, R., Eter, N., … Blenkinsop, T. A. (2014). Human RPE stem cells grown into polarized RPE monolayers on a polyester matrix are maintained after grafting into rabbit subretinal space. *Stem Cell Reports*, *2*(1), 64–77.

Strauss, O. (2005). The retinal pigment epithelium in visual function. *Physiological Reviews*, *85*(3), 845–81.

Sugino, I. K., Sun, Q., Wang, J., Nunes, C. F., Cheewatrakoolpong, N., Rapista, A., … Zarbin, M. A. (2011). Comparison of fRPE and human embryonic stem cell-derived RPE behavior on aged human Bruch's membrane. *Investigative Ophthalmology & Visual Science*, *52*(8), 4979–97.

Tabar, V., & Studer, L. (2014). Pluripotent stem cells in regenerative medicine: challenges and recent progress. *Nature Reviews. Genetics*, *15*(2), 82–92.

Takahashi, K., Tanabe, K., Ohnuki, M., Narita, M., Ichisaka, T., Tomoda, K., & Yamanaka, S. (2007). Induction of pluripotent stem cells from adult human fibroblasts by defined factors. *Cell*, *131*(5), 861–72.

Tezel, T. H., & Del Priore, L. V. (1997). Reattachment to a substrate prevents apoptosis of human retinal pigment epithelium. *Graefe's Archive for Clinical and Experimental Ophthalmology = Albrecht von Graefes Archiv Für Klinische Und Experimentelle Ophthalmologie*, *235*(1), 41–47.

Tezel, T. H., & Del Priore, L. V. (1999). Repopulation of different layers of host human Bruch's membrane by retinal pigment epithelial cell grafts. *Investigative Ophthalmology & Visual Science*, *40*(3), 767–74.

Tezel, T. H., Kaplan, H. J., & Del Priore, L. V. (1999). Fate of human retinal pigment epithelial cells seeded onto layers of human Bruch's membrane. *Investigative Ophthalmology & Visual Science*, *40*(2), 467–76.

Thomson, J., Itskovitz-Eldor, J., Shapiro, S., Waknitz, M., Swiergiel, J., Marshall,

V., & Jones, J. (1998). Embryonic stem cell lines derived from human blastocysts. *Science*, *282*, 1145–47.

Thumann, G., Aisenbrey, S., Schraermeyer, U., Lafaut, B., Esser, P., Walter, P., & Bartz-Schmidt, K. U. (2000). Transplantation of autologous iris pigment epithelium after removal of choroidal neovascular membranes. *Archives of Ophthalmology*, *118*(10), 1350–55.

Thumann, G., Bartz-Schmidt, K. U., El Bakri, H., Schraermeyer, U., Spee, C., Cui, J. Z., … Heimann, K. (1999). Transplantation of autologous iris pigment epithelium to the subretinal space in rabbits. *Transplantation*, *68*(2), 195–201.

Thumann, G., & Walter, P. (2008). Non-pharmacological interventional perspectives in AMD [German]. *Klinische Monatsblätter Für Augenheilkunde*, *225*, 699–702.

Travis, G. H., Golczak, M., Moise, A. R., & Palczewski, K. (2007). Diseases caused by defects in the visual cycle: retinoids as potential therapeutic agents. *Annual Review of Pharmacology and Toxicology*, *47*, 469–512.

Ugarte, M., Hussain, A. A., & Marshall, J. (2006). An experimental study of the elastic properties of the human Bruch's membrane-choroid complex: relevance to ageing. *The British Journal of Ophthalmology*, *90*(5), 621–26.

Van Zeeburg, E. J. T., Maaijwee, K. J. M., Missotten, T. O. A. R., Heimann, H., & Van Meurs, J. C. (2012). A free retinal pigment epitheliumchoroid graft in patients with exudative age-related macular degeneration: Results up to 7 years. *American Journal of Ophthalmology*, *153*(1), 120–27.

Vepari, C., & Kaplan, D. L. (2007). Silk as a Biomaterial. *Progress in Polymer Science*, *32*(8-9), 991–1007.

Vrhovski, B., & Weiss, A. S. (1998). Biochemistry of tropoelastin. *European Journal of Biochemistry*, *258*(1), 1–18.

Wachi, H., Sato, F., Murata, H., Nakazawa, J., Starcher, B. C., & Seyama, Y. (2005). Development of a new in vitro model of elastic fiber assembly in human pigmented epithelial cells. *Clinical Biochemistry*, *38*(7), 643–53.

Wang, N.-K., Tosi, J., Kasanuki, J., Chou, C., Kong, J., Parmalee, N., … Tsang, S. (2010). Transplantation of reprogrammed embryonic stem cells improves visual function in a mouse model for retinitis pigmentosa. *Transplantation*, *89*, 911–19.

Wang, Y., Kim, H.-J., Vunjak-Novakovic, G., & Kaplan, D. L. (2006). Stem cell-based tissue engineering with silk biomaterials. *Biomaterials*, *27*(36), 6064–82.

Wassell, J., Davies, S., Bardsley, W., & Al., E. (1999). The photo-reactivity of the retinal age pigment lipofuscin. *Journal of Biological Chemistry*, *274*, 23828–32.

Wenk, E., Merkle, H., & Meinel, L. (2011). Silk fibroin as a vehicle for drug delivery applications. *Journal of Controlled Release*, *150*, 128–41.

Williams, R. A., Brody, B. L., Thomas, R. G., Kaplan, R. M., & Brown, S. I. (1998). The psychosocial impact of macular degeneration. *Archives of Ophthalmology*, *116*(4), 514–20.

Wise, S. G., Mithieux, S. M., & Weiss, A. S. (2009). Engineered tropoelastin and elastin-based biomaterials. In A. McPherson (Ed.), *Advances in protein chemistry and structural biology* (Vol. 78, pp. 1–24). Elsevier Science.

Wray, L. S., Hu, X., Gallego, J., Georgakoudi, I., Omenetto, F. G., Schmidt, D., & Kaplan, D. L. (2011). Effect of processing on silk-based biomaterials: Reproducibility and biocompatibility. *Journal of Biomedical Materials Research - Part B Applied Biomaterials*, *99 B*(1), 89–101.

Yu, J., Vodyanik, M. A., Smuga-Otto, K., Antosiewicz-Bourget, J., Frane, J. L., Tian, S., … Thomson, J. A. (2007). Induced pluripotent stem cell lines derived from human somatic cells. *Science (New York, N.Y.)*, *318*(5858), 1917–20.

Zhang, H. R. (1994). Scanning electron-microscopic study of corrosion casts on retinal and choroidal angioarchitecture in man and animals. *Progress in Retinal and Eye Research*, *13*(1), 243–70.

Zhang, Y., & Marmorstein, L. (2010). Focus on molecules: fibulin-3 (EFEMP1). *Experimental Eye Research*, *90*, 374–75.